



**Trace Analysis of Polycyclic Aromatic Hydrocarbons
in Water Sample by Gas Chromatography**

Sathida Malee

**Master of Science Thesis in Analytical Chemistry
Prince of Songkla University**

2003

T

เลขที่	QD.341.H9 927 2003 c.2
Bib Key	287217
	- 6 W.A. 2547

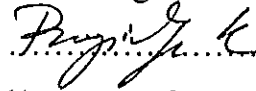
Thesis Title Trace analysis of Polycyclic Aromatic Hydrocarbons in Water Sample
by Gas Chromatography
Author Miss Sathida Malée
Major Program Analytical Chemistry

Advisory Committee

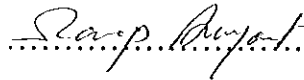
..... Chairman

(Assoc. Prof. Dr. Proespichaya Kanatharana)

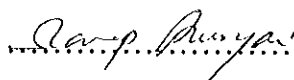
Examining Committee

..... Chairman


(Assoc. Prof. Dr. Proespichaya Kanatharana)

..... Committee

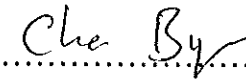
(Assist. Prof. Dr. Manop Arunyanart)

..... Committee

(Assist. Prof. Dr. Manop Arunyanart)

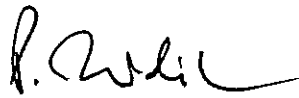
..... Committee

(Assoc. Prof. Dr. Panote Thavarungkul)

..... Committee

(Assist. Prof. Dr. Charun Bunyakan)

The Graduate School, Prince of Songkla University, has approved this thesis
as partial fulfillment for the Master of Science degree in Analytical Chemistry.



.....
(Piti Trisdikoon, Ph. D.)

Associate Professor and Dean

Graduate School

ชื่อวิทยานิพนธ์	วิเคราะห์สารประกอบโพลีไซคลิก อะโรมาติก ไฮโดรคาร์บอนที่มีปริมาณน้อยในตัวอย่างน้ำโดยเทคนิคโครมาโตกราฟี
ผู้เขียน	นางสาวสาธิตา มะลี
สาขาวิชา	เคมีวิเคราะห์
ปีการศึกษา	2546

บทคัดย่อ

วิเคราะห์เชิงคุณภาพและปริมาณสารประกอบโพลีไซคลิก อะโรมาติก ไฮโดรคาร์บอน (พีเอเอช) 7 ตัวซึ่งจัดอยู่ในกลุ่มบี 2 โดย US EPA ได้แก่ เบนโซ(เอ)แอนทราซีน, ไครซีน, เบนโซ(บี)ฟลูออแรนทีน, เบนโซ(เค)ฟลูออแรนทีน, เบนโซ(เอ)ไพรีน, ไคเบนโซ(เอ, เอช)แอนทราซีน และ อินดีโน(1,2,3-ซีดี)ไพรีน ที่มีปริมาณน้อยในน้ำด้วยเทคนิคแก๊สโครมาโตกราฟีที่ใช้คาปิลลารีคอลัมน์ชนิดเฮกซ์พี 5 (HP 5) ยาว 30 เมตร ขนาดเส้นผ่าศูนย์กลาง 0.32 มิลลิเมตร และความหนาของฟิล์ม 0.25 ไมโครเมตร ร่วมกับตัวตรวจวัดชนิดเฟลมไอออไนเซชัน สภาวะการทดลองที่เหมาะสม ได้แก่ อัตราการไหลของแก๊สพา (ฮีเลียม) 1.5 มิลลิลิตรต่อนาที โปรแกรมอุณหภูมิคอลัมน์ อุณหภูมิเริ่มต้นจาก 130 องศาเซลเซียส และเพิ่มอุณหภูมิด้วยอัตรา 15 องศาเซลเซียสต่อนาทีจนถึง 220 องศาเซลเซียส คงอุณหภูมิไว้ 1 นาที แล้วเพิ่มอุณหภูมิต่อด้วยอัตรา 3 องศาเซลเซียสต่อนาทีไปจนถึง 290 องศาเซลเซียส และคงอยู่ที่อุณหภูมิสุดท้าย 2 นาที อุณหภูมิหัวฉีด 280 องศาเซลเซียสและอุณหภูมิตัวตรวจวัด 300 องศาเซลเซียส การฉีดสารเป็นแบบสปลิตเลส (splitless mode) ผลการศึกษาได้ขีดจำกัดต่ำสุดของการตรวจวัดสารพีเอเอชทั้งเจ็ดอยู่ในช่วง 50 ถึง 250 นาโนกรัมต่อมิลลิลิตร โดยมีช่วงความเป็นเส้นตรง 25 นาโนกรัมต่อมิลลิลิตร ถึง 80 ไมโครกรัมต่อมิลลิลิตร ด้วยค่าสหสัมพันธ์ของเส้นตรง (R^2) มากกว่า 0.99 และให้ความแม่นยำสูงโดยมีค่าเบี่ยงเบนมาตรฐานสัมพัทธ์ต่ำกว่า 4%

ได้ทำการศึกษาเทคนิคการเตรียมตัวอย่างที่เหมาะสมสำหรับการวิเคราะห์สารพีเอเอชที่มีปริมาณต่ำกว่าขีดจำกัดต่ำสุด พบว่าตัวอย่างต้องผ่านอุปกรณ์กรองอนุภาค

แขวนลอยอยู่ในน้ำซึ่งประคิษฐ์ขึ้นในห้องปฏิบัติการ ก่อนเพิ่มความเข้มข้นโดยเทคนิคการสกัดด้วยตัวดูดซับของแข็งชนิดแบบแผ่นสกัด (C_{18} extraction disk) โดยใช้ 2-โพรพานอล 0.5% โดยปริมาตรเป็น โมดิฟายเออร์ หลังจากผ่านตัวอย่างน้ำทำให้แผ่นสกัดแห้งเป็นเวลา 3 นาทีก่อนจะสารพีเอเอชจากแผ่นสกัดด้วยตัวชะที่เหมาะสมคือ เอทิลอะซิเตต (ethyl acetate) 3.0 มิลลิลิตร 2 ครั้ง ค่าเปอร์เซ็นต์การได้กลับคืนของสาร พีเอเอชทั้งเจ็ดอยู่ในช่วง 67 ถึง 113 เปอร์เซ็นต์ ผลจากการวิเคราะห์ปริมาณสารประกอบพีเอเอชในตัวอย่างน้ำโดยวิธีที่ศึกษานี้ ในพื้นที่บริเวณบ่อบำบัดน้ำ 3 แห่งของโรงพยาบาลสงขลานครินทร์ โดยเทคนิคแก๊สโครมาโตกราฟี-เฟลมไอออไนเซชัน ร่วมกับเทคนิคการสกัดด้วยตัวดูดซับของแข็งด้วยสภาวะการทดลองดังกล่าวข้างต้น พบว่าทุกพื้นที่มีการปนเปื้อนของสารพีเอเอชทั้งเจ็ดต่ำกว่าขีดจำกัดการตรวจวัดของวิธี ดังนั้นการวิเคราะห์ปริมาณของพีเอเอชในตัวอย่างน้ำทำโดยนำวิธี Standard Addition มาร่วมด้วยได้ค่าการปนเปื้อนของพีเอเอชอยู่ในช่วง 1.1 ถึง 11.2 นาโนกรัมต่อมิลลิลิตร

Thesis Title	Trace analysis of Polycyclic Aromatic Hydrocarbons in Water Sample by Gas Chromatography
Author	Miss Sathida Malee
Major Program	Analytical Chemistry
Academic Year	2003

Abstract

Qualitative and quantitative analysis of seven PAHs, group B2 classified by US EPA, *i.e.* Benzo(a)anthracene, Chrysene, Benzo(b)fluoranthene, Benzo(k)fluoranthene, Benzo(a)pyrene, Dibenzo(a,h)anthracene and Indeno(1,2,3-cd)pyrene in water were carried out by gas chromatography equipped with a 30 m \times 0.25 mm i.d. \times 0.32 μ m film thickness HP 5 capillary column and flame ionization detector. Optimum conditions were obtained, *i.e.* the carrier gas (helium) flow rate at 1.5 ml/min; the column temperature programming was achieved as: initial temperature 130°C, ramped to 220°C at 15°C/min, hold at 220°C for 1 min, ramped to 290°C at 3°C/min, and finally hold for 2 min. The sample was introduced into the column with splitless injection mode injector temperature 280°C, and detector temperature 300°C. The system at optimum conditions provided limit of detections in the range of 50 to 250 ng ml⁻¹, and a linear dynamic range in the range of 25 ng ml⁻¹ to 80 μ g ml⁻¹ with a linear regression (R^2) greater than 0.99 and the relative standard deviation (% RSD) of less than 4%.

The water sample was filtered through the lab-built prefiltration unit before being preconcentrated by solid phase extraction technique using C₁₈ extraction disk. 2-propanol (0.5% v/v) was used as modifier. After the samples passed through the disk, the disk was dried for 3 min and eluted with two portions of 3 ml ethyl acetate which provided high recovery in the range of 67 to 113%. The three sampling sites were waste water ponds of Songklanakarind

Hospital. Samples were extracted by solid phase extraction and analyzed by gas chromatography-flame ionization detector. The results showed that PAHs in water were less than the limit of detections. The standard addition method was implemented for quantitative analysis of PAHs in water samples. The results showed PAHs in water in the range of 1.1 to 11.2 ng ml⁻¹.

ACKNOWLEDGEMENTS

The completion of this thesis would be quite impossible without the help of many people, whom I would like to thank.

I express my sincere thanks to my advisors Associate Professor Dr. Proespichaya Kanatharana for her valuable advice and suggestions throughout the course of this work, and Assistant Professor Dr. Manop Arunyanart for this instructing and providing me with the useful knowledge for my thesis.

I would also like to thank:

Associate Professor Dr. Panote Thvarungkul for her advice which is a valuable encourage for my thesis;

The examination committee members of this thesis for their valuable time;

Staffs of the Department of Chemistry for their help in some technical aspects of this thesis;

Higher Education Development Project: Postgraduate Education and Research Program in Chemistry (PERCH), Funded by the Royal Thai Government, for the scholarship and research supporting;

The Graduate and School Chemistry Department, Prince of Songkla University;

My parents, my sister and my brother for their loves and attentions throughout my life;

And lastly, my friends in Analytical & Environment Chemistry/Trace Analysis Research Unit and Biophysics Research Unit: Biosensors & Biocurrents who help in many ways.

Sathida Malee

CONTENTS

	Page
Abstract (Thai)	(3)
Abstract (English)	(5)
Acknowledgements	(7)
Contents	(8)
Lists of Tables	(11)
Lists of Figures	(16)
Chapter	
1 Introduction	1
1.1 Introduction	1
1.2 Review of literature	7
1.3 Objectives	23
2 Experimental	24
2.1 Chemicals and materials	24
2.2 Instruments and apparatus	25
2.3 Methods	26
2.3.1 Preparation of PAHs standard stock solution	26
2.3.2 Preparation of PAHs standard working solutions	27
2.3.3 GC-FID conditions for PAHs analysis	28
Optimization of split injection mode	28
2.3.3.1 Optimization of carrier gas flow rate	28
2.3.3.2 Optimization of column temperature programming	29
2.3.3.3 Optimization of injector temperature	31
2.3.3.4 Optimization of detector temperature	31
2.3.3.5 Optimization of flow rate of gaseous used in FID	31
2.3.3.6 Limit of Detection	32
2.3.3.7 Linear dynamic range	32

CONTENTS (CONT.)

	Page
Chapter	
Optimization of splitless injection mode	32
2.3.3.8 Optimization of carrier gas flow rate	32
2.3.3.9 Optimization of column temperature programming	33
2.3.3.10 Optimization of injector temperature	34
2.3.3.11 Optimization of detector temperature	34
2.3.3.12 Limit of Detection	34
2.3.3.13 Linear dynamic range	35
2.3.3.14 Response Factor (RF)	35
2.3.3.15 Internal standardization plot method	35
2.3.4 Sample preparation by Solid Phase Extraction	36
2.3.4.1 Elution solvent	38
2.3.4.2 Volume of eluting solvent	39
2.3.4.3 Drying time	39
2.3.4.4 Percentage of modifier	39
2.3.5 Qualitative and quantitative analysis of PAHs in water	40
2.3.5.1 Sampling sites	40
2.3.5.2 Sample collection	41
2.3.5.3 Qualitative analysis	42
2.3.5.4 Quantitative analysis	42
3 Results and Discussion	44
3.1 GC-FID conditions for PAHs analysis	45
Optimization of split injection mode	45
3.1.1 Optimization of carrier gas flow rate	45
3.1.2 Optimization of column temperature programming	49

CONTENTS (CONT.)

Chapter	Page
3.1.3 Optimization of injector temperature	73
3.1.4 Optimization of detector temperature	75
3.1.5 Optimization of make up gas flow rate	77
3.1.6 Optimization of fuel gas flow rate	78
3.1.7 Optimization of oxidant gas flow rate	80
3.1.8 Limit of detection	81
3.1.9 Linear dynamic range	82
Optimization of splitless injection mode	84
3.1.10 Optimization of carrier gas flow rate	84
3.1.11 Optimization of column temperature programming	86
3.1.12 Optimization of injector temperature	95
3.1.13 Optimization of detector temperature	96
3.1.14 Limit of Detection	97
3.1.15 Linear dynamic range	98
3.1.16 Response Factor (RF)	103
3.1.17 Internal standardization plot method	103
3.2 Sample preparation by Solid Phase Extraction	105
3.2.1 Elution solvent	105
3.2.2 Volume of eluting solvent	107
3.2.3 Drying time	109
3.2.4 Percentage of modifier	111
3.3 Qualitative and quantitative analysis of PAHs in water	114
4 Conclusions	123
References	126
Vitae	132

LISTS OF TABLES

Table	Page
1 The carcinogenic potency of PAHs included in US EPA priority pollutant list	3
2 The TEFs currently utilized by EPA Region VI for PAHs	4
3 Physical properties of PAHs including in the group B2 of the US EPA priority pollutant list	11
4 Summarises the techniques for preparation and determination of PAHs	22
5 Optimization of column temperature programming	29
6 Optimization of flow rate of gaseous used in FID	31
7 Optimization of column programming temperature in splitless mode	33
8 Sequential concentrations of 7 PAHs mixture for standard addition method	43
9 The Height Equivalent to a Theoretical Plate (HETP) of $10 \mu\text{g ml}^{-1}$, 1- μl seven PAHs mixture at various flow rate	48
10 The response of B(a)an on isothermal column temperature	49
11 The effect of initial temperature on the response and analysis time of $10 \mu\text{g ml}^{-1}$, 1- μl PAHs standard working solution	50
12 The effect of holding time on the response of $10 \mu\text{g ml}^{-1}$, 1- μl standard working solution	51
13 The effect of ramp rate on the response and the analysis time of $10 \mu\text{g ml}^{-1}$, 1- μl standard working solution	52
14 The effect of initial temperature on the response and analysis time of $10 \mu\text{g ml}^{-1}$, 1- μl standard working solution	54
15 The effect of holding time on the response and analysis time of $10 \mu\text{g ml}^{-1}$, 1- μl PAHs standard working solution	55

LISTS OF TABLES (CONT.)

Table	Page
16 The effect of ramp rate on the response and analysis time of 10 $\mu\text{g ml}^{-1}$, 1- μl PAHs standard working solution	56
17 The effect of initial temperature on the response and analysis time of 10 $\mu\text{g ml}^{-1}$, 1- μl PAHs standard working solution	57
18 The effect of holding time on the response and analysis time of 10 $\mu\text{g ml}^{-1}$, 1- μl PAHs standard working solution	58
19 The effect of ramp rate on the response and analysis time of 10 $\mu\text{g ml}^{-1}$, 1- μl PAHs standard working solution	59
20 The effect of initial temperature on the response and analysis time of 10 $\mu\text{g ml}^{-1}$, 1- μl PAHs standard working solution	60
21 The effect of holding time on the response and analysis time of 10 $\mu\text{g ml}^{-1}$, 1- μl PAHs standard working solution	61
22 The effect of ramp rate on the response and analysis time of 10 $\mu\text{g ml}^{-1}$, 1- μl PAHs standard working solution	62
23 The effect of initial temperature on the response and analysis time of 10 $\mu\text{g ml}^{-1}$, 1- μl PAHs standard working solution	63
24 The effect of holding time on the response and analysis time of 10 $\mu\text{g ml}^{-1}$, 1- μl PAHs standard working solution	64
25 The effect of ramp rate on the response and analysis time of 10 $\mu\text{g ml}^{-1}$, 1- μl PAHs standard working solution	65
26 The effect of initial temperature on the response and analysis time of 10 $\mu\text{g ml}^{-1}$, 1- μl PAHs standard working solution	66
27 The effect of holding time on the response and analysis time of 10 $\mu\text{g ml}^{-1}$, 1- μl PAHs standard working solution	67
28 The effect of ramp rate on the response and analysis time of 10 $\mu\text{g ml}^{-1}$, 1- μl PAHs standard working solution	68

LISTS OF TABLES (CONT.)

Table		Page
29	The effect of initial temperature on the response and analysis time of $10 \mu\text{g ml}^{-1}$, 1- μl PAHs standard working solution	70
30	The effect of holding time on the response and analysis time of $10 \mu\text{g ml}^{-1}$, 1- μl PAHs standard working solution	71
31	The effect of ramp rate on the response and analysis time of $10 \mu\text{g ml}^{-1}$, 1- μl PAHs standard working solution	72
32	The effect of injector temperature on the response of $10 \mu\text{g ml}^{-1}$, 1- μl PAHs standard working solution	74
33	The effect of detector temperature on the response of $10 \mu\text{g ml}^{-1}$, 1- μl PAHs standard working solution	76
34	The effect of make up gas flow rate on the response of $10 \mu\text{g ml}^{-1}$, 1- μl PAHs standard working solution	78
35	The effect of fuel gas flow rate on the response of $10 \mu\text{g ml}^{-1}$, 1- μl PAHs standard working solution	79
36	The effect of oxidant gas flow rate on the response of $10 \mu\text{g ml}^{-1}$, 1- μl PAHs standard working solution	81
37	The relationship between the response of PAHs ($S/N > 3$) and concentration	82
38	The limits of detection for individual PAHs with split mode injection	82
39	The response of individual PAHs at various concentration	83
40	The Height Equivalent to a Theoretical Plate (HETP) of $10 \mu\text{g ml}^{-1}$, 1- μl seven PAHs mixture at various carrier gas flow rate	85
41	The effect of initial temperature on the response and analysis time of $10 \mu\text{g ml}^{-1}$, 1- μl PAHs standard working solution	87

LISTS OF TABLES (CONT.)

Table	Page
42 The effect of hold time on the response and analysis time of 10 $\mu\text{g ml}^{-1}$, 1- μl PAHs standard working solution	88
43 The effect of the first stage ramp rate on the response and analysis time of 10 $\mu\text{g ml}^{-1}$, 1- μl standard working solution	89
44 The effect of second stage temperature on the response and the analysis time of 10 $\mu\text{g ml}^{-1}$, 1- μl standard working solution	90
45 The effect of hold time at the second stage temperature on the response and the analysis time of 10 $\mu\text{g ml}^{-1}$, 1- μl standard working solution	91
46 The effect of ramp rate at the second stage temperature on the response and the analysis time of 10 $\mu\text{g ml}^{-1}$, 1- μl standard working solution	92
47 The effect of ramp rate at the second stage temperature on the response and the analysis time of 10 $\mu\text{g ml}^{-1}$, 1- μl standard working solution	93
48 The effect of injector temperature on the response of 10 $\mu\text{g ml}^{-1}$, 1- μl PAHs standard working solution	95
49 The effect of detector temperature on the response of 10 $\mu\text{g ml}^{-1}$, 1- μl PAHs standard working solution	96
50 The relationship between the response of PAHs and concentrations	97
51 The limits of detection for individual PAHs with the optimum splitless mode injection GC conditions	98
52 The response of individual PAHs at various concentration	99
53 Relative response factor of seven PAHs at various concentration	103
54 The relation between the concentration of PAHs and the ratio of peak area of analyte to internal standard (A_a/A_{is})	104

LISTS OF TABLES (CONT.)

Table		Page
55	The percentage recovery of seven PAHs extraction with dichloromethane, ethyl acetate, methanol and dichloromethane: ethyl acetate (1:1)	106
56	The percentage recovery of seven PAHs with 2×2 ml, 2×3ml, 2×4 ml and 2×5 ml ethyl acetate	108
57	The percentage recovery of drying time as 3, 5, 7 and 10 min	110
58	Comparison of percentage recovery of percentage organic modifier as 0, 5 and 10	112
59	The recovery of seven PAHs from C ₁₈ disk	113
60	The response of B(a)an for sample site 1, 2 and 3 at various spiked concentration level	115
61	The response of Chry for sample site 1, 2 and 3 at various spiked concentration level	116
62	The response of B(b)fl for sample site 1, 2 and 3 at various spiked concentration level	117
63	The response of B(k)fl for sample site 1, 2 and 3 at various spiked concentration level	118
64	The response of B(a)p for sample site 1, 2 and 3 at various spiked concentration level	119
65	The response of In(123-cd)p for sample site 1,2 and 3 at various spiked concentration level	120
66	The response of D(a,h)an for sample site 1,2 and 3 at various spiked concentration level	121
67	The PAHs concentrations of samples determined by standard addition method	122

LISTS OF FIGURES

Figure		Page
1	Solid phase extraction apparatus	36
2	The location of the three sampling sites	40
3	The van Deemter plot	46
4	Measurements used in calculating total theoretical plates	47
5	The van Deemter plot of the seven PAHs	48
6	The responses of 10 $\mu\text{g ml}^{-1}$, 1- μl PAHs standard working solution at different initial temperature	50
7	The responses of 10 $\mu\text{g ml}^{-1}$, 1- μl PAHs standard working solution at different hold time	51
8	The responses of 10 $\mu\text{g ml}^{-1}$, 1- μl PAHs standard working solution at different ramp rate	52
9	The responses of 10 $\mu\text{g ml}^{-1}$, 1- μl PAHs standard working solution at different initial temperature	54
10	The responses of 10 $\mu\text{g ml}^{-1}$, 1- μl PAHs standard working solution at different hold time	55
11	The responses of 10 $\mu\text{g ml}^{-1}$, 1- μl PAHs standard working solution at different ramp rate	56
12	The responses of 10 $\mu\text{g ml}^{-1}$, 1- μl PAHs standard working solution at different initial temperature	57
13	The responses of 10 $\mu\text{g ml}^{-1}$, 1- μl PAHs standard working solution at different hold time	58
14	The responses of 10 $\mu\text{g ml}^{-1}$, 1- μl PAHs standard working solution at different ramp rate	59
15	The responses of 10 $\mu\text{g ml}^{-1}$, 1- μl PAHs standard working solution at different initial temperature	60

LISTS OF FIGURES (CONT.)

Figure		Page
16	The responses of $10 \mu\text{g ml}^{-1}$, 1- μl PAHs standard working solution at different hold time	61
17	The responses of $10 \mu\text{g ml}^{-1}$, 1- μl PAHs standard working solution at different ramp rate	62
18	The responses of $10 \mu\text{g ml}^{-1}$, 1- μl PAHs standard working solution at different initial temperature	63
19	The responses of $10 \mu\text{g ml}^{-1}$, 1- μl PAHs standard working solution at different hold time	64
20	The responses of $10 \mu\text{g ml}^{-1}$, 1- μl PAHs standard working solution at different ramp rate	65
21	The responses of $10 \mu\text{g ml}^{-1}$, 1- μl PAHs standard working solution at different initial temperature	66
22	The responses of $10 \mu\text{g ml}^{-1}$, 1- μl PAHs standard working solution at different hold time	67
23	The responses of $10 \mu\text{g ml}^{-1}$, 1- μl PAHs standard working solution at different ramp rate	68
24	The responses of $10 \mu\text{g ml}^{-1}$, 1- μl PAHs standard working solution at different initial temperature	70
25	The responses of $10 \mu\text{g ml}^{-1}$, 1- μl PAHs standard working solution at different hold time	71
26	The responses of $10 \mu\text{g ml}^{-1}$, 1- μl PAHs standard working solution at different ramp rate	72
27	The optimum column temperature programming by split injection	73
28	The responses of $10 \mu\text{g ml}^{-1}$, 1- μl PAHs standard working solution at different injector temperature	74

LISTS OF FIGURES (CONT.)

Figure		Page
29	The responses of $10 \mu\text{g ml}^{-1}$, 1- μl PAHs standard working solution at different detector temperature	76
30	The responses of $10 \mu\text{g ml}^{-1}$, 1- μl PAHs standard working solution at different make up gas flow rate	78
31	The responses of $10 \mu\text{g ml}^{-1}$, 1- μl PAHs standard working solution at different fuel gas flow rate	79
32	The responses of $10 \mu\text{g ml}^{-1}$, 1- μl PAHs standard working solution at different oxidant gas flow rate	81
33	The linear dynamic range of seven PAHs	83
34	The van Deemter plot of seven PAHs	85
35	The responses of $10 \mu\text{g ml}^{-1}$, 1- μl PAHs standard working solution at different initial temperature	87
36	The responses of $10 \mu\text{g ml}^{-1}$, 1- μl PAHs standard working solution at different hold time	88
37	The responses of $10 \mu\text{g ml}^{-1}$, 1- μl PAHs standard working solution at different first stage ramp rate	89
38	The responses of $10 \mu\text{g ml}^{-1}$, 1- μl PAHs standard working solution at different second stage temperature	90
39	The responses of $10 \mu\text{g ml}^{-1}$, 1- μl PAHs standard working solution at different second stage temperature holding time	91
40	The responses of $10 \mu\text{g ml}^{-1}$, 1- μl PAHs standard working solution at different second stage of ramp rate	92
41	The responses of $10 \mu\text{g ml}^{-1}$, 1- μl PAHs standard working solution at different final temperature	93
42	The optimum column temperature programming by splitless injection mode	94

LISTS OF FIGURES (CONT.)

Figure		Page
43	The responses of 10 $\mu\text{g ml}^{-1}$, 1- μl PAHs standard working solution at different injector temperature	95
44	The responses of 10 $\mu\text{g ml}^{-1}$, 1- μl PAHs standard working solution at different detector temperature	96
45	The linear dynamic range of seven PAHs	99
46	Split liner	101
47	Splitless liner	101
48	Comparison the response and analysis time obtained from split and splitless injection	102
49	The relationship between concentration of PAHs and the ratio of peak area of analyte to internal standard	104
50	The effect of type of eluting solvent to the recovery of PAHs extraction	106
51	The effect of volume of solvent to the recovery of PAHs extraction	108
52	The effect of drying time to the recovery of PAHs extraction	110
53	The effect of percentage of 2-propanol to the recovery of PAHs extraction	112
54	The standard addition calibration curve of B(a)an	115
55	The standard addition calibration curve of Chry	116
56	The standard addition calibration curve of B(b)fl	117
57	The standard addition calibration curve of B(k)fl	118
58	The standard addition calibration curve of B(a)p	119
59	The standard addition calibration curve of In(123-cd)p	120
60	The standard addition calibration curve of D(a,h)an	121

Chapter 1

INTRODUCTION

1.1 Introduction

In the 20th century, the environment is continuously loaded with foreign organic chemicals. Humans are daily exposed to a number of potentially harmful substances of natural or anthropogenic origin. Distribution and dispersion of pollutants can be via air, water, soils, sediment, food, tobacco (ASTDR, 1996) smoke, transport, and industrial activities. Many thousands organic trace pollutants, such as polycyclic aromatic hydrocarbons (PAHs), have been produced and, in part, released into the environment (van der Oost *et al.*, 2003). These pollutants are ubiquitous in nature due to environmental persistency and are subject to bioaccumulation and/or exhibit high toxicity. Most of these pollutants are listed as controlled substances by the regulatory agencies, such as U.S. Environmental Protection Agency (US EPA), European Unions (EU), and World Health Organization (WHO) (Urbe and Ruana, 1997) due to their potentially persistent and hazardous to non-target organisms including humans. They are usually present as complex mixtures and may vary vastly in the relative abundance of the individual components (Marriott *et al.*, 2003).

Polycyclic aromatic hydrocarbons (PAHs) are ubiquitous organic compounds which are non-essential for the growth of plants, animals or humans. PAHs are introduced into the environmental mainly via natural and anthropogenic combustion processes. As a consequence, their loading to aquatic and terrestrial systems all have a component which is atmospheric in origin. Volcano eruptions and forest and prairie fires are among the major natural sources of PAHs. Important anthropogenic sources include combustion

of fossil fuels, waste incineration, coke and asphalt production, oil refinery, and many other industrial activities. As a result, they are widely distributed in environment. PAHs have received considerable attention because of the documented carcinogenic in experimental animals of several of its members. When they are present in sufficient quantity, even in trace level, certain PAHs are toxic, mutagenic and carcinogenic to living things (Manoli and Samara, 1999). Mammals and many lower organisms metabolize PAHs primarily by enzymatic oxygenation to peroxides, phenols, dihydrodiols, quinones, and water-soluble conjugates in an attempt to make them more soluble and thus facilitate their excretion from the organism. In this way, the pre carcinogen is converted to the ultimate carcinogen which covalently binds to the information molecules (*e.g.* DNA and RNA) and leads to carcinogenesis (tumour formation) (Townshend, 1997). Several PAHs, especially those with four or more benzene ring, have been established as carcinogens in animals. Among the most potent and best reported carcinogenic is Benzo(a)pyrene or (B(a)p). It is shown to cause lung and skin cancer in laboratory animals. A significant amount of the knowledge of toxicological actions of PAHs is based on extrapolation of studies with B(a)p to the other carcinogenic members of the class.

More than 100 PAHs have been found in nature, however, only 16 have been selected as priority pollutants by the US EPA (Barranco *et al.*, 2003), as listed in Table 1. US EPA has also classified seven PAHs compounds, *i.e.* Benzo(a)pyrene, B(a)p; Benzo(a)anthracene, B(a)an; Chrysene, Chry; Benzo(b)fluoranthene, B(b)fl; Benzo(k)fluoranthene, B(k)fl; Indeno(1,2,3-cd)pyrene, I(123-cd)p; and Dibenzo(a,h)anthracene, D(a,h)p, as group B2 carcinogenics. They are indicating sufficient evidence of carcinogenesis in animals, and they are possibly carcinogenic to humans (ASTDR, 1995).

Table 1 The carcinogenic potency of PAHs included in US EPA priority pollutant list

PAHs	Carcinogenic potency IARC/US EPA* classification
Acenaphthene	-
Acenaphthylene	-
Fluorene	-
Naphthalene	-
Anthracene	3
Fluoranthene	3
Phenanathrene	3
Pyrene	3
Benzo(ghi)perylene	3
Benzo(a)anthracene	2A/B2
Benzo(a)pyrene	2A/B2
Benzo(b)fluoranthene	2B/B2
Benzo(k)fluoranthene	2B/B2
Chrysene	3/B2
Dibenzo(a,h)anthracene	2A/B2
Indeno(1,2,3-cd)pyrene	2B/B2

2A: Probably carcinogenic to humans;

2B: Possibly carcinogenic to humans;

B2: Probable human carcinogen;

3: Not classifiable as to human carcinogenicity.

* IARC: International Agency for Research on Cancer;

U. S. EPA: U. S. Environmental Protection Agency.

Source: Manoli and Samara (1999)

Because cancer potency factors for the carcinogenic PAHs other than B(a)p have not been developed, the potency factor for B(a)p is used as a basis for determining relative carcinogenic potential for the other PAHs. The US EPA has developed Toxicity Equivalence Factors (TEFs) to rank the relative carcinogenic potential of others to B(a)p. The TEFs currently utilized by EPA Region VI for PAHs are listed in Table 2 (ASTDR, 1992). The TEFs can be used for estimating the relative carcinogenicity of an environmental mixture with a known distribution of PAHs. Specially, the concentration of each carcinogenic PAH is multiplied by the appropriate TEF and then summed to provide an estimate of the B(a)p equivalent concentration.

Table 2 The TEFs currently utilized by EPA Region VI for PAHs

Compound	TEF
Benzo(a)pyrene	1.0
Dibenzo(a,h)anthracene	1.0
Benzo(a)anthracene	0.1
Benzo(b)fluoranthene	0.1
Benzo(k)fluoranthene	0.1
Indeno(1,2,3-cd)pyrene	0.1
Chrysene	0.01

Despite their large source strength in urban/industrial sites, PAHs occur at relative high concentrations in rural and remote areas due to their ability to be transported over long distance as gases or aerosols, and their apparent resistance to degradation on atmospheric particulates. Thus, PAHs emission into urban/industrial atmospheres may significantly affect coastal and inland surface waters. PAHs enter surface waters via atmospheric fallout, urban run-off, municipal effluents, industrial effluents and oil spillage or leakage.

Atmospheric fallout includes wet and dry deposition of particles and vapors. PAHs are discharged into the atmosphere in gaseous and particulate phases. They are subjected to either vapor and particle washout from the atmosphere during precipitation. Atmospheric deposition is considered to be an important input of PAHs to surface waters. It has been estimated that 10-80% input to the world's oceans is from atmospheric sources. A significant amount of PAHs carried to surface waters by sewer derives from urban run-off, industrial effluent, and municipal wastewaters. In groundwater, PAHs may originate from pollute surface water bodies, agricultural irrigation with effluents, or contaminated soil. The presence of PAHs in drinking water may be due to the surface or groundwater used as raw water sources, or to the use of coal tar-coated pipes in public water supply systems. Regarding the chlorination of drinking water, it has been found that this disinfection technique may lead to formation of oxygenated or chlorinated PAHs, *i.e.* quinones or polychlorinated aromatics compounds that are more toxic than the parent PAHs (Manoli and Samara, 1999).

Different laws on water for public consumption passed by the EU, US EPA, and WHO include control over PAHs. The recent European Community Directive 80/778/EEC states a maximum level for PAHs in drinking water of $0.2 \mu\text{g l}^{-1}$ for Fluoranthene [fl], B(a)p, B(b)fl, B(k)fl, Benzo(ghi)perylene [B(ghi)pe] and limits to $0.01 \mu\text{g l}^{-1}$ for B(a)p. Maximum levels for the sum of PAHs in surface waters can reach $1 \mu\text{g l}^{-1}$ depending on the surface water treatment process. The US EPA legislation includes B(a)p and limits it to a concentration of $0.2 \mu\text{g l}^{-1}$. WHO in its latest "Guidelines for drinking water quality", considers only B(a)p with a reference level of $0.7 \mu\text{g l}^{-1}$ (Urbe and Ruana, 1997; Manoli and Samara, 1999).

Most people are exposed to PAHs when they breath smoke, auto emissions or industrial exhausts. Drinking or eating exposure is usually from charcoal-broiled or fried foods, especially meats. Shellfish living in

contaminated water may be another major source of exposure. People may be exposed to PAHs which exist in groundwater near disposal sites where construction waters or ash are buried (www.dhfs.state.wi.us/ch, 2000). PAHs can also be absorbed through skin. Exposure can come from handling contaminated soil or bathing in contaminated water. In general, chemicals affect the same organ systems in all people who are exposed. However, the seriousness of the effects vary from person to person. A person's reaction depends on several things, including individual health, heredity, previous exposure to chemicals (medicines), and personal habit (smoking or drinking). It is also important to consider the length of exposure, the amount of exposure and whether the chemical was inhaled, touched or eaten.

From the above reasons, PAHs have received increasing attention in recent years in water pollution. However, due to their hydrophobic nature ($\log K_{ow} = 3-8$) (Manoli and Samara, 1999) concentrations of dissolved PAHs in water are very low. Therefore, trace-level determination of PAHs in water has become laborious and complicated. PAHs also associate easily with particulate matter which are deposited in the sediment. Thus, it is necessary to separate these PAHs from the complex matrix and enhance their concentration before determination.

This thesis emphasized on the methodology for the determination of trace PAHs in water, *i.e.* the seven PAHs group B2. The method consists of two parts, the optimization of a Gas Chromatograph equipped with Flame Ionization detector (GC-FID), and a sample preparation technique, which includes extraction, pre-concentration, and clean up, by Solid Phase Extraction (SPE). This method is simple, rapid and produce a minimum amount of waste from the process, *i.e.* environmental friendly. On the other hand high accuracy, good precision, high efficiency of extraction and high recovery yield are obtained.

1.2 Review of literature

1.2.1 Name, synonyms, and chemical structure

Polycyclic aromatic hydrocarbons, PAHs (also as known as polynuclear aromatic hydrocarbons) are composed of two or more aromatic rings which are fused together when a pair of carbon atoms is shared between them and there is no other element except carbon and hydrogen. The resulting structure is a molecule where all carbon and hydrogen atoms lie in one plane. The group B2 PAHs include 7 compounds as follows (Irwin, 1997)

Benzo(a)anthracene ; B(a)an

Synonyms: 1,2-Benzo(a)anthracene;

1,2-Benzanthracene;

1,2-Benzanthrene

1,2-Benzoanthracene;

2,3-Benzophenanthrene;

Benzanthracene;

Benzanthrene;

Benz(a)anthracene;

Benzo(b)phenanthrene;

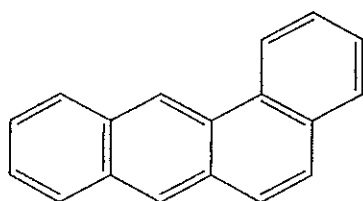
Benzoanthracene;

Tetraphene;

Naphthanthracene

Molecular formula: C₁₈H₁₂

Chemical structure:



Benzo(a)pyrene; B(a)p

Benzo(a)pyrene; B(a)p

Synonyms: 1,2-Benzopyrene;

1,2-Benzopyrene;

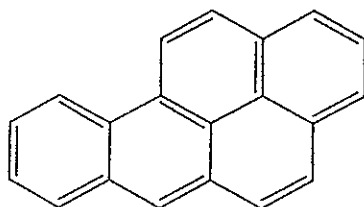
1,2-Benzopyrene;

4,5-Benzopyrene;

B(e)p

Molecular formula: C₂₀H₁₂

Chemical structure:



Benzo(b)fluoranthene; B(b)fl

Synonyms: 2,3-benzfluoranthene;

2,3-benzofluoranthene;

2,3-benzofluoranthrene;

3,4-benz(e)acephenanthrylene;

3,4-benzfluoranthene;

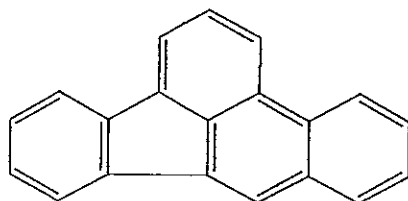
2,3-benzofluoranthene;

Benz(e)acephenanthrylene;

Benzo(e)fluoranthene;

Molecular formula: C₂₀H₁₂

Chemical structure:



Benzo(k)fluoranthene; B(k)fl*Synonyms:* 2,3,1',8'-Binaphthylene;

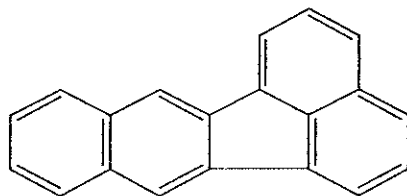
8,9-Benzofluoranthene;

8,9-Benzfluoranthene;

11,12-Benzo(k)fluoranthene;

11,12-Benzofluoranthene;

Dibenzo(b,jk)fluorene

Molecular formula: C₂₀H₁₂*Chemical structure:*Dibenzo(a,h)anthracene; D(a,h)an*Synonyms:* 1,2,5,6-Dibenzanthracene;

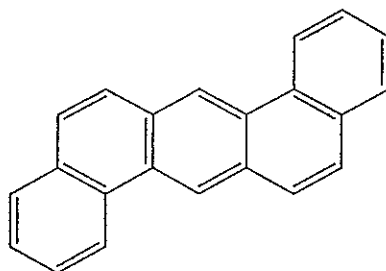
1,2:5,6-benzanthracene;

1,2:5,6-Dibenz(a)anthracene;

1,2:5,6-Dibenzanthracene;

1,2:5,6-Dibenzoanthracene;

1,2,7,8-dibenzanthracene;

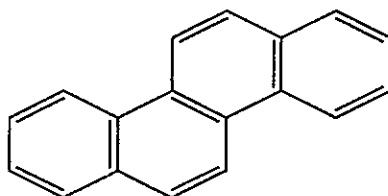
Molecular formula: C₂₂H₁₄*Chemical structure:*

Chrysene; Chry

Synonym: 1,2-Benzphenanthrene

Molecular formula: C₁₈H₁₂

Chemical structure:



Indeno(1,2,3-cd)pyrene; In(123-cd)p

Synonyms: 1,10-(1,2-Phenylene)Pyrene;

1,10-(O-Phenylene)Pyrene;

2,3-O-Phenylenepyrene;

2,3-Phenylenepyrene;

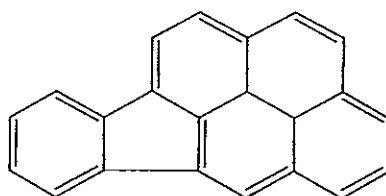
O-Phenylenepyrene;

Indenopyrene;

Indeno(1,2,3-cd)pyrene

Molecular formula: C₂₂H₁₂

Chemical structure:



1.2.2 Physical properties

The physical properties of the seven PAHs are summarized in Table 3.

Table 3 Physical properties of PAHs including in the group B2 of the US EPA priority pollutant list

PAHs	Molecular weight (g mol ⁻¹)	Density (g l ⁻¹)	Color	Vapor pressure (torr)	Solubility in water (mg l ⁻¹)	Log K _{oc} *	Log K _{ow} **	Boiling point (°C)
B(a)an	228.29	1.274	Colorless platelets	5×10^{-9} at 20°C	0.01 at 25°C	6.3	5.61-5.91	435
B(a)p	252.30	1.351	Yellowish plates	5×10^{-9}	0.0038 at 25°C	4.00-7.20	6.44-7.40	495
B(b)fl	252.32	Unknown	Colorless needles	10^{-11} to 10^{-6} at 20°C	0.014 at 25°C	5.74	5.80-6.57	398
B(k)fl	252.32	Unknown	Pale yellow needles	9.6×10^{-7} at 20°C	0.008 at 25°C	5.74-5.99	6.06-7.20	481
Chry	228.28	1.274	Colorless platelets	10^{-11} to 10^{-6} at 20°C	0.002 at 25°C	5.3	5.61-5.91	448
D(a,h)an	278.33	1.282	Colorless platelets	$\sim 10^{-10}$	0.002 at 25°C	5.20-6.52	5.80-7.19	524
In(123-cd)p	276.33	Unknown	Yellowish plates	$\sim 10^{-10}$	0.0062	4.3	6.58-7.00	530

Source: Manoli and Samara (1999), Marce and Borruil (2000) and Irwin (1997)

* Log K_{ow}: Partition coefficients octanol-water

** Log K_{oc}: Sorption partition coefficient

1.2.3 Environmental impact and environmental fate in water

The pattern of PAHs release into the environment are quite general since they are the universal products of combustion of organic matter. Both in air and water, it is largely associated with particulate matter. When release into water it will rapidly become adsorbed to sediment or particulate matter in the water column including phytoplankton and zooplankton. PAHs are accumulated in aquatic organisms which cannot metabolize them (organism which lack microsomal oxidase, the enzyme enables the rapid metabolism of PAHs). In the dissolved state, they were degraded by photolysis (in a matter of hours to days) in eutrophic bodies of water, and oxidation by alkyl radicals and hydroperoxy radicals may be important. Its slow desorption from sediment and particulate matter resulted in a low concentration of PAHs in the water. PAHs are very slowly biodegraded when colonies of microorganism are acclimated but this is a very slow process (half-life *ca* 1 year to be significant) (www.speclab.com/compund.htm, 2001).

1.2.4 Sample preparation and analysis method

PAHs compounds are usually determined by chromatographic techniques because wide range of different compounds with similar characteristics can be separated, and their individual concentration can be determined. These include High Performance Liquid Chromatography (HPLC), Gas Chromatography (GC), Supercritical Fluid Chromatography (SFC), and Capillary Electrophoresis (CE) (Nguyen and Luong, 1997; Szolar *et al.*, 1995).

Reverse phase liquid chromatography on chemically bonded octadecylsilane (C₁₈) stationary phase has been shown to provide excellent separation of PAHs. However, not all C₁₈ stationary phases provide the same resolution (*i.e.* relative separation) since resolution is greatly influenced by the type of synthesis used to prepare the bonded phase. Popp *et al.*, (2000) coupled

off-line SPME with a Vydac 201 TP 52 column (250 × 2.1 mm i.d.) LC-FLD, the results provided detection limits of PAHs ranged from 1 to 6 ng l⁻¹.

For GC analysis, fused silica capillary columns coated with non-polar liquid phase, such as methyl-silicone, are widely employed. Packed column with similar stationary phase are also used (US EPA, 1984). Singh *et al.*, (1998) quantitatively analyzed the semi-volatile pollutant in soil, water and plasma samples by using 30 m × 0.25 mm i.d. HP-5 GC-MS programmed to monitoring selected ions (SIM). The samples were extracted by forisil SPE column. The result provided clear separation of some compounds but partial to incomplete separation of others. To validate the analytical procedure for polychlorinated biphenyls (PCBs) and PAHs, Jaouen-Madoulet *et al.* (2000) selected various GC columns and detectors for their analysis. For the detection of PAHs, three different columns and two detectors were used. These were (1) a 60 m × 0.25 mm i.d. × 0.25 μm thickness DB-5 equipped with FID; (2) a 30 m × 0.53 mm i.d. × 0.5 μm thickness DB-608 equipped with FID and (3) a 60 m × 0.25 mm i.d. × 0.25 μm thickness HP-5 MS equipped with MSD. They provided the similar linear dynamic range from 2.0 to 40.0 ng ml⁻¹ and limit of detection for PAHs was in the range of 0.90 to 2.47 ng ml⁻¹. Li and Lee (2001) studied the negative effect of humic acid which was a particular problem of surface water analysis. PAHs separation was accomplished with a 30 m × 0.32 mm i.d. × 0.25 μm thickness DB-5 fused silica capillary column GC-MS. For PAHs quantified by GC-FID or GC-MS, the concentration tested were in the range 2 to 40 ng μl⁻¹ and 0.1 to 1 ng μl⁻¹, respectively.

GC is the most widely used separation technique. Many of the target pollutants are volatile enough to be analyzed by GC. For semivolatiles such as PAHs, PCBs, and some pesticides HPLC is widely used. GC has several advantages over HPLC. GC column provided a larger number of plates, and a variety of highly sensitivity and selective detector are available. Since environmental samples are complex, the high separation capability is

important. If there is a choice between GC and HPLC, GC is usually preferred. An example of a difficult separation of some metabolites of benzo(a)pyrene, too non-volatile to be separated, can easily be separated by GC (Kebbekus and Mitra, 1998).

Due to the complexity of the matrix, PAHs determination in environmental samples is often a difficult task, even after fractionation of sample extracts, therefore, good chromatographic selectivity, both in separation and in detection are required during environmental analysis. Moreover, since their concentration in water sample is extremely low, owing to their low solubility, the determination of PAHs is rather difficult (Bruzzoniti *et al.*, 2000).

In general, most organic pollutant of interest in aqueous environmental samples have to be extracted and enriched before the instrumental determination. This isolation from a sample matrix is often achieved by sampling and extraction steps, separated from the instrumental analysis. In the past, sample preparation was dominated by the conventional liquid – liquid extraction (LLE), a time consuming multi-step method for which large amount of solvents were necessary. Today many sampling and extraction methods are still based on classical techniques, such as the common Soxhlet extraction method (Eisert and Levsen, 1996).

Liquid–liquid extraction is a popular method for extracting organic pollutants from liquid matrices, especially water. Extraction technique is usually employed for compounds which could not be analyzed efficiently by purge and trap, because the analyte is not volatile enough to be purged in a reasonable time. The aqueous sample containing the pollutant is shaken with an immiscible organic solvent. The sample components distribute themselves between the aqueous and the solvent phase. When the two solutions reach equilibrium, the ratio of the concentration of the solute in the two phases is constant (Kebbekus and Mitra, 1998). Liquid–liquid extraction has been largely

replaced in the past few years by SPE using a variety of different sorbents. An optimized selectivity could be achieved by using analyte-specific sorbent for different compound classes.

Solid Phase Extraction (SPE) is also known as liquid-solid extraction. Few milligram of SPE adsorbent was packed in a cartridge or embedded on surface of a membrane. The liquid sample from which the analytes are to be extracted is passed through the SPE adsorbent, and the analytes are retained by the sorbent. The sample is then extracted by passing a few milliliters of a suitable solvent through the cartridge or disk. In this way, the analytes are separated from the sample matrix and transferred into a small quantity of solvent. The analytes are not only extracted from the water but also concentrated in a small volume of solvent (Kebbekus and Mitra, 1998).

The SPE method is simple and less time-consuming than classical liquid-liquid extraction as many samples can be enriched in parallel. Moreover, it is inexpensive and less (toxic) solvents are needed. Kootstra *et al.*, (1995) compared the C₈ SPE and LLE method for extraction of PAHs from soil sample. The concentrated PAHs were analyzed by HPLC, with acetonitrile-water (50:50, v/v) as mobile phase. Both fluorescence and UV detection were used for all analytes. Recoveries of the volatile PAHs, naphthalene, acenaphthylene, and acenaphthene were 80 – 90%. All other recoveries were compared with the standard LLE and they ranged from 75 – 90%. The results from the SPE method was compared with the conventional LLE method for different type of real soil samples of the Dutch monitoring program. The linear regressions between the two methods were better than 0.9 with relative standard deviations for SPE between 0.9 and 9.1%. LLE standard deviations range from 1.1 to 1.5% (Koostra *et al.*, 1995). These results indicated that SPE is a good method for sample preparation for the analysis PAHs in soil sample.

Concerning on-line sampling, the successful application of solid adsorbents for the extraction for trace organic compounds dissolved in water

creates opportunities for automation of the extraction at the sample site. This method involves passing a known volume of water directly from the water body through a suitable SPE column. This largely eliminates the problems associated with losses of analytes on the surface containers. An advantage is that the SPE samples can be stabilized by storage at -20°C until they are eluted with solvent. The main problems are associated with the sampling of suspended solids and insuring that the sample is representative.

Michor *et al.* (1996) introduced an empore disk extraction for the analysis of 23 PAHs in natural water. Experimental investigation included determination of solvent type, extraction number, preconditioning requirements, breakthrough, and the use of an in-line drying agent. The stability of PAHs stored extracted on empore disk was compared to samples left unextracted. The analyte was injected into $60\text{ m} \times 0.25\text{ mm i.d.} \times 0.25\text{ }\mu\text{m}$ thickness RTX 5 capillary column. The results indicated disks stored at -19°C for 60 days had higher recoveries than samples left in sampling bottles unextracted at 4°C . In general, less decomposition of the target analytes occurred when extracted and stored on the disks. The accuracy of this method was evaluated through the use of certified reference material analyzed as blind samples. The empore disk extraction method achieved equivalent or better detection limits, used significantly less amounts of solvent, and was faster to use than traditional LLE method. Method detection limits for the 23 PAHs ranged from 9 to 56 ng l^{-1} .

Subsequently, Urbe and Ruana (1997) reported the application of SPE to extract aqueous sample on a glass fiber matrix. Three different SPE systems were studied and compared *i.e.* (1) SPE column with a glass body and 500 mg of C_{18} filling; (2) C_{18} disk with a PTFE matrix; and (3) C_{18} disk with a glass fiber matrix. The resulting extract was analyzed by HPLC-FLD and the use of glass fiber matrix allowed the extraction time of PAHs to be shortened by between 3 and 12 times in comparison with other systems. The glass fiber

matrix could concentrate a volume sample of up to 1 l, with PAHs recoveries higher than $80 \pm 10\%$.

Wolska *et al.* (1999) also applied SPE for analysis of PAHs and PCBs in water containing suspended particulate matter (SPM). A specially design filtration vessel coupled directly on an SPE cartridge was used for their work, to provide the SPM separation and analyte isolation/concentration were carried out in a single step. Both the SPE cartridge and the suspended matter collected on the filter were extracted by solvent, and analyte recoveries were determined. A $30 \text{ m} \times 0.25 \text{ mm i.d.} \times 0.25 \text{ }\mu\text{m}$ thickness SPB-5TM GC column was used with helium as carrier gas to determine the extracts. Analyte recoveries from the filtrate range from 64 to 100% of the spiked amount for PAHs with the highest aqueous solubilities, and did not exceed 20% for those with the lowest solubilities. Total recoveries of PAHs from surface water SPM ranged from 65 to 121%. PCBs recoveries from the particulate matter reached over 10% of the spiked amount, while those from the filtrate ranged from 20 to 57%. Total PCBs recoveries ranged from 34 to 69%.

Several sorbents have been used in the SPE of PAHs, and the one which has been used most is C₁₈-bonded silica. SPE was also used to clean up sample. Barranco *et al.* (2003) determined PAHs in edible oils using SPE in the sample clean up step, followed by a separation by HPLC $250 \times 4.6 \text{ mm i.d.}$, $5 \text{ }\mu\text{m}$ reverse phase Vydac C₁₈ column and a $20 \times 3.9 \text{ mm i.d.}$, $4 \text{ }\mu\text{m}$ Waters C₁₈ guard column HPLC-FLD, with acetonitrile-water as mobile phase. The effects of variables, such as washing and elution solvents, sample solvent and drying time have been studied using C₁₈ cartridges include the recoveries and selectivity with other materials *i.e.* C₈, C₂, CH, PH, NH₂. The results showed, C₁₈ and C₈ sorbents to have the same behavior. With CH sorbent, good recoveries were obtained for the PAHs of 4 – 6 rings, but the low molecular mass ones were less retained. With more polar sorbents, *i.e.* C₂, PH, and NH₂, poor recoveries were obtained, because PAHs were not retained. The

selectivity provided by C₁₈ and C₈ sorbents was assayed with coconut oil and no significant difference. The recoveries ranged between 50 and 103% depending on molecular mass of the analytes. Sagenti and Mcnair (1998, cited by Marce and Borrull, 2000) also compared three different bonded silica sorbent *i.e.* C₁₈, cyano, and phenyl and showed that C₁₈ was the best.

In most situation the cleaning up is necessary for the contaminated sample. The most frequently used clean up procedure is simple SPE with various adsorbent phases. For sample preparation for the determination of PAHs in water, E-DIN 38407 F18 recommends clean up on a silica SPE column (Reupert and Brausen, 1994 cited by Manoli and Samara, 1999). Other used adsorbent phases are aminopropyl-, cyanopropyl-, and octadecyl-bonded silica and forisil. Classical column adsorption chromatography with alumina and silica gel has also been used as clean up procedures for water extracts. A new methodology involving highly selective isolation by an antigen – antibody, so called immunosorbent (IS) (Pichon *et al.*, 1998), has been proposed as an alternative to SPE of PAHs. The IS can be used either for recovery or as a clean up procedure. The method offers higher selectivity compared to conventional extraction and clean up.

Supercritical Fluid Chromatography (SFC) has aroused increasing interest for environmental analyses due to its high separation efficiency and the short analysis times it provides (Bernal *et al.*, 1997). A Supercritical Fluid (SF) is a substance above its critical temperature and pressure. The properties of gas-like mass transfer coefficients and liquid-like solvent characteristics make SF very attractive as extraction solvents. The process of using SF as extraction solvent is known as Supercritical Fluid Extraction (SFE) (Kebbekus and Mitra, 1998). In 1997 the studied of the chromatographic separation by Bernal *et al.* led to the use of SPE coupled to SFC, which improved detection limits. Disks of two different materials, *i.e.* C₁₈ and polystyrene-divinylbenzene (PS-DVB), were assayed in terms of variables influencing the extraction step. From the

experiment, the membranes were activated with 10-ml of methanol and 10-ml of nanopure water containing 20% isopropanol. Then, the standard solution was pre-concentrated. Disks were then dried for 10 min and after that, the retained analytes were eluted by the mobile phase. The best results were obtained by serially connecting a 150 × 4.6 mm Spherisorb ODS2 column and a 125 × 4.6 mm Envirosep-PP column. The best recovery was obtained from C₁₈ disk which was higher than 86%, while PS-DVB disk provided below 60%.

A year later Sargenti *et al.* (1998 cited by Marce and Borrull, 2000) compared four different extraction techniques *i.e.* SPE, SFE, SPE followed by SFE, and LLE for the extraction of 16 PAHs from drinking water. The results showed that recoveries were good for SPE and SPE/SFE for all compounds. Recoveries for SFE were less than SPE/SFE, and LLE had the least recovery and reproducibility.

A special device of SPE is solid-phase microextraction (SPME), which consists of a fused-silica fiber mounted in a syringe-like device. The fiber is coated by a sorbent, usually other than those used for SPE. The following sorbents, or a mixture of any two of them, can be used for SPME: polydimethylsiloxane, polyacrylate, carboxen, carbowax, and divinyl benzene. The mechanism of SPME is based on the equilibrium between analyte concentration in the aqueous phase and that is in the polymeric phase of the fiber. The SPME can be easily coupled to GC and also to HPLC with a special device. The main advantage of this technique is that it is solvent free and it requires a small volume of sample (Marce and Borrull, 2000).

SPME consists of two steps: first, the adsorption of the analyte from the aqueous matrix by dipping the SPME fiber into the matrix, and second, the desorption of the analytes from the polymeric layer into the carrier gas stream of the heated GC injector (Eisert and Levsen, 1996). Even though, the SPME provided many advantages, there are also limitations *i.e.* (1) a fiber is quite fragile; (2) in many situations difficult to select fiber coating of polarity close to

polarity of analytes; (3) in combination with GC, high mass compounds cannot be analyzed; (4) if partition coefficient is high and/or a sample is small it can be analyzed only once (Namieśnik *et al.*, 2000) (5) prediction of the amount of compounds extracted are different and no straightforward relationship has been shown between partition coefficients ($\text{Log } K_{\text{OW}}$) and characteristic of the analytes; (6) although the relationship has been established for analytes having low molecular weights, the correlation between the apparent SPME distribution coefficient (K_{SPME}) and K_{OW} values appear to fail as the molecular weights of the analytes increase (Doong and Chang, 2000).

US EPA/600/4-88/039 (US EPA, 1988) suggests the use of SPE for the recovery of PAHs from drinking water. The cartridges are proposed to be packed with silica, whose surface has been modified by chemically bonded octadecyl (C_{18}) groups, while methylene chloride is proposed as eluting solvent. Recently, the US EPA also adopted SPE as the pre-concentration technique for PAHs in water and biological sample. PAHs are separated from the sample onto a non-polar solid matrix by reverse phase mechanisms. The adsorbent phases are packaged in two basic formats: cartridges or membranes. For water analysis, membranes are preferred over cartridges, since the larger cross-sectional area and the shorter depth of extraction disks result in high flow rates and short analyses time (Hagestuen and Campiglia, 1999).

According to E-DIN38407 F18 (Manoli and Samara, 1999), HPLC-FLD is adequate for the determination of the 15 PAHs (acenaphthylene is excluded) in water sample, while US EPA method 610 suggests reverse phase HC-ODS Sil-X, 5 micron particle diameter, in a 25 cm \times 2.6 mm i.d. HPLC with UVD or FLD, or 1.8 m \times 2 mm i.d. glass, packed with 3% OV-17 on Chromosorb W-AW-DCMS (100/120 mesh) GC-FID for the determination of 16 PAHs in wastewaters. It should be noted that the gas chromatographic procedure does not adequately resolve the following four pairs of compounds: Anthracene–Phenanthrene, Benzo(a)anthracene–

Chrysene, Benzo(b)fluoranthene - Benzo(k)fluoranthene, and Dibenzo(a,h)anthracene – Indeno(1,2,3-cd)pyrene (US EPA, 1984). To solve the GC limitation in EPA method 610, method 8100 has been considered. The method provides the GC-FID conditions for detection of ppb levels of PAHs. The use of a capillary column instead of the pack column, also described in this method, may be adequately resolve these pairs PAHs (US EPA, 1986).

Table 4 Summary of analytical method for recovery, clean up, and determination of PAHs in natural waters.

Recovery	Clean up	Determination
<ul style="list-style-type: none"> • Liquid-liquid extraction (LLE) • Solid Phase extraction (SPE) • Solid Phase Microextraction (SPME) • Immunosorbents (IS) 	<ul style="list-style-type: none"> • Solid Phase extraction (SPE) • Classical column adsorption chromatography • High Performance Liquid Chromatography (HPLC) • Immunosorbents (IS) 	<ul style="list-style-type: none"> • Gas Chromatography (GC) with Flame Ionization Detector (FID) or Mass Spectrometry Detector (MSD) • High Pressure Liquid Chromatography (HPLC) with Ultraviolet Detector (UVD) or Fluorometric Detector (FLD) or Mass Spectrometry Detector (MSD) or Photodiode Array Detector (PAD) • Supercritical Fluid Chromatography (SFC) with Ultraviolet Detector (UVD) or Mass Spectrometry Detector (MSD)

Source: Manoli and Samara (1999)

1.3 Objectives

The aims of this research are

- 1.3.1 To study the use of appropriate solid phase extraction procedure as sample preparation technique for trace PAHs of group B2 in water.
- 1.3.2 To optimize Gas Chromatography - Flame Ionization Detector conditions for the determination of seven PAHs of group B2.
- 1.3.3 To use the appropriate solid phase extraction procedure and optimum Gas Chromatography - Flame Ionization Detector conditions for the qualitative and quantitative analyse of PAHs in real water sample.

Chapter 2

EXPERIMENTAL

2.1 Chemicals and materials

2.1.1 Standard chemicals (Certified solution with purity 99%, Restek, USA) ;

Benzo (a) anthracene	: 1000 $\mu\text{g ml}^{-1}$
Benzo (a) pyrene	: 1000 $\mu\text{g ml}^{-1}$
Benzo (b) fluoranthene	: 1000 $\mu\text{g ml}^{-1}$
Benzo (k) fluoranthene	: 1000 $\mu\text{g ml}^{-1}$
Chrysene	: 1000 $\mu\text{g ml}^{-1}$
Dibenzo (a, h) anthracene	: 1000 $\mu\text{g ml}^{-1}$
Indeno (1,2,3- cd) pyrene	: 1000 $\mu\text{g ml}^{-1}$
Anthracene-d ₁₀	: 1000 $\mu\text{g ml}^{-1}$

2.1.2 General solvents and chemicals

Acetone (AR grade, Carlo Erba, USA)

Dichloromethane (AR grade, Lab-scan, Thailand)

Ethyl acetate (AR grade, Analar , England)

Methanol (AR grade, Merck, USA)

2-Propanol (AR grade, Merck, USA)

Acetonitrile (AR grade, Lab-scan, Thailand)

Ultra pure water (H₂O, Synthesis in laboratory by Maxima, ELGA, England)

2.1.3 Samples

Water samples were collected from the water treatment ponds of Songklanagarind Hospital, Prince of Songkla University, Hat Yai, Songkhla.

2.2 Instruments and apparatus

2.2.1 Gas chromatography-Flame Ionization Detector (GC-FID)

- Gas Chromatograph model 6890 series equipped with Flame Ionization Detector (Agilent, USA)
- Capillary column was fused silica HP-5 30 m × 0.32 I. D. × 0.25 μm film thickness of 5% phenyl and 95% dimethylpolysiloxane (Agilent, USA).
- Computer system model VL Vectra (Hewlette Packard, USA),
- Chemstation software (Agilent, USA).
- Helium gas, high purity 99.99%, (TIG, Thailand)
- Nitrogen gas, high purity grade 99.99%,(TIG, Thailand)
- Hydrogen gas, high purity 99.99%, (TIG, Thailand)
- Air, zero grade 99.995% (TIG, Thailand)

2.2.2 Solid Phase Extraction (SPE)

- ENVITM-18 DSK 47 mm Solid Phase Extraction Vacuum Disks (Supelco, USA)
- Filter Aid 400 (3M, USA)
- Glass fiber filter 47 mm (Whatman, USA)
- Vacuum pump (Gast, USA)
- Rotary evaporator (EYELA, Japan)
- Ultrasonic bath (Elma, Germany)
- Nitrogen gas (TIG, Thailand)

2.2.3 Apparatus

- Amber vial 2 ml with polypropylene screw cap and white silica/red rubber septa (Agilent, USA)
- Amber vial 2 ml with silver aluminatesium cap (Agilent, USA)
- Clear vial 1 ml with cap (waters, USA)
- 11-mm crimper and 11-mm decrimper (Agilent, USA)
- Microlitre pipette: model P200, 50-200 μl ; and model P20, 5-20 μl (Gilson France)
- General Glassware such as Glass round bottom 50ml; volumetric flask 100 ml.

2.3 Methods

2.3.1 Preparation of PAHs standard stock solution

Experiments were optimized and validated with seven PAHs, classified by US EPA as group B2. These consisted of Benzo (a) anthracene, Chrysene, Benzo (b) fluoranthene, Benzo (k) fluoranthene, Benzo (a) pyrene, Indeno (1,2,3-cd) pyrene, and Dibenzo (a,h) anthracene. Two individual standard stock solutions, series A and B, were prepared. Series A concentration was $1000 \mu\text{g ml}^{-1}$ and series B was prepared by diluting the standard stock solution, $1000 \mu\text{g ml}^{-1}$, to the concentration of $100 \mu\text{g ml}^{-1}$ in dichloromethane. Each standard stock solution was transferred into glass bottle with the screw cap. All bottles were wrapped with aluminum foil and then stored at 4°C , to keep them from degradation by high temperature and photochemical reaction.

2.3.2 Preparation of PAHs standard working solutions

The PAHs standard working solutions used in the experiments were prepared as mixture of the seven PAHs. The standard stock solutions of series A or B were diluted with dichloromethane to obtain the desired PAHs mixture concentration over the range of 0.02 - 100.00 $\mu\text{g ml}^{-1}$.

Special sequential preparation of working standard solution used for optimizing column programmed temperature are as followed:

- I. Benzo (a) anthracene standard stock solution from series B was diluted with dichloromethane to obtained the final concentration 10 $\mu\text{g ml}^{-1}$.
- II. Benzo (a) anthracene and Chrysene standard stock solution from series B were mixed then diluted with dichloromethane to the final concentration of 10 $\mu\text{g ml}^{-1}$.
- III. Benzo (a) anthracene, Chrysene, and Benzo (b) fluoranthene standard stock solution from series B were mixed and diluted with dichloromethane to the final concentration of 10 $\mu\text{g ml}^{-1}$.
- IV. Benzo (a) anthracene, Chrysene, Benzo (b) fluoranthene and Benzo (k) fluoranthene standard stock solution from series B were mixed and diluted with dichloromethane to the final concentration of 10 $\mu\text{g ml}^{-1}$.
- V. Benzo (a) anthracene, Chrysene, Benzo (b) fluoranthene, Benzo (k) fluoranthene, and Benzo (a) pyrene standard stock solution from series B were mixed and diluted with dichloromethane to the final concentration of 10 $\mu\text{g ml}^{-1}$.
- VI. Benzo (a) anthracene, Chrysene, Benzo (b) fluoranthene, Benzo (k) fluoranthene, Benzo (a) pyrene, and Indeno (1,2,3-cd) pyrene standard stock solution from series B were mixed and diluted with dichloromethane to the final concentration of 10 $\mu\text{g ml}^{-1}$.
- VII. Benzo (a) anthracene, Chrysene, Benzo (b) fluoranthene, Benzo (k) fluoranthene, Benzo (a) pyrene, Indeno (1,2,3-cd) pyrene, and Dibenzo (a,h)

anthracene standard stock solution from series B were mixed and diluted with dichloromethane to the final concentration of $10 \mu\text{g ml}^{-1}$.

2.3.3 GC-FID conditions for PAHs analysis

The temperature programming was started with an initial temperature of 150°C , then ramped the temperature at $15^{\circ}\text{C}/\text{min}$ to 300°C and hold for 5 min. The injector and detector temperatures set points were held at 250°C and 300°C , respectively. These parameters were described as default conditions as cited by the Certificate of Analysis from Materials Safety Data Sheet (Restek, USA). Nitrogen, hydrogen and air were used as make up, fuel and oxidant gas. These gasses were initially maintained at the flow rate of 30, 30, and 300 ml/min, respectively. These recommended set points were suggested in the Operating Manual of GC-FID model HP 6890 series.

1- μl aliquot of $10 \mu\text{g ml}^{-1}$, PAHs mixture standard working solution was injected into the GC system. The qualitative and quantitative data would be compared by two modes of injection, split and splitless modes, were compared.

First injection mode: Optimization of split injection mode

2.3.3.1 Optimization of carrier gas flow rate

A 1- μl of $10 \mu\text{g ml}^{-1}$, PAHs working standard solution (2.3.2 VII) was injected into the GC system. In this study Helium gas (He) was used as carrier gas. The carrier gas flow rate was varied *i.e.* 1.0, 1.5, 2.0, 2.5, 3.0, 3.5, 4.0, 4.5, and 5.0 ml/min. The retention times and peak heights of the seven PAHs compounds were obtained from the chromatogram. The van Deemter graph was then plotted to obtain the optimum carrier gas flow rate, *i.e.* the flow rate that showed the lowest HETP.

2.3.3.2 Optimization of column temperature programming

The seven PAHs studied in this work consisted of three single compounds and two pairs of isomer compounds. According to EPA 610 (US EPA, 1984) normal gas chromatographic procedures could not adequately resolved the following group of PAHs, *i.e.*, Benzo (a) anthracene and Chrysene; Benzo (b) fluoranthene and Benzo (k) fluoranthene; and Dibenzo (a, h) anthracene and Indeno (1,2,3-cd) pyrene. The optimizations were carried out step by step to obtain a high resolution of the seven compounds. To optimize the column temperature programming parameter, 1- μ l of each PAHs standard working solution from 2.3.2 I – 2.3.2 VII was injected into the GC system by varying one parameter at a time, as shown in Table 5. The response (peak area) and the resolution obtained from the chromatograms were then compared. The selected optimum of each parameter was the one that provided the highest response and the best resolution. The values found were used in the optimization of the next parameters.

Table 5 Optimization of column temperature programming.

Step	Parameters	Optimized value
I column temperature programming of B(a)an	<ul style="list-style-type: none"> • isothermal • initial temperature • hold time • ramp rate 	100, 150, 200 and 250°C 80, 90, 100 and 110°C 0, 1, 2 and 3 min 15, 20, 25 and 30 °C/min
II column temperature programming of B(a)an+Chry	<ul style="list-style-type: none"> • initial temperature • hold time • ramp rate 	80, 90, 100 and 110°C 0, 1, 2 and 3 min 15, 20, 25 and 30 °C/min

Table 5 Optimization of column temperature programming (continue)

Step	Parameters	Optimized value
<i>III</i> column temperature programming of B(a)an+Chry+B(b)fl	<ul style="list-style-type: none"> • initial temperature • hold time • ramp rate 	90, 100, 110and 120°C 0, 1, 2 and 3 min 15, 20 and 25°C/min
<i>IV</i> column temperature programming of B(a)an+Chry+B(b)fl+B(k)fl	<ul style="list-style-type: none"> • initial temperature • hold time • ramp rate 	100, 110, 120and 130°C 0, 1, 2 and 3 min 5, 10, 15 and 20°C/min
<i>V</i> column temperature programming of B(a)an+Chry+B(b)fl+B(k)fl+B(a)p	<ul style="list-style-type: none"> • initial temperature • hold time • ramp rate 	120, 130, 140and 150°C 0, 1, 2 and 3 min 5, 10 and 15°C/min
<i>VI</i> column temperature programming of B(a)an+Chry+B(b)fl+B(k)fl+B(a)p+In(123-cd)p	<ul style="list-style-type: none"> • initial temperature • hold time • ramp rate 	120, 130, 140and 150°C 0, 1, 2 and 3 min 3, 5, 7 and 10°C/min
<i>VII</i> column temperature programming of B(a)an+Chry+B(b)fl+B(k)fl+B(a)p+In(123-cd)p+D(a,h)an	<ul style="list-style-type: none"> • initial temperature • hold time • ramp rate 	120, 130, 140and 150°C 0, 1, 2 and 3 min 3, 5, 7 and 10°C/min

For the rest of optimization procedures, when not stated otherwise, the optimum condition of the parameter was done by comparing the chromatograms from several values of the optimized parameters. The selected

optimum was the one which provided the highest response and the best resolution.

2.3.3.3 Optimization of injector temperature

The GC conditions were set following the results from 2.3.3.1 – 2.3.3.2. The injector temperature was varied at 240, 250, 260, and 270°C.

2.3.3.4 Optimization of detector temperature

The detector temperature was varied *i.e.* 270, 280, 290 and 300°C. Because of the maximum temperature the column can take is 325°C, the temperature varying was kept less than 325°C.

2.3.3.5 Optimization of flow rate of gaseous used in FID

A 1- μ l of PAHs standard working solution 2.3.2 VII was injected into GC system which operated with the optimum conditions obtained from 2.3.3.1-2.3.3.4. One parameter was varied at a time, while the others were fixed as described in 2.3.3. The gaseous flow rates were varied as shown in Table 6.

Table 6 Optimization of flow rate of gaseous used in FID

Parameters	Gas	Optimized value
Make up gas flow rate	N ₂	10, 20 and 30 min
fuel gas flow rate	H ₂	20, 30, 40 and 50 min
oxidant gas flow rate	Air	200, 300, 400 and 500 min

2.3.3.6 Limit of Detection

The PAHs standard working solutions were prepared at concentration in the range of 0.35 – 0.75 $\mu\text{g ml}^{-1}$. 1- μl aliquot of each concentration was injected into the GC system which operated at optimum conditions obtained from experiments 2.3.3.1-2.3.3.7.

Limit of detection was considered as the lowest concentration that the detector could provide a signal on the chromatogram, and the signal to noise ratio (S/N) was calculated from the chromatogram, S/N was more than 3.

2.3.3.7 Linear dynamic range

The PAHs standard working solutions were prepared at concentration between 0.50 to 75.00 $\mu\text{g ml}^{-1}$. A 1- μl aliquot of each concentration was injected into GC system which operated at the optimum conditions were achieved from experiments 2.3.3.1-2.3.3.7.

Linearity of PAHs analysis was determined from the calibration curve by plotting the peak areas versus PAHs concentrations. The linearity was reflected by using the linear regression.

Second injection mode: Optimization of splitless injection mode.

2.3.3.8 Optimization of carrier gas flow rate

The achieved optimum conditions from 2.3.3.1-2.3.3.7 were set. 1- μl of 10 $\mu\text{g ml}^{-1}$, PAHs working standard solution 2.3.2 VII was injected to GC system. The carrier gas flow rate was varied at 1.0, 1.5, 2.0, 2.5, 3.0, 3.5, 4.0, 4.5, and 5.0 ml/min. The retention time and peak height of the seven PAHs were obtained from chromatogram, The van Deemter graph was

then plotted to obtain the optimum carrier gas flow rate at, that is the flow rate that showed the lowest HETP.

2.3.3.9 Optimization of column temperature programming

In the splitless injection mode when operating at the optimum column temperature programming for the split mode the chromatogram gave overlapping peaks. Therefore, the column temperature programming was optimized by using splitless mode to obtain the appropriate conditions for separation of PAHs. In starting, initial temperature was set at 130°C then ramped immediately with a ramp rate of 20°C/min to 200°C. Then increased the temperature, 200°C, with a rate of 10°C/min to 300°C, held at that temperature for 5 min. To optimize the column temperature programming parameter for splitless mode injection, 1- μ l of each PAHs standard working solution (2.3.2 VII) was injected into the GC system by varying one parameter at a time, as shown in Table 7. The response (peak area) and the resolution obtained from the chromatograms were then compared. The selected optimum of each parameter was the one that provided the highest response and the best resolution.

Table 7 Optimization of column programming temperature in splitless mode

Step	Parameters	Optimized value
<i>I</i>	initial temperature	120, 130, 140 and 150°C
<i>II</i>	first hold time	0, 1, 2 and 3 min
<i>III</i>	first stage of ramp rate	10, 15, 20, and 25°C/min
<i>IV</i>	second stage of temperature	200, 210, 220 and 230°C
<i>V</i>	second hold time	0, 1, 2 and 3 min
<i>VI</i>	second stage of ramp rate	2, 3, 5, and 10°C/min
<i>VII</i>	final temperature	270, 280, 290 and 300°C

2.3.3.10 Optimization of injector temperature

The optimum carrier gas flow rate was set as found in 2.3.3.8. The column temperature programming by using splitless injection mode were set as found in 2.3.3.9, that is, initial temperature 130°C, then ramped temperature with ramp rate 15°C/min to 220°C and held this temperature for 1 minute, then ramped temperature at 3°C/min to final temperature 300°C. The injector temperature varied as 250, 260, 270, 280 and 290°C.

2.3.3.11 Optimization of detector temperature

Other parameters were set at the optimum conditions found earlier. The detector temperature was varied at 270, 280, 290, and 300°C.

2.3.3.12 Limit of Detection

The PAHs standard working solutions were prepared at concentration in the range of 0.025–0.750 $\mu\text{g ml}^{-1}$. 1- μl aliquot of each concentration was injected into the GC system which operated at optimum conditions obtained from experiments 2.3.3.5 and 2.3.3.8-2.3.3.11.

Limit of detection was considered as the lowest concentration that the detector could provide a signal on the chromatogram, and the signal to noise ratio (S/N) was calculated from the chromatogram, S/N was more than 3.

2.3.3.13 Linear dynamic range

The PAHs standard working solutions were prepared at concentration between 0.25 to 80.00 $\mu\text{g ml}^{-1}$. A 1- μl aliquot of each concentration was injected into GC system which operated at the optimum conditions were achieved from experiments 2.3.3.5 and 2.3.3.8-2.3.3.11.

Linearity of PAHs analysis was determined from the calibration curve by plotting the peak areas versus PAHs concentrations. The linearity was reflected by using the linear regression.

2.3.3.14 Response Factor (RF)

The mixed PAHs standard working solution was prepared at five concentrations, 0.50, 0.75, 1.00, 1.25 and 1.50 $\mu\text{g ml}^{-1}$. A 1- μl aliquot of each concentration was injected into GC system run with the optimum conditions were achieved from experiment.

The response factor was the ratio between the integrated peak response of each analyte at various concentration and the integrated peak response of B(a)p. That is B(a)p was assigned with a response factor of 1.

2.3.3.15 Internal standardization plot method

The mixed standard working solution was prepared at five concentrations, 0.50, 0.75, 1.00, 0.25, and 1.50 $\mu\text{g ml}^{-1}$. Anthracene_{d10} 1.00 $\mu\text{g ml}^{-1}$ was added as internal standard in each working solution. A 1- μl aliquot of each concentration was injected into the GC system which operated at optimum conditions obtained from experiments 2.3.3.5 and 2.3.3.8-2.3.3.11.

Quantitative analysis of PAHs was determined by plotting the relationship between concentrations of the seven PAHs and the ratio of analyte to internal standard peaks.

2.3.4 Sample preparation by Solid Phase Extraction

A blank was prepared from ultra pure water, the same water being used to prepare the water sample. A 100-ml of blank was placed in a 100-ml volumetric flask. A 300- μl of working standard solution at concentration $5 \mu\text{g ml}^{-1}$ was spiked into the blank. It was stirred and mixed well before being stored in the dark at room temperature overnight. The concentration of PAHs in the blank solution 100- ml was equal to 15 ng ml^{-1} . 2-propanol was then added to the spiked water before loading to the C_{18} Empore disk, the amount of added 2-propanol in the blank was as equal to that in the sample.

Figure 1 shows the standard filter SPE apparatus for sample preparation and preconcentration of PAHs in water.

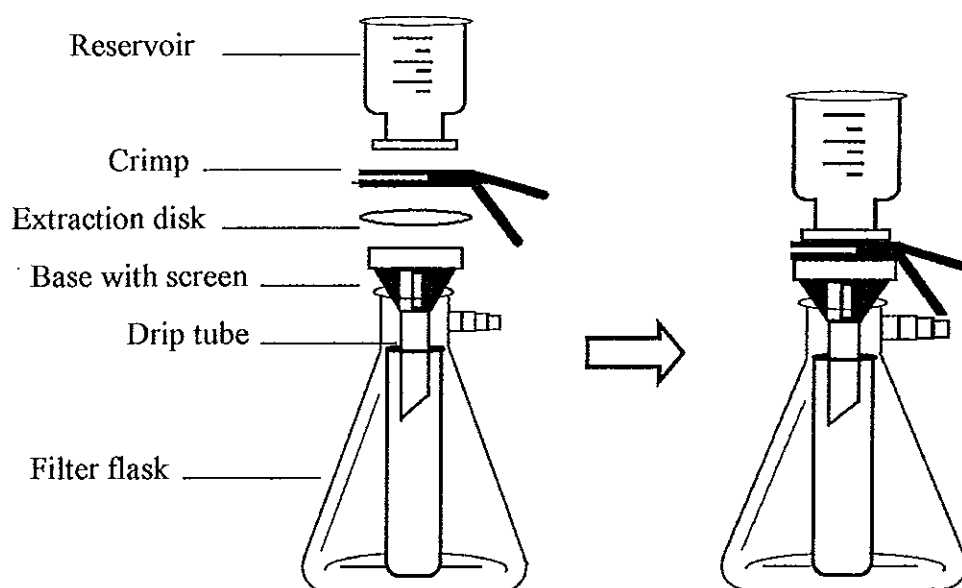


Figure 1 Solid phase extraction apparatus

SPE procedures on ENVI-18 DSK disks consisted of disk cleaning, disk condition, sample extraction, disk drying, and sample elution respectively.

The extraction disk was cleaned by rinsing with 10.0-ml dichloromethane followed by 5.0-ml ethyl acetate down the sides of the glass

reservoir. The solvent was pulled through the disk under vacuum. The disk was allowed to soak with the solvent for one minute by turning off the vacuum. The remaining solvent was pumped through the disk till the disk was dried.

Typical conditioning involved wetting the disk with organic solvent, followed by conditioning solvent matching with the sample matrix. The conditioning solvent should sufficiently wet the hydrophobic bonded phase, yet be water miscible. Therefore, 10.0-ml methanol was added to the extraction disk where vacuum was applied. When a drop of methanol passed through the disk, turned off the vacuum and soaked the disk with solvent for 1 minute. Then applied the vacuum again to draw the remaining solvent through the disk until only a thin layer of solvent covered the disk, that is, the disk surface had no contact with air. A 10.0-ml water sample was then poured onto the disk, while the vacuum was applying and left a small amount of water above the disk surface. The disk surface must be prevented from air exposure until the entire sample passed through the disk.

After the disk was cleaned and preconditioned, 100-ml of water sample was pour into the apparatus reservoir, adding it directly to the left over water film on the disk after the conditioning step. The vacuum allowed the sample to automatically feed onto the disk. Adjusted the vacuum to approximately 10 in Hg, to achieve a flow rate of 100 ml/min for a clean water sample (Instruction for using ENVITM-18 DSK 47 mm SPE Disks, catalog No. 57171, Supelco, USA). Most of the water must be removed from the disk prior to eluting the analyte. This was done by maintaining the vacuum for at least 3 minutes. Once the disk was dried, the filtration support and the reservoir was removed from the vacuum flask without disturbing the disk. Empty the processed water from the flask, then inserted a 60-ml sample collection tube into the receiving flask, and reassemble the apparatus. The drip tip of the filtration apparatus was sealed below the neck of the collection tube to prevent

the analyte loss due to splattering when vacuum was applied. PAHs were initially eluted from the disk with 5.0-ml acetone where the disk was allowed to soak in this solvent for 20. The sample flask was added with 10.0-ml acetonitrile, and gently twirled it to rinse all of the inside surface. Allow the bottle to stand for 1 – 2 minutes. Transferred the acetonitrile to the disk. Drew the solvent through the disk (5 in Hg). Both acetone and acetonitrile were used to draw the remaining water in the disk. Finally, two portions of 5.0-ml dichloromethane were poured to the disk as the last elution solvent for PAHs extraction from C₁₈ Empore disk. The solvent extract was transferred to a 50-ml round bottom flask and dried by evaporating rotator until dryness. A 1.5-ml of dichloromethane was then added to the residue PAHs and transferred to a 2-ml amber vial (or clear vial with foil-wrapped), then the solvent was evaporate again under gentle stream of nitrogen gas till dry. A 0.3-ml dichloromethane was then added to vial and analyzed by GC-FID at the optimum conditions.

The absolute recovery of PAHs, was obtained by optimizing the C₁₈ Empore disk extraction conditions.

2.3.4.1 Elution solvent

The elution solvent should be strong with respected to the analyte for high selectivity and maximum efficiency. The elution solvents for PAHs extraction were studied to achieve the appropriate solvent. The procedures of sample preparation by C₁₈ Empore disk SPE were followed as described in 2.3.4. Four elution solvents were tested, dichloromethane, ethyl acetate, methanol, and dichloromethane-ethyl acetate 1:1 v/v. Two portions of 5.0-ml of each solvent was used as the last eluent (the solvent was added when acetonitrile was drawn through the disk). Each experiment was done in five replicates. The resulting extract was analyzed by GC-FID and calculated to

obtain the percentage of recovery. The solvent that provided the best recovery was then selected.

2.3.4.2 Volume of eluting solvent

The procedures for sample preparation by C₁₈ Empore disk SPE followed those in 2.3.4, and using the last eluent found in 2.3.4.1. In order to minimize solvent used and at the same time maintained the good recovery, the volume of the last eluting solvent, ethyl acetate, was studied using 2 × 5.0, 2 × 4.0, 2 × 3.0, and 2 × 2.0 ml. Each experiment was done in five replicates. The extractant was analyzed by GC-FID at optimum conditions and calculated the percentage of recovery. The least solvent volume that provided the best recovery was then selected.

2.3.4.3 Drying time

Since the elution solvent is water-immiscible it was important to remove as much water as possible from the disk prior to the elution of PAHs. The drying time was varied at 3, 5, 7, and 10 minutes and each experiment was done in five replicates. The extractant was analyzed by GC-FID percentage of recovery was calculated. The least drying time that provided the best recovery was selected.

2.3.4.4 Percentage of modifier

An organic solvent is usually added to the sample as modifier to increase the solubility of PAHs. The concentration of the organic solvent is a critical parameter because if it is too low it may not be enough to solubilize the high molecular weight PAHs. Marce and Borrull (2000) found that 2-propanol was a compatible organic modifier and this was used as the organic modifier in this work. The percentage of modifier was tested at 0, 0.5, and 1.0%. The resulting extract was analyzed by GC-FID and calculated to

give percentage recovery. The least percentage of modifier that provided the best recovery was selected.

2.3.5 Qualitative and quantitative analysis of PAHs in water

2.3.5.1 Sampling sites

Three water treatment ponds of Songklanagarind Hospital, Prince of Songkla University, Hat Yai, Songkhla were selected as the sampling sites

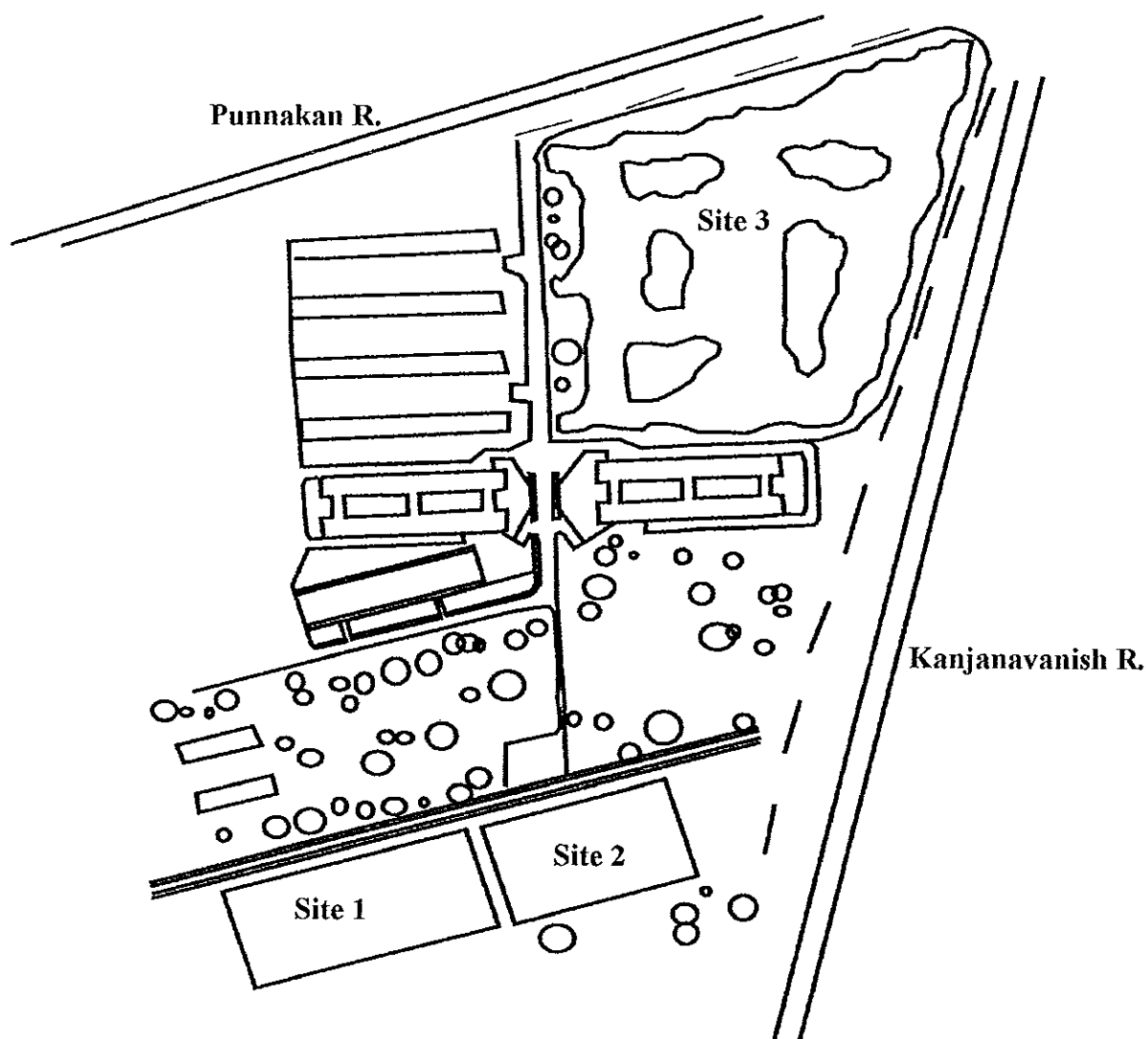


Figure 2 The location of the three sampling sites

Site 1: the first water treatment pond which received the wastewater from the hospital, three faculties, and the residence that located in the south side of Prince of Songkla University. Oxygen was added to water by two rower machines.

Site 2: the second water treatment pond. This is connected to the first water treatment pond and received the water by overflow through connection pipe. In this pond, water was treated by sunlight.

Site 3: Sri trang pond. After leaving the second water treatment pond, chlorine was added to the water and it was transported through underground pipe to this pond. Water was treated by natural treatment. The pond has a complete aquatic ecosystem and water from this pond was flow to the municipal effluent.

2.3.5.2 Sample collection

Water sample was pumped through a lab built filtration unit using a small fish tank pump. This was to eliminate the particulate matter before extraction. Water sample was then collected in a 2.5 l clean amber glass container.

PAHs are known to be light sensitive; therefore, all samples were stored at 4°C in amber or foil-wrapped bottles in order to minimize photolytic decomposition. All samples must be extracted within seven days after collection and completely analyzed within forty days of extraction as set by EPA method-610 (US EPA, 1984).

2.3.5.3 Qualitative analysis

Qualitative analysis was carried out by using the retention data from the chromatogram of the PAHs standard.

2.3.5.4 Quantitative analysis

Quantitative analysis was carried out by considering the response from GC-FID, *i.e.*, peak area of the chromatogram which is proportional to the amount of PAHs, by taking the response factor into consideration. The analytical standardization techniques applied to this work were "Internal standardization plot method" (see 2.3.3.16) and "Standard addition method". In this latter method, the sample was analyzed, then a measured portion of standard was added to the sample, and the determination was repeated. The standard was added as a small quantity of a fairly concentrated solution, so that the matrix was not significantly diluted. Four concentrations were added to extractant as shown in Table 5. The resulting solution was injected to GC-FID at optimum conditions. The results were plotted, and the response from the chromatogram per unit of component was determined from the slope of the line. The concentration of PAHs in the original sample can then be determined.

Table 8 Sequential concentrations of 7 PAHs mixture for standard addition method

PAHs	Concentration (ng ml ⁻¹)			
	1 st concentration	2 nd concentration	3 rd concentration	4 th concentration
B(a)an	50	70	90	110
Chry	30	50	70	90
B(b)fl	50	70	90	110
B(k)fl	100	120	140	160
B(a)p	100	120	140	160
In(123-cd)p	250	270	290	310
D(a,h)an	500	520	540	560

Chapter 3

RESULTS AND DISCUSSION

Trace analysis of Polycyclic Aromatic Hydrocarbon in water sample was carried out using a Gas-liquid Chromatography (GLC) technique. In this thesis, a 30 m × 0.32 mm i.d. × 0.25 μm film thickness fused silica HP 5 capillary column was used. The separation process of analytes was done by the HP 5 stationary phase, when analytes were eluted from the column, they were detected by Flame Ionization Detector. The HP 5 capillary column is a processed commercial stationary phase from Hewlett Packard, USA. Chemical composition of HP 5 consists of 5% diphenyl and 95% dimethyl siloxane. HP 5 is a non-polar phase, therefore it is a suitable column to separate PAHs, which are non-polar compounds. The same stationary phase (5% diphenyl and 95% dimethyl siloxane), HP 5 or other names was used by Singh *et al.*, (1998), McGowin *et al.*, (2001), Wolska *et al.*, (1999) used SPB-5 (Supelco, Bellefonte, USA), Michor *et al.*, (1996) applied RTX 5 (Restek, USA), Li and Lee, (2001) DB-5 (J & W, USA) and Wong and Wang, (2001) applied PTE-5 QTM (Supelco, USA). The optimum chromatographic conditions were optimized as follows.

3.1 GC-FID conditions for PAHs analysis

First injection mode: Optimization of split injection mode

3.1.1 optimization of carrier gas flow rate, helium gas

The carrier gas flow rate was optimized (2.3.3.1) by considering the relationship between the height equivalent to a theoretical plate (HETP) and the carrier gas flow rate. Theoretically HETP can be calculated by the van Deemter equation.

$$HETP = A + B/u + (C_G + C_L)u \quad (1)$$

Where A is the eddy diffusion term, the represent the band broadening that occurs because of a solute in a gas or liquid stream has a natural and unavoidable tendency to diffuse both forward and backward in the stream of analytes in packed columns. The only factor that can change this is the viscosity of the mobile phase, which is not unusually very easy to change. A faster flow, gives the peak less time to diffuse

B/u describes the longitudinal, diffusion term, represents the diffusion of the analyte in the mobile phase. This term becomes smaller as the velocity increases, because less time is available for the solute to diffuse.

$(C_G + C_L)u$ is the resistance to mass transfer rate term, C_G refers to mass transfer of the analyte in gas phase and C_L related mass transfer of the analyte in liquid phase. Both of these terms increase with flow, because the solute is less able to reach equilibrium between the two phases as the flow becomes faster. Figure 3 shows the change in HETP versus average linear velocity of carrier gas.

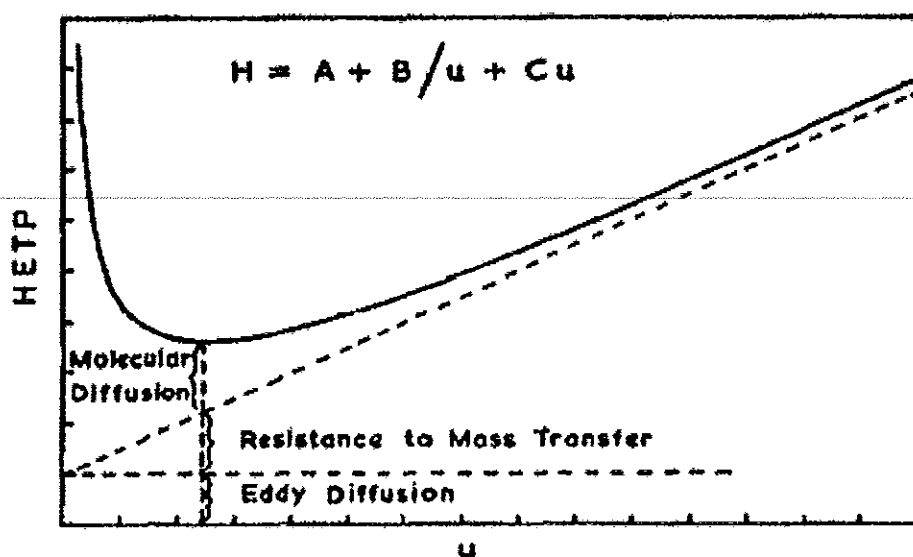


Figure 3 The van Deemter plot

In this research, a 30 m wall-coated open tubular (WCOT) column (0.32 mm i.d.) was applied. In this column a liquid phase is coated on fused silica wall with no packing material, therefore, the A term is nonexistent. The resistance to mass transfer term C has the greatest effects on band broadening, and its effect in capillary columns is controlled by the mass transfer in the gas phase. Equation (1) takes a different form for capillary columns, and this is known as the Golay equation (Grob, 1985) where

$$HETP = B/u + (C_G + C_L)u \quad (2)$$

The above equation showed that $HETP$ is proportional to the flow rate of carrier gas (u). It is also known that an optimum carrier gas flow rate will give an optimum column resolution which give the narrowest $HETP$ (Grob, 1985).

In practice it is difficult to know the term B , C_G and C_L . Since $HETP$ is related to the effective number of plate " N " and the length of the column. To indicate column efficiency the $HETP$ can be determined according to the equation

$$HETP = L/N \quad (3)$$

where L is the length of the column in centimeters and N is the number of theoretical plates. N can be calculated from the equation

$$N = 16 (t_R / W_b)^2 \quad (4)$$

or

$$N = 5.54 (t_R / W_{1/2})^2 \quad (5)$$

In this research, a capillary column was employed, and sharp peaks were obtained. Therefore it is difficult to determine the base peak width. Thus, the plate number N can be calculated directly from the value obtained from a chromatogram as shown in Figure 4 by the relationship

$$N = 2\pi(t_R h / A)^2 \quad (6)$$

where t_R is the retention time, h is integral peak height and A is integral peak area.

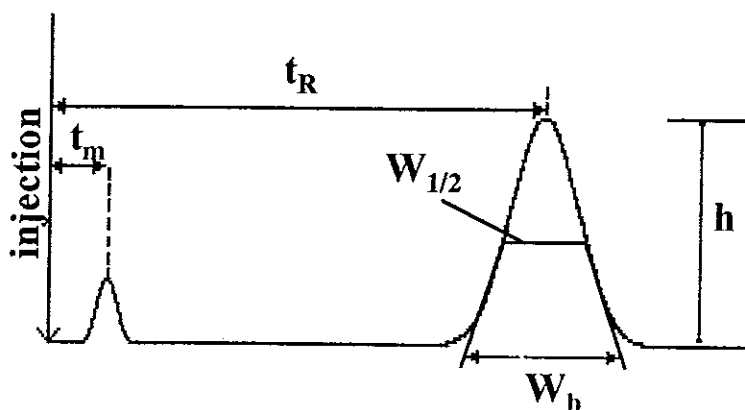


Figure 4 Measurements used in calculating total theoretical plates

N was calculated using equation (4), and substituted in equation (3), with a known L term, to obtain $HETP$. The $HETP$ and the carrier flow rates were plotted as in the van Deemter graph (Table 9 and Figure 5) which

indicated the narrowest *HETP* at the carrier gas flow rate of 1.5 ml/min for all seven PAHs.

Table 9 The Height Equivalent to a Theoretical Plate (*HETP*) of $10 \mu\text{g ml}^{-1}$, $1\text{-}\mu\text{l}$ seven PAHs mixture at various flow rate

Flow rate (ml/min)	<i>HETP</i> (cm)*						
	B(a)an	Chry	B(b)fl	B(k)fl	B(a)p	In(123-cd)p	D(a,h)an
1.5	0.82	0.86	0.60	0.65	0.57	0.44	0.43
2.0	0.86	0.87	0.66	0.64	0.59	0.48	0.52
2.5	0.99	0.95	0.72	0.71	0.65	0.54	0.52
3.0	1.10	1.06	0.79	0.78	0.73	0.58	0.57
3.5	1.26	1.23	0.94	0.91	0.85	0.66	0.66
4.0	1.41	1.39	1.04	1.03	0.95	0.74	0.76
4.5	1.63	1.58	1.15	1.11	1.03	0.82	0.82
5.0	1.80	1.72	1.25	1.30	1.15	0.92	0.91

* 5 replication, RSD < 4%

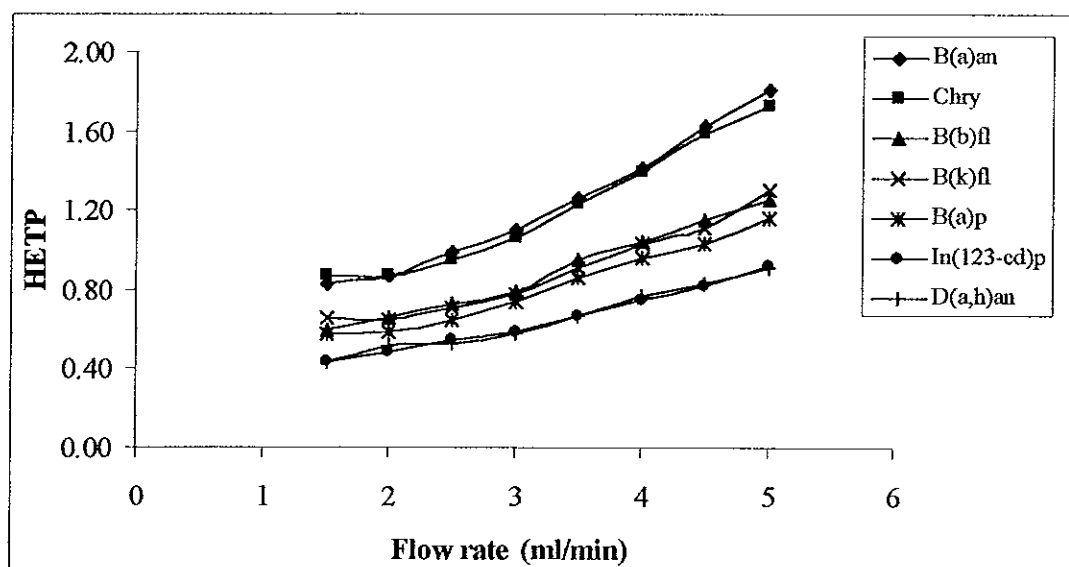


Figure 5 The van Deemter plot of the seven PAHs

3.1.2 Optimization of column temperature programming

In gas chromatography, besides the stationary phase, column temperature is another important parameter to give a good peak resolution. Initially only isothermal temperature was optimized, but it gave no response as shown in Table 10. This is probably because B(a)an has a high boiling point (435°C) and the isothermal temperature was not sufficient to elute the analyte from the GC column. Therefore, the column temperature program was optimized (2.3. 3.2).

Table 10 The response of B(a)an on isothermal column temperature

Temperature (°C)	Response (pAs)*
100	N.D
150	N.D
200	N.D
250	N.D

* 3 replication

Initially, the column temperature programming was operated as the initial temperature 150°C was ramped immediately with ramp rate 15°C/min to 300°C, hold the temperature for 5 min according to Certificate of Analysis from Materials Safety Data Sheet (Restek, USA). However we would like to optimize this system to give the best response. Therefore, optimization steps were carried out as followed. In step I, the results of initial temperature were shown in Table 11 and Figure 6 which indicated that the analysis time decreased when the temperature increased. The response of FID showed that 90°C provided the highest response, thus the optimum initial temperature was 90°C. Different holding time of this initial temperature were tested and the response (Table 12 and Figure 7) were approximately the same, differed less

than 10%. Therefore, the initial temperature was not hold, but was immediately ramped to 300°C. Table 13 and Figure 8 show the results of the ramp rate. At 30°C/min the peak of B(a)an could not be observed. This was because the operating time was too short to elute B(a)an. From the FID responses (Table 13 and Figure 8) the ramp rate at 20°C/min provided the highest response. Thus, the optimum ramp rate of 20°C/min was selected.

Table 11 The effect of initial temperature on the response and analysis time of 10 µg ml⁻¹, 1-µl PAHs standard working solution

Temperature (°C)	Response (pAs)*	Analysis time (min)*
80	25.42	19.67
90	30.31	19.00
100	27.14	18.33
110	26.84	17.67

* 5 replication, RSD < 4%

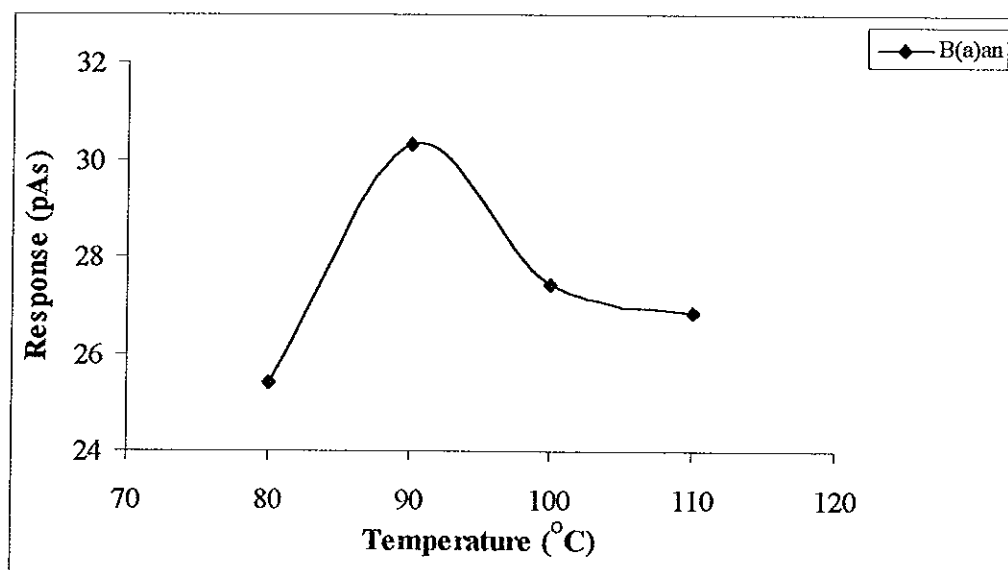


Figure 6 The responses of 10 µg ml⁻¹, 1-µl PAHs standard working solution at different initial temperature

Table 12 The effect of holding time on the response of $10 \mu\text{g ml}^{-1}$, $1\text{-}\mu\text{l}$ standard working solution

Time (min)	Response (pAs)*	Analysis time (min)*
0	30.31	19.00
1	30.35	20.00
2	30.21	21.00
3	30.35	22.00

* 5 replication, RSD < 4%

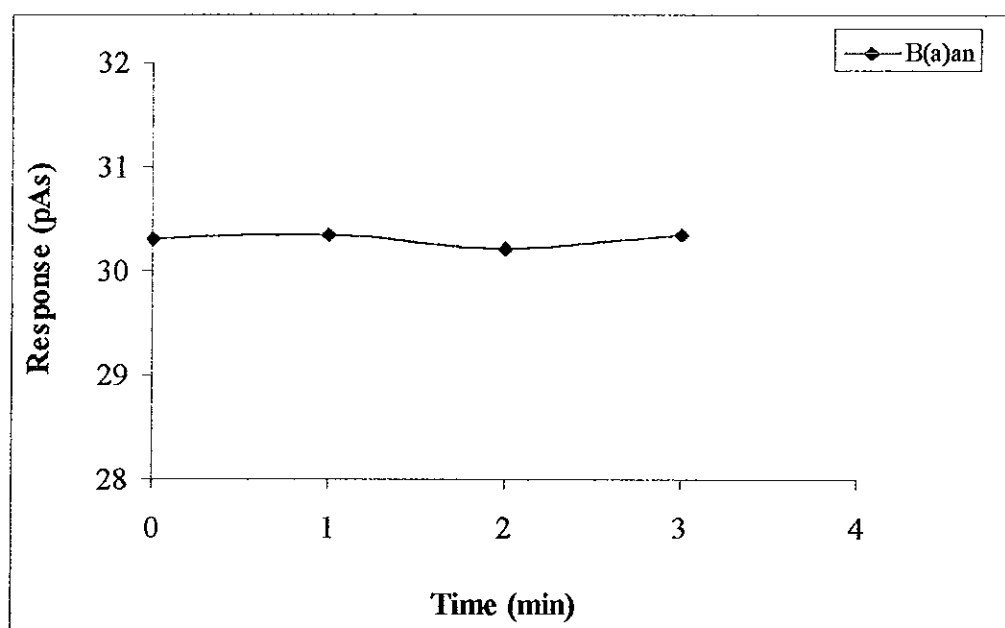


Figure 7 The responses of $10 \mu\text{g ml}^{-1}$, $1\text{-}\mu\text{l}$ PAHs standard working solution at different hold time

Table 13 The effect of ramp rate on the response and the analysis time of $10 \mu\text{g ml}^{-1}$, $1\text{-}\mu\text{l}$ standard working solution

Ramp rate ($^{\circ}\text{C}/\text{min}$)	Response (pAs)*	Analysis time (min)*
15	28.31	14.00
20	30.57	10.50
25	20.89	9.40
30	N.D	8.67

* 5 replication, RSD < 4%

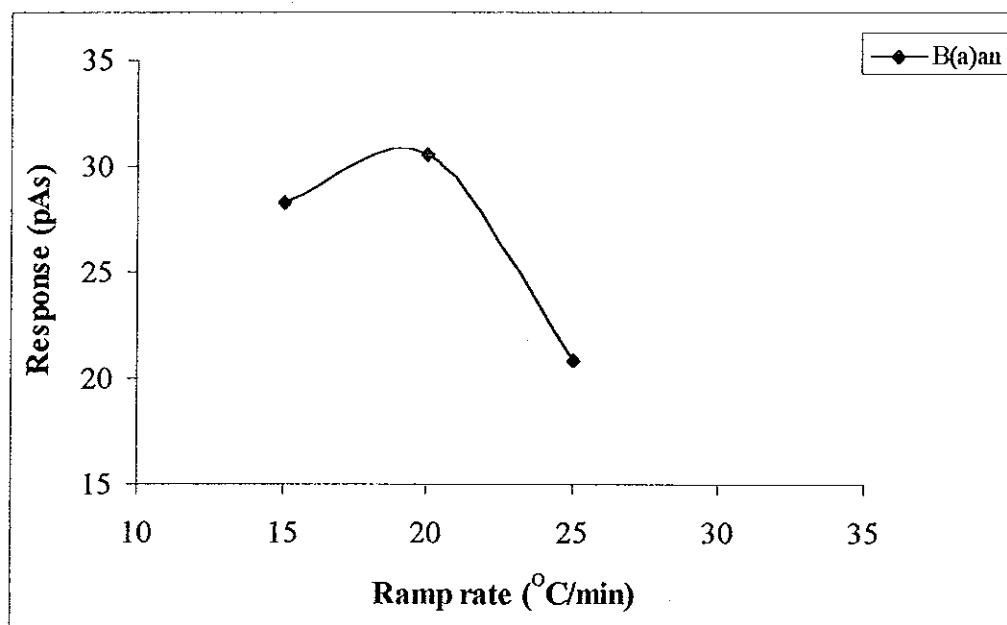


Figure 8 The responses of $10 \mu\text{g ml}^{-1}$, $1\text{-}\mu\text{l}$ PAHs standard working solution at different ramp rate

In step II the column programming temperature was to separate B(a)an from Chry, and the standard working solution 2.3.2 II was used. The results of the initial temperature are shown in Table 14 and Figure 9. The responses at 90 and 100°C were not much difference, therefore, to minimize the analysis time 100°C was chosen. The effect of the holding time on the response is shown in Table 15 and Figure 10. The responses are closed to each other with differences of less than 10%. Therefore, the initial temperature was not hold.

The temperature was ramped to the final temperature at 300°C with various ramp rate (table 16 and Figure 11). Similar to step I the ramp rate 30°C/min could not elute B(a)an and Chry. The ramp rate at 20°C/min provided the highest and this was selected as the optimum ramp rate for the separation for B(a)an and Chry mixture.

Table 14 The effect of initial temperature on the response and analysis time of $10 \mu\text{g ml}^{-1}$, $1\text{-}\mu\text{l}$ standard working solution

Temperature (°C)	Response (pAs)*		Analysis time (min)*
	B(a)an	Chry	
80	25.39	24.42	19.67
90	31.24	32.68	19.00
100	31.02	33.00	18.00
110	29.68	30.90	17.67

* 5 replication, RSD < 4%

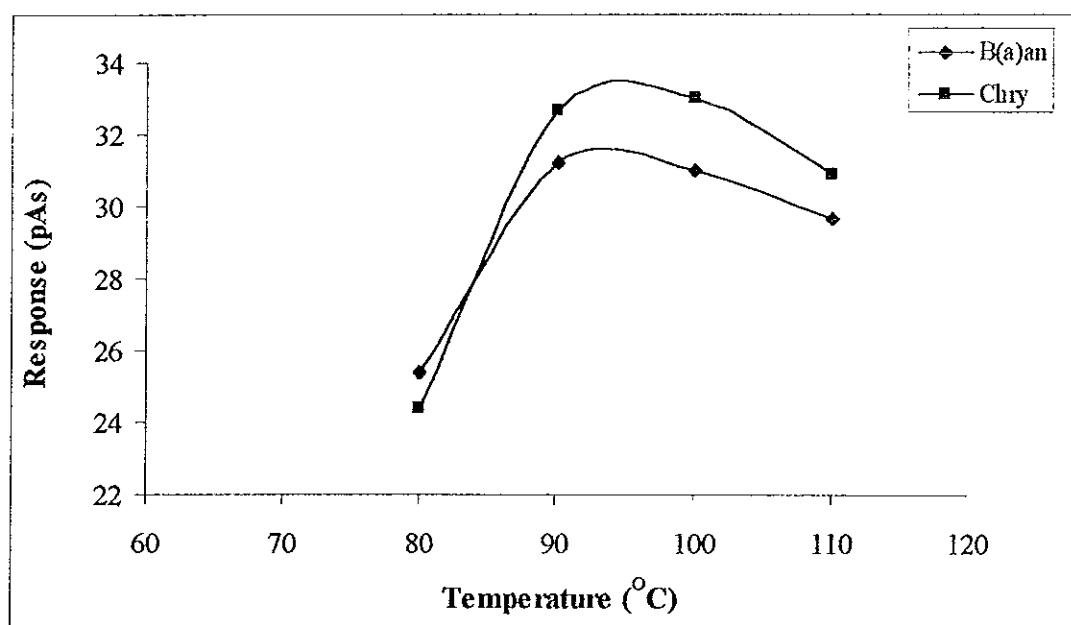


Figure 9 The responses of $10 \mu\text{g ml}^{-1}$, $1\text{-}\mu\text{l}$ PAHs standard working solution at different initial temperature

Table 15 The effect of holding time on the response and analysis time of $10 \mu\text{g ml}^{-1}$, $1\text{-}\mu\text{l}$ PAHs standard working solution

Time (min)	Response (pAs)*		Analysis time (min)*
	B(a)an	Chry	
0	31.24	32.68	18.00
1	30.55	32.75	19.00
2	30.10	31.85	20.00
3	30.05	31.89	21.00

* 5 replication, RSD < 4%

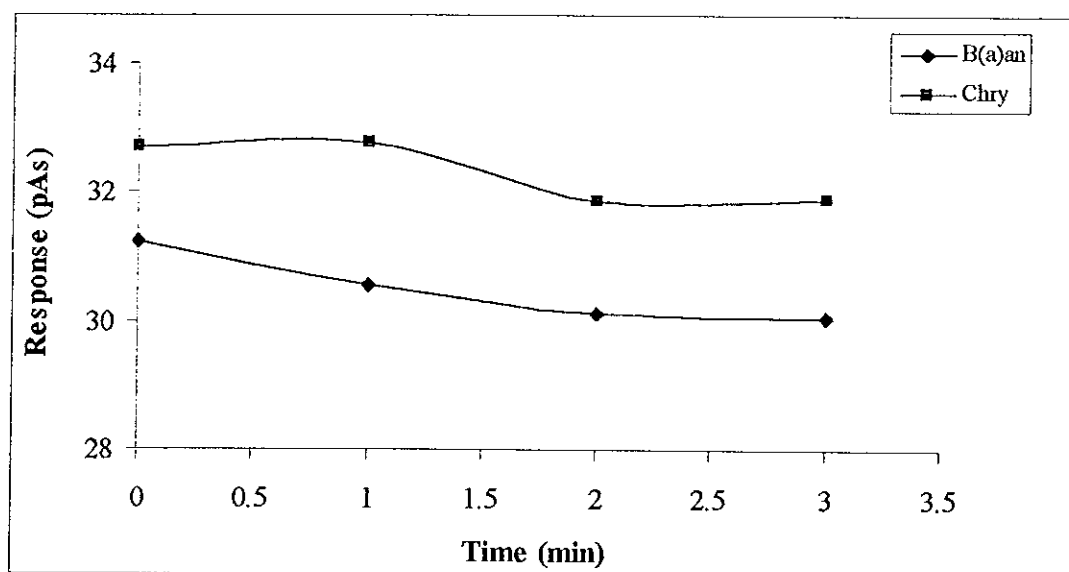


Figure 10 The responses of $10 \mu\text{g ml}^{-1}$, $1\text{-}\mu\text{l}$ PAHs standard working solution at different hold time

Table 16 The effect of the ramp rate on the response and analysis time of $10 \mu\text{g ml}^{-1}$, 1- μl standard working solution

Ramp rate ($^{\circ}\text{C}/\text{min}$)	Response (pAs)*		Analysis time (min)*
	B(a)an	Chry	
15	26.55	30.84	18.33
20	31.24	32.68	15.00
25	22.65	25.02	13.00
30	N.D	N.D	6.67

* 5 replication, RSD < 4%

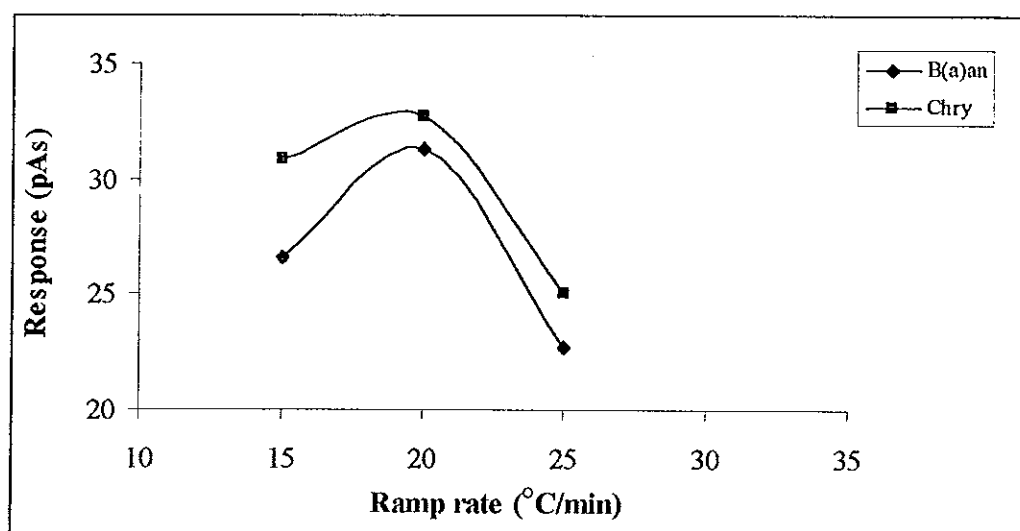


Figure 11 The responses of $10 \mu\text{g ml}^{-1}$, 1- μl PAHs standard working solution at different ramp rate

Step III is the column programming temperature to separate B(a)an, Chry, and B(b)fl in standard working solution 2.3.2 III. The results of initial temperature (Table 17 Figure 12) showed that 110°C provided the highest response, therefore it was chosen. Similar to the previous two programs different holding time only showed slight differences *i.e.* less than 10% (Table 18 and Figure 13). Therefore, the initial temperature was not hold. The

initial temperature was ramped to 300°C with ramp rates as shown in Table 19 and Figure 14. the ramp rate of 20°C/min provided the highest response and this was considered as the optimum ramp rate for separation for B(a)an, Chry and B(b)fl mixture.

Table 17 The effect of the initial temperature on the response and analysis time of 10 µg ml⁻¹, 1-µl PAHs standard working solution

Temperature (°C)	Response (pAs)*			Analysis time (min)*
	B(a)an	Chry	B(b)fl	
90	25.27	27.08	26.57	15.50
100	26.69	27.92	27.13	15.00
110	31.45	33.00	29.68	14.50
120	29.56	31.52	28.06	14.00

* 5 replication, RSD < 4%

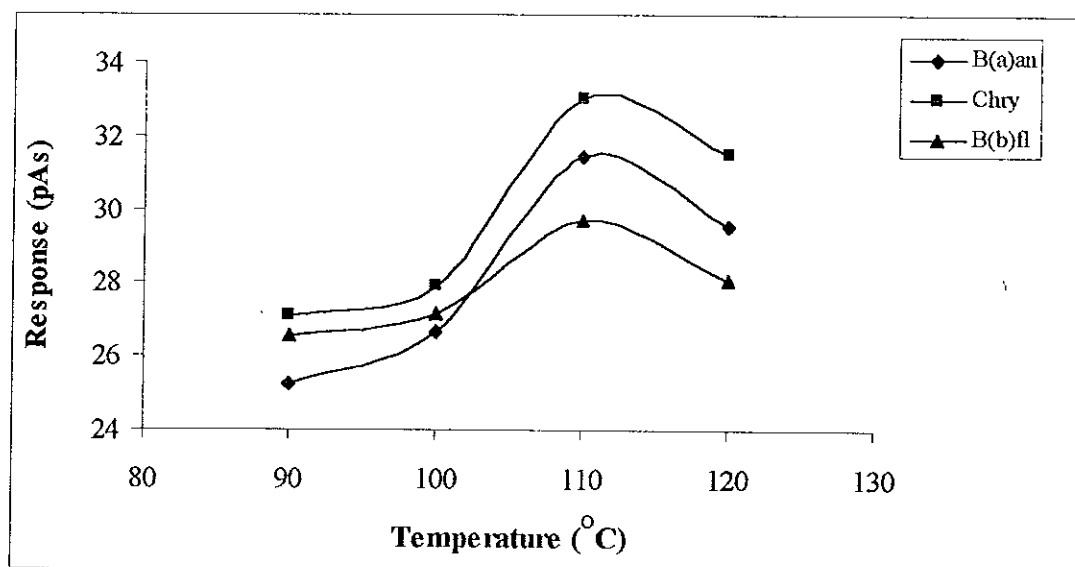


Figure 12 The responses of 10 µg ml⁻¹, 1-µl PAHs standard working solution at different initial temperature

Table 18 The effect of the holding time on the response and analysis time of $10 \mu\text{g ml}^{-1}$, $1\text{-}\mu\text{l}$ PAHs standard working solution

Time (min)	Response (pAs)*			Analysis time (min)*
	B(a)an	Chry	B(b)fl	
0	31.02	32.99	29.68	14.50
1	30.98	32.63	29.41	15.50
2	30.68	31.67	29.22	16.50
3	29.96	31.45	29.35	17.50

* 5 replication, RSD < 4%

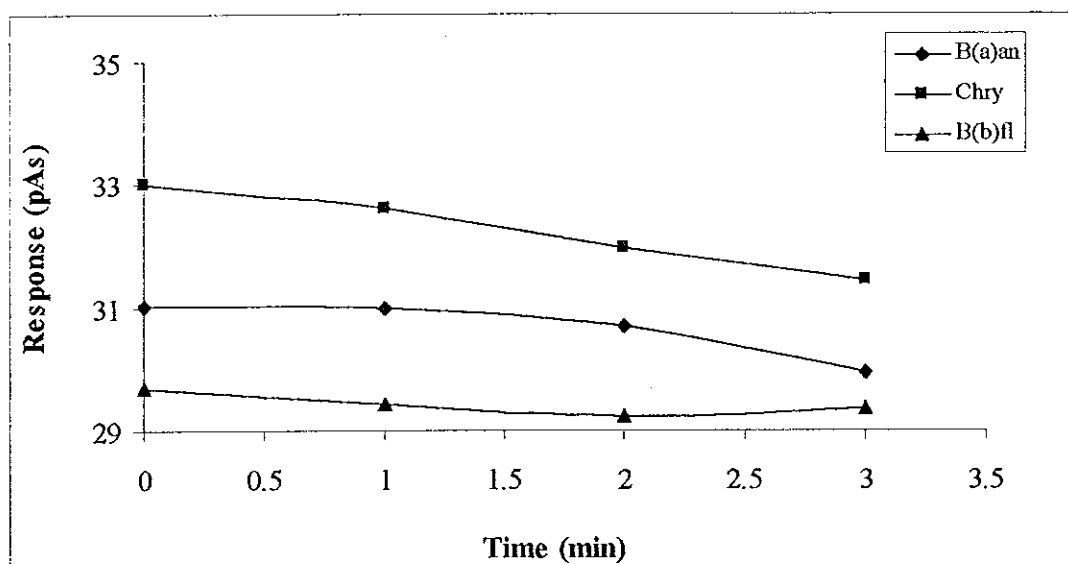


Figure 13 The responses of $10 \mu\text{g ml}^{-1}$, $1\text{-}\mu\text{l}$ PAHs standard working solution at different hold time

Table 19 The effect of the ramp rate on the response and analysis time of $10 \mu\text{g ml}^{-1}$, $1\text{-}\mu\text{l}$ PAHs standard working solution

Ramp rate (°C/min)	Response (pAs)*			Analysis time (min)*
	B(a)an	Chry	B(b)fl	
15	29.54	31.65	29.52	17.67
20	32.42	33.91	30.34	14.00
25	31.02	32.99	29.68	12.60

* 5 replication, RSD < 4%

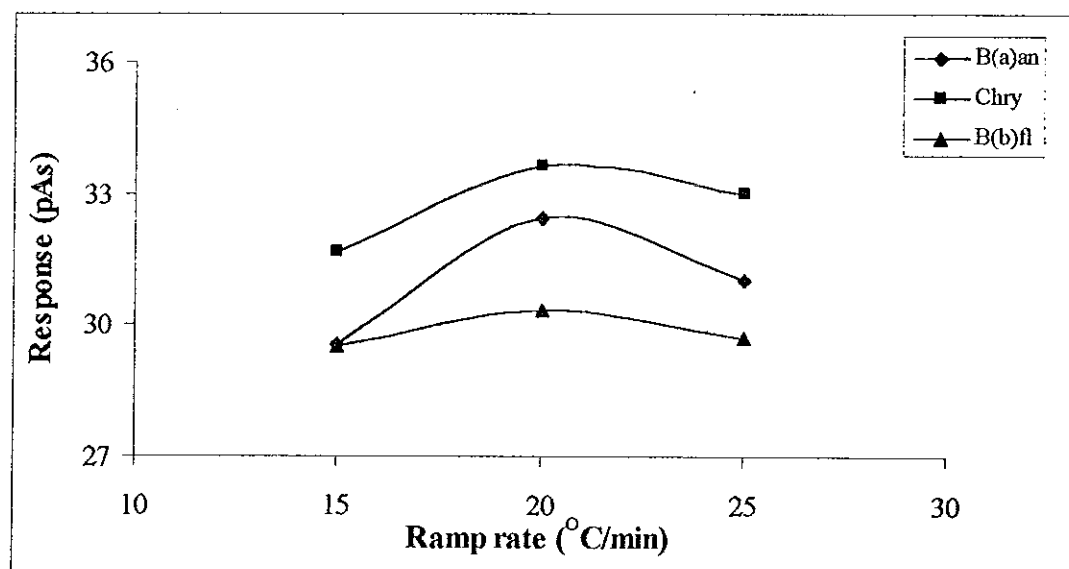


Figure 14 The responses of $10 \mu\text{g ml}^{-1}$, $1\text{-}\mu\text{l}$ PAHs standard working solution at different ramp rate

Step IV, the column programming temperature was for the separation of the mixture of B(a)an, Chry, B(b)fl and B(k)fl, and standard working solution 2.3.2 IV was used. The results are shown in Tables 20-22 and Figures 15-18. The values chosen followed the same reasoning as the previous these steps. The optimum values chosen were, initial temperature 120°C and the initial temperature was not hold. The ramp rate of $20^{\circ}\text{C}/\text{min}$ provided the

highest response (Table 22 and Figure 17) but the baseline resolution between 3rd and 4th peak than was poorer than at 15°C/min. thus, the ramp rate 15°C/min was considered as the optimum ramp rate to separate B(a)an, Chry, B(b)fl and B(k)fl.

Table 20 The effect of initial temperature on the response and analysis time of 10 µg ml⁻¹, 1-µl PAHs standard working solution

Temperature (°C)	Response (pAs)*				Analysis time (min)*
	B(a)an	Chry	B(b)fl	B(k)fl	
100	25.38	29.67	29.31	25.94	15.00
110	27.37	30.68	29.46	26.35	14.50
120	32.65	33.46	30.571	28.65	14.00
130	30.90	32.45	29.44	27.96	13.50

* 5 replication, RSD < 4%

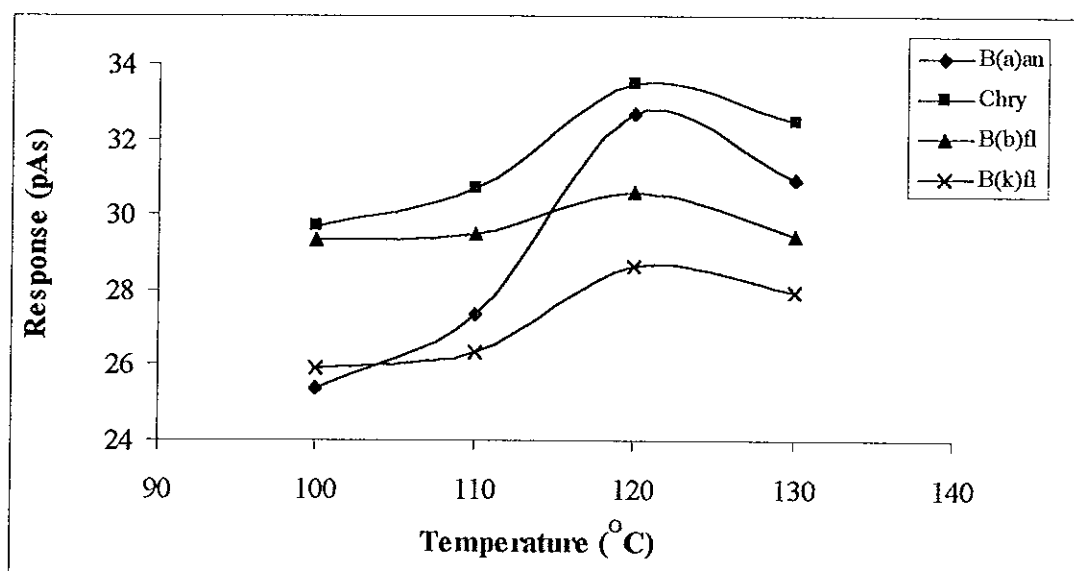


Figure 15 The responses of 10 µg ml⁻¹, 1-µl PAHs standard working solution at different initial temperature

Table 21 The effect of holding time on the response and analysis time of $10 \mu\text{g ml}^{-1}$, 1- μl PAHs standard working solution

Time (min)	Response (pAs)*				Analysis time (min)*
	B(a)an	Chry	B(b)fl	B(k)fl	
0	25.38	29.67	29.31	25.94	15.00
1	27.37	30.68	29.46	26.35	14.50
2	32.65	33.46	30.57	28.65	14.00
3	30.90	32.45	29.44	27.96	13.50

* 5 replication, RSD < 4%

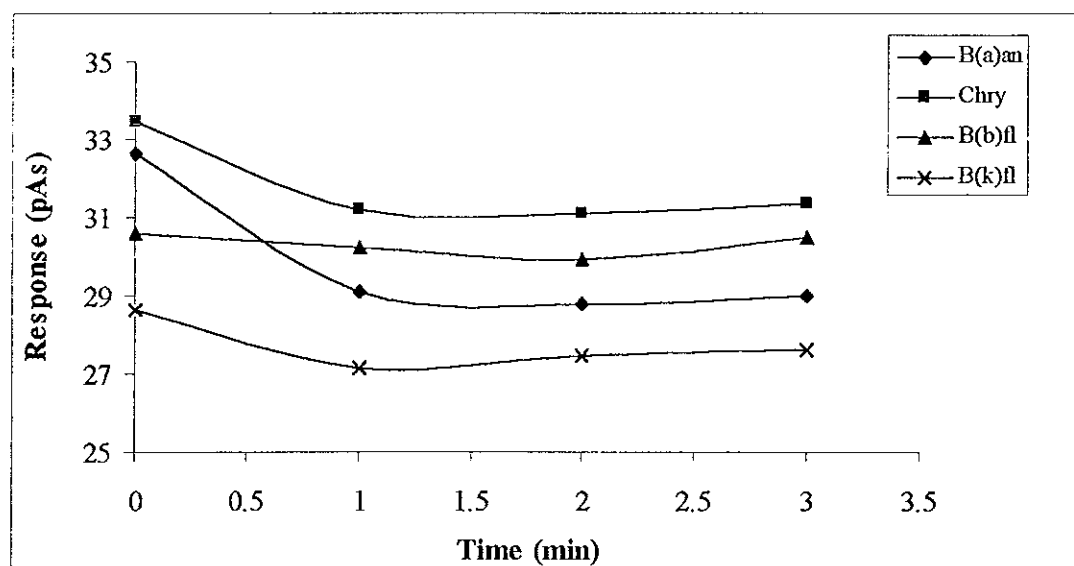


Figure 16 The responses of $10 \mu\text{g ml}^{-1}$, 1- μl PAHs standard working solution at different hold time

Table 22 The effect of the ramp rate on the response and analysis time of $10 \mu\text{g ml}^{-1}$, $1\text{-}\mu\text{l}$ PAHs standard working solution

Ramp rate ($^{\circ}\text{C}/\text{min}$)	Response (pAs)*				Analysis time (min)*
	B(a)an	Chry	B(b)fl	B(k)fl	
5	28.98	31.14	28.64	27.68	41.00
10	32.01	32.85	29.35	27.84	23.00
15	32.32	33.02	29.84	28.42	17.00
20	32.65	33.46	30.57	28.65	14.00

* 5 replication, RSD < 4%

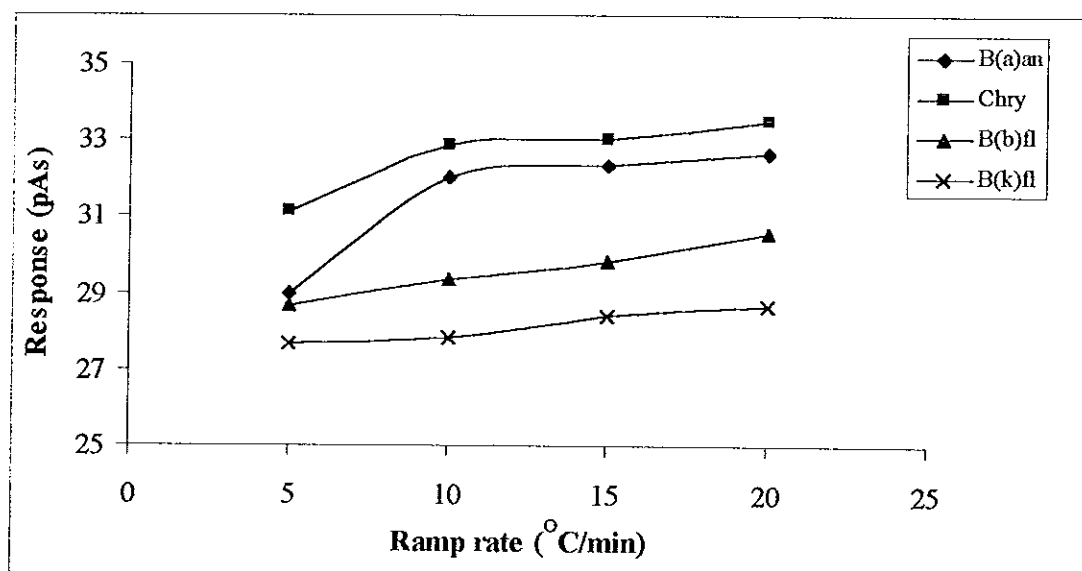


Figure 17 The responses of $10 \mu\text{g ml}^{-1}$, $1\text{-}\mu\text{l}$ PAHs standard working solution at different ramp rate

Step V, this is to separate B(a)an, Chry, B(b)fl, B(k)fl and B(a)p, and standard working solution 2.3.2 V was used. The results are shown in Tables 23-25 Figures 18-20. The values chosen were those which gave the highest response with best resolution. That is initial temperature 130°C the

initial temperature was not hold, then ramped to 300°C with the ramp rate of 10°C/min

Table 23 The effect of the initial temperature on the response and analysis time of 10 µg ml⁻¹, 1-µl PAHs standard working solution

Temperature (°C)	Response (pAs)*					Analysis time (min)*
	B(a)an	Chry	B(b)fl	B(k)fl	B(a)p	
120	29.58	31.65	28.65	26.98	26.21	17.00
130	32.25	33.65	30.64	28.96	27.65	16.33
140	31.20	33.25	31.98	29.65	29.66	15.67
150	31.64	33.96	32.66	30.35	30.64	15.00

* 5 replication, RSD < 4%

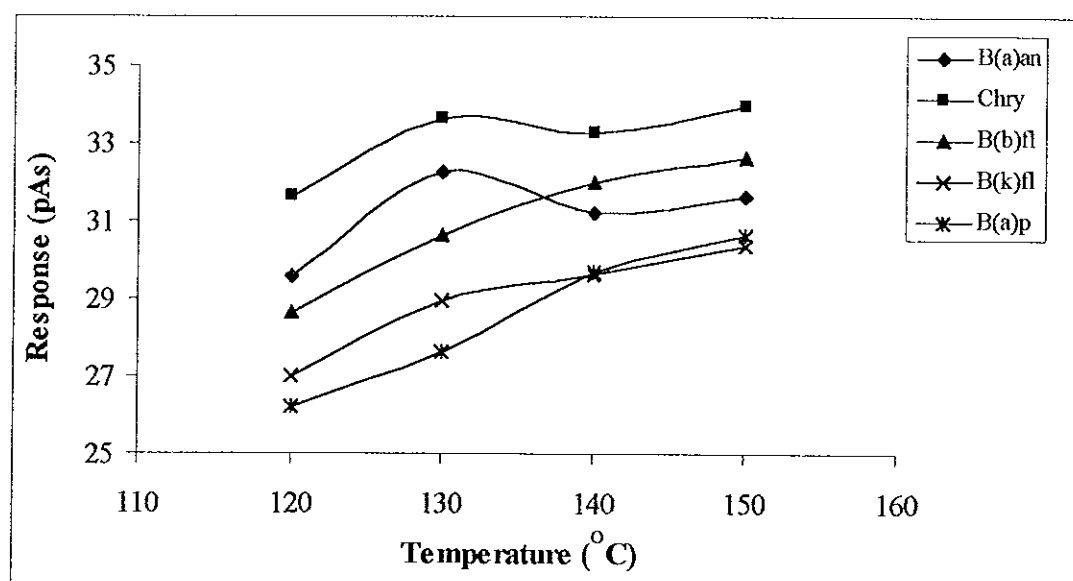


Figure 18 The responses of 10 µg ml⁻¹, 1-µl PAHs standard working solution at different initial temperature

Table 24 The effect of the holding time on the response and analysis time of $10 \mu\text{g ml}^{-1}$, $1\text{-}\mu\text{l}$ PAHs standard working solution

Time (min)	Response (pAs)*					Analysis time (min)*
	B(a)an	Chry	B(b)fl	B(k)fl	B(a)p	
0	32.25	33.64	30.64	28.95	27.65	16.33
1	28.92	30.95	29.62	27.95	27.33	17.33
2	28.52	30.26	29.95	27.13	27.00	18.33
3	28.49	29.96	29.85	26.74	25.99	19.33

* 5 replication, RSD < 4%

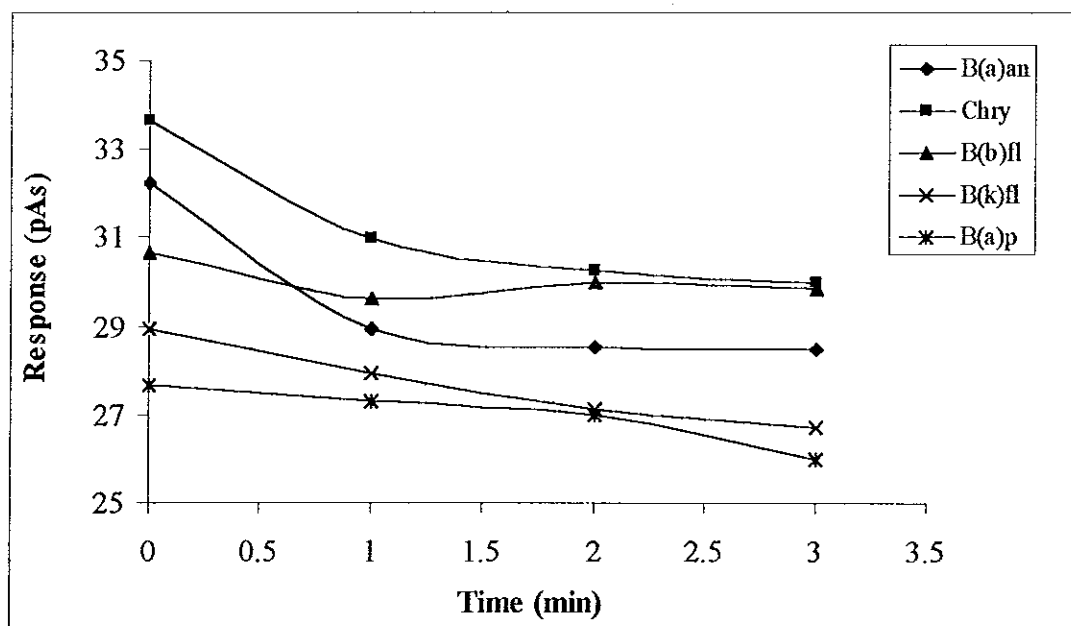


Figure 19 The responses of $10 \mu\text{g ml}^{-1}$, $1\text{-}\mu\text{l}$ PAHs standard working solution at different hold time

Table 25 The effect of the ramp rate on the response and analysis time of $10 \mu\text{g ml}^{-1}$, 1- μl PAHs standard working solution

Ramp rate ($^{\circ}\text{C}/\text{min}$)	Response (pAs)*					Analysis time (min)*
	B(a)an	Chry	B(b)fl	B(k)fl	B(a)p	
5	30.13	32.65	28.59	28.01	25.86	39.00
10	32.25	33.64	30.64	28.95	27.65	22.00
15	30.99	31.95	29.66	28.26	27.00	16.33

* 5 replication, RSD < 4%

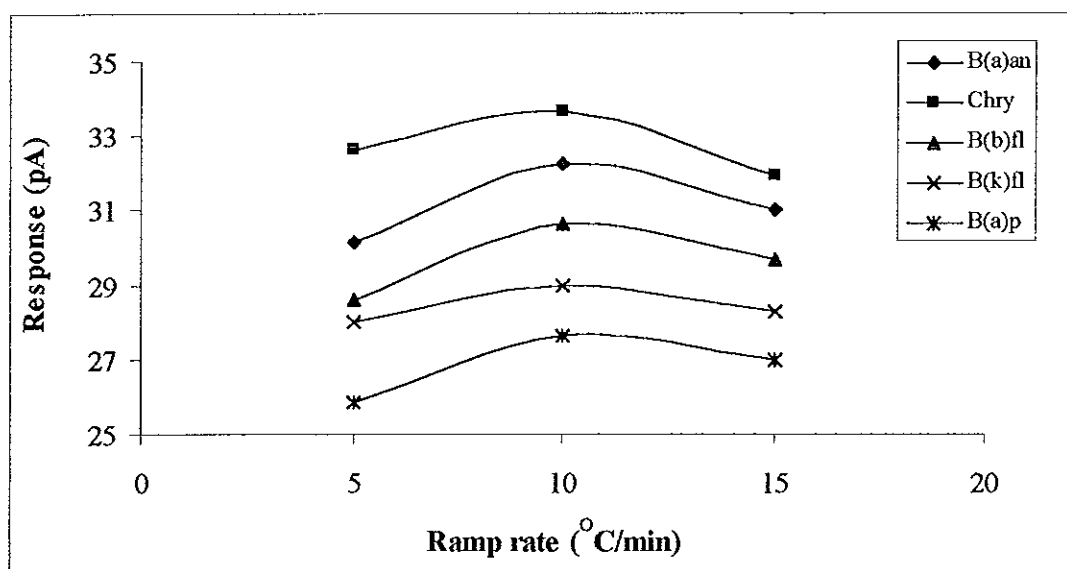


Figure 20 The responses of $10 \mu\text{g ml}^{-1}$, 1- μl PAHs standard working solution at different ramp rate

Step VI, separation of the mixture of B(a)an, Chry, B(b)fl, B(k)fl, B(a)p and In(123-cd)p, with the standard working solution 2.3.2 VI. The initial temperature at 150°C provided the highest response (Table 26, Figure 21). But the baseline resolution between the 3rd and the 4th peaks obtained from 140°C and 150°C were less than 130°C . Thus, the initial temperature of 130°C was selected. These was not much difference (<10%) between the response of

different hold time, (Table 27 and Figure 22) therefore, this was unnecessary. Initial temperature was then ramped to 300°C with the optimum ramp rate of 10°C/min (Table 28 and Figure 23).

Table 26 The effect of the initial temperature on the response and analysis time of 10 µg ml⁻¹, 1-µl PAHs standard working solution

Temperature (°C)	Response (pAs)*						Analysis time (min)*
	B(a)an	Chry	B(b)fl	B(k)fl	B(a)p	In(123-cd)p	
120	30.15	32.65	28.32	27.68	25.36	21.35	23.00
130	32.32	33.45	30.84	29.42	28.64	25.34	22.00
140	33.36	34.25	32.74	29.65	29.70	24.85	21.00
150	33.85	34.61	32.85	30.35	29.98	25.01	20.00

* 5 replication, RSD < 4%

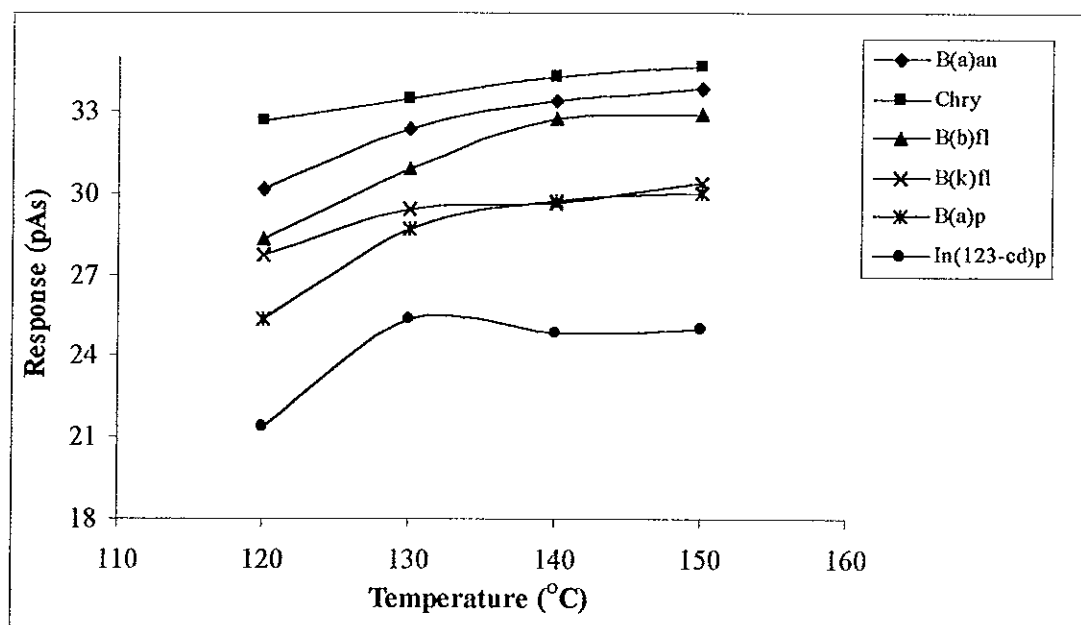


Figure 21 The responses of 10 µg ml⁻¹, 1-µl PAHs standard working solution at different initial temperature

Table 27 The effect of the holding time on the response and analysis time of $10 \mu\text{g ml}^{-1}$, $1\text{-}\mu\text{l}$ PAHs standard working solution

Time (min)	Response (pAs)*						Analysis time (min)*
	B(a)an	Chry	B(b)fl	B(k)fl	B(a)p	In(123-cd)p	
0	32.32	33.45	30.84	29.42	28.64	25.34	22.00
1	30.15	31.89	29.26	28.06	27.74	20.65	23.00
2	28.74	31.58	28.88	27.86	26.62	20.89	24.00
3	28.85	29.60	28.98	27.45	26.87	19.85	25.00

* 5 replication, RSD < 4%

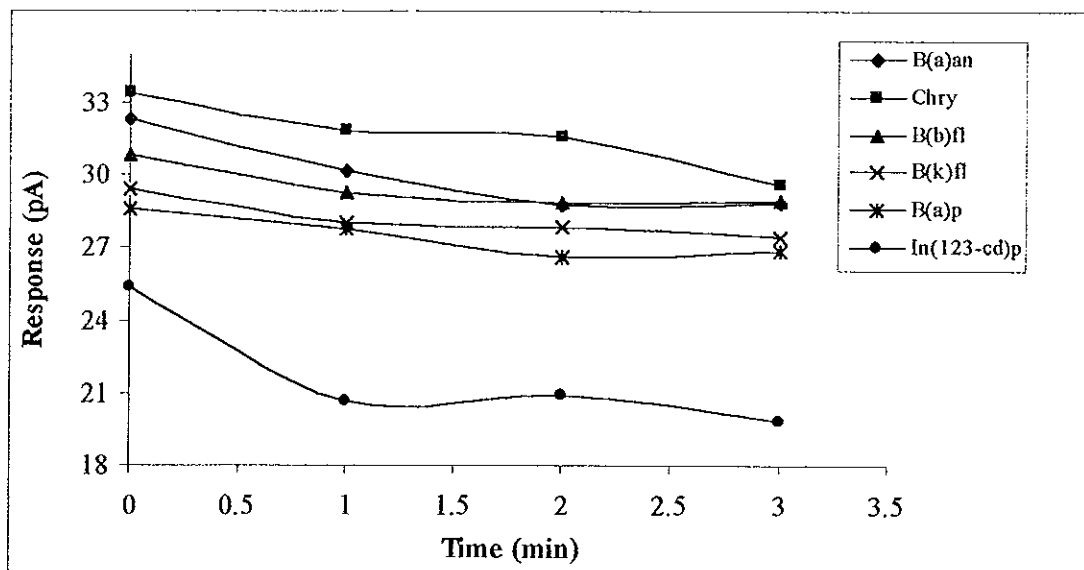


Figure 22 The responses of $10 \mu\text{g ml}^{-1}$, $1\text{-}\mu\text{l}$ PAHs standard working solution at different hold time

Table 28 The effect of ramp rate on the response and analysis time of $10 \mu\text{g ml}^{-1}$, $1\text{-}\mu\text{l}$ PAHs standard working solution

Ramp rate (°C/min)	Response (pAs)*						Analysis time (min)*
	B(a)an	Chry	B(b)fl	B(k)fl	B(a)P	In(123-cd)p	
3	29.14	30.62	27.01	26.35	24.95	23.65	61.67
5	31.89	32.51	29.98	27.34	25.75	24.32	39.00
7	32.05	33.12	30.25	28.62	26.98	24.89	29.29
10	32.32	33.45	30.84	29.42	28.64	2534	22.00

* 5 replication, RSD < 4%

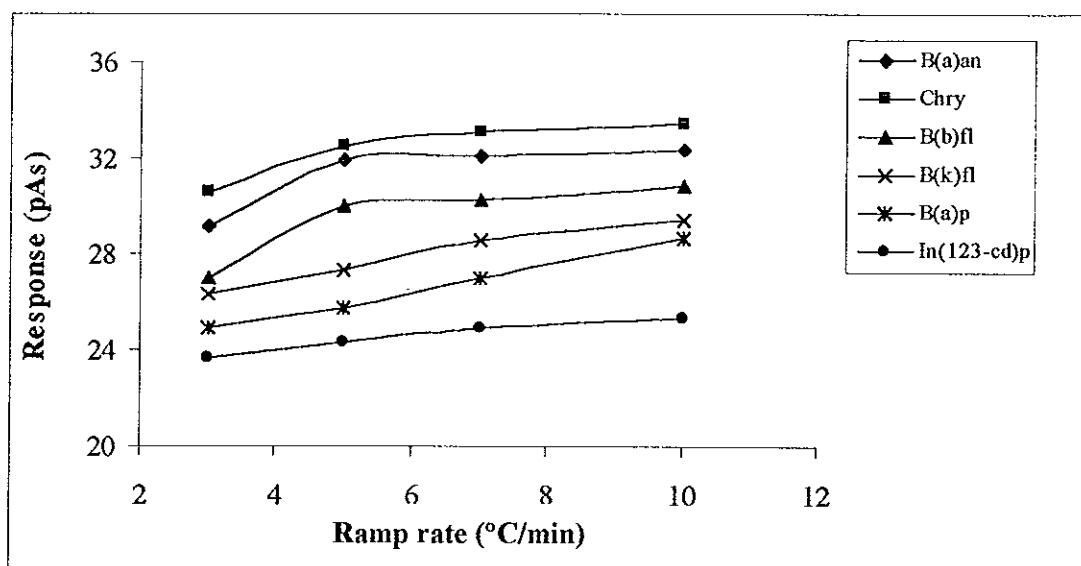


Figure 23 The responses of $10 \mu\text{g ml}^{-1}$, $1\text{-}\mu\text{l}$ PAHs standard working solution at different ramp rate

Step VII, the column programming temperature for the separation of the mixture of B(a)an, Chry, B(b)fl, B(k)fl, B(a)p, In(123-cd)p and D(a,h)an, using standard working solution 2.3.2 VII. The initial temperature at 150°C provided the highest response (Table 29, Figure 24), but the baseline resolution between the 3rd and the 4th peak obtained from 140 and 150°C were less than 130°C. Although in many literatures, the initial temperature was generally recommended to be lower than the boiling point of the solvent about 10-20°C (Grob, 1985). Due to the high boiling points of PAHs, therefore, at that temperature the analyte would volatilize gradually and would have gone into the column without lost. Similar to previous results holding time is unnecessary since the differences of the responses were less than 10% (Table 30 and Figure 25). As for the ramp rate, 7 and 10°C/min gave higher response and less analysis time than 5°C/min (Table 31 and Figure 26), but they provided unacceptable baseline resolution ($R_s < 1.0$). The ramp rate at 5°C/min was the one which gave the highest responses with an acceptable baseline resolution. Therefore it was selected for separation of B(a)an, Chry, B(b)fl, B(k)fl, B(a)p, In(123-cd)p and D(a,h)an in a mixture.

Table 29 The effect of the initial temperature on the response and analysis time of $10 \mu\text{g ml}^{-1}$, $1\text{-}\mu\text{l}$ PAHs standard working solution

Temperature (°C)	Response (pAs)*							Analysis time (min)*
	B(a)an	Chry	B(b)fl	B(k)fl	B(a)p	In(123-cd)p	D(a,h)an	
120	30.45	32.85	28.52	27.98	25.66	23.35	20.65	23.00
130	31.92	33.65	30.98	28.65	27.34	25.34	23.68	2.00
140	32.24	33.98	31.58	30.34	28.64	26.34	24.34	21.00
150	32.69	34.34	32.61	31.35	29.35	27.62	25.31	20.00

* 5 replication, RSD < 4%

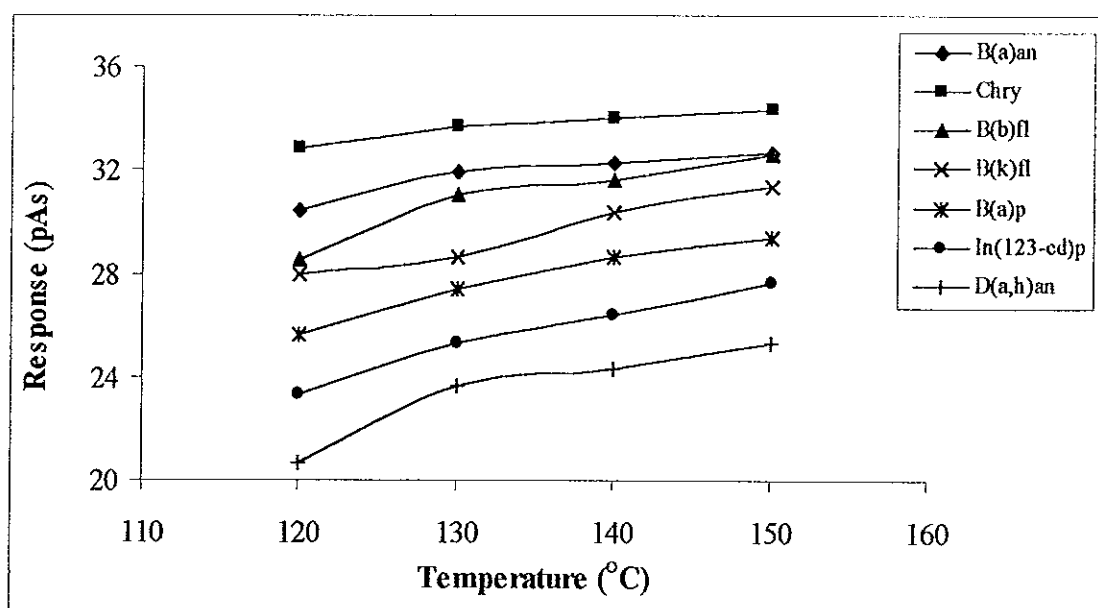


Figure 24 The responses of $10 \mu\text{g ml}^{-1}$, $1\text{-}\mu\text{l}$ PAHs standard working solution at different initial temperature

Table 30 The effect of the holding time on the response and analysis time of $10 \mu\text{g ml}^{-1}$, $1\text{-}\mu\text{l}$ PAHs standard working solution

Time (min)	Response (pAs)*							Analysis time (min)*
	B(a)an	Chry	B(b)fl	B(k)fl	B(a)p	In(123-cd)p	D(a,h)an	
0	31.92	33.65	30.98	28.65	27.34	25.34	23.68	22.00
1	31.00	32.64	29.24	28.02	26.01	24.20	21.97	23.00
2	30.85	31.95	28.84	27.64	25.81	23.64	21.48	24.00
3	31.02	31.97	28.46	27.14	24.97	23.87	20.95	25.00

* 5 replication, RSD < 4%

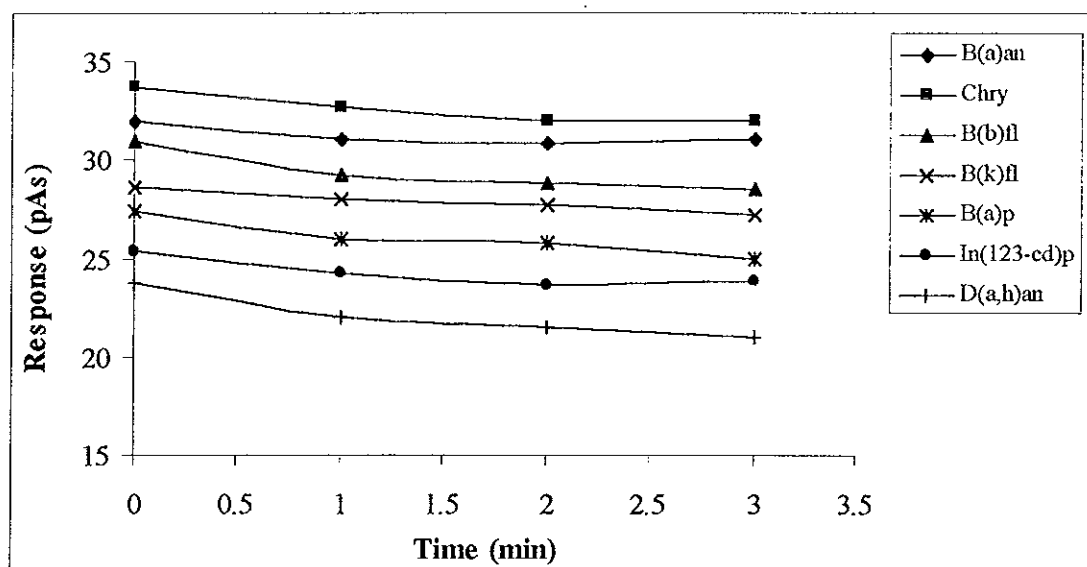


Figure 25 The responses of $10 \mu\text{g ml}^{-1}$, $1\text{-}\mu\text{l}$ PAHs standard working solution at different hold time

Table 31 The effect of the ramp rate on the response and analysis time of $10 \mu\text{g ml}^{-1}$, 1- μl PAHs standard working solution

Ramp rate ($^{\circ}\text{C}/\text{min}$)	Response (pAs)*							Analysis time (min)*
	B(a)an	Chry	B(b)fl	B(k)fl	B(a)p	In(123-cd)p	D(a,h)an	
3	30.24	30.85	26.95	27.67	26.12	24.24	20.34	61.67
5	31.24	32.65	28.99	27.92	26.35	25.02	22.54	39.00
7	31.75	33.25	29.36	28.63	26.84	25.07	23.14	29.29
10	31.92	33.65	30.98	28.65	27.34	25.34	23.68	22.00

* 5 replication, RSD < 4%

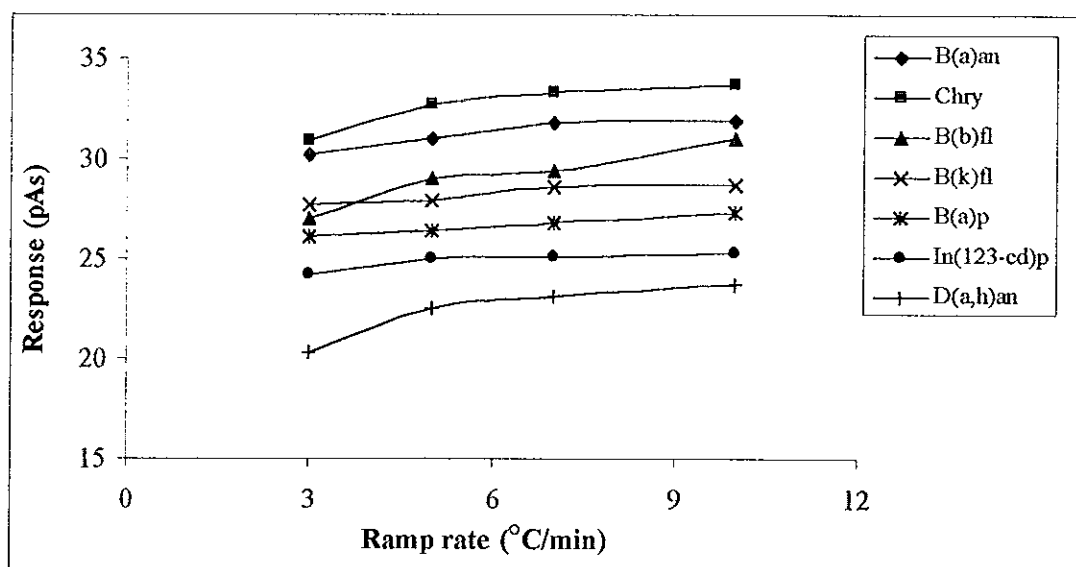


Figure 26 The responses of $10 \mu\text{g ml}^{-1}$, 1- μl PAHs standard working solution at different ramp rate

In conclusion, the optimum conditions of the column temperature programming was the initial temperature, 130°C then ramped at 5°C/min to 300°C as shown in Figure 27. At this final temperature, it was held until the signal returned to the baseline. The holding time at this final temperature had effect on the response and baseline resolution. Therefore, to decrease analysis time, the final temperature at 300°C was only held for 2 min. This was enough to allow the signal to go back to the baseline. The total analysis time was 36.00 min. Figure 27 shows this optimum temperature programming.

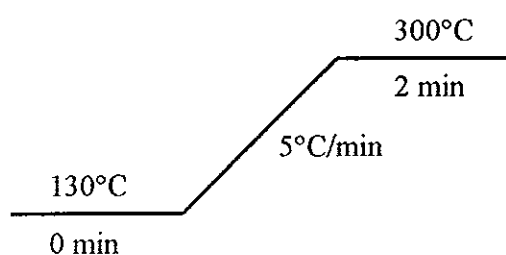


Figure 27 The optimum column temperature programming by split injection

3.1.3 Optimization of injector temperature

Table 32 and Figure 28 show the responses of PAHs at injector temperature between 240 to 270°C. The highest responses of all seven PAHs were obtained at 250°C. Therefore, the temperature of 250°C is selected to be an optimum injector temperature for split mode injection analysis.

Table 32 The effect of injector temperature on the response of $10 \mu\text{g ml}^{-1}$, $1\text{-}\mu\text{l}$ PAHs standard working solution

Temperature (°C)	Response (pAs)*						
	B(a)an	Chry	B(b)fl	B(k)fl	B(a)p	In(123-cd)p	D(a,h)an
240	29.62	30.32	26.54	25.64	24.85	23.18	20.64
250	31.02	32.65	28.99	27.92	26.35	25.02	22.54
260	30.99	31.78	27.65	27.15	26.04	24.89	22.11
270	30.66	30.96	26.99	26.24	25.62	24.51	21.65

* 5 replication, RSD < 4%

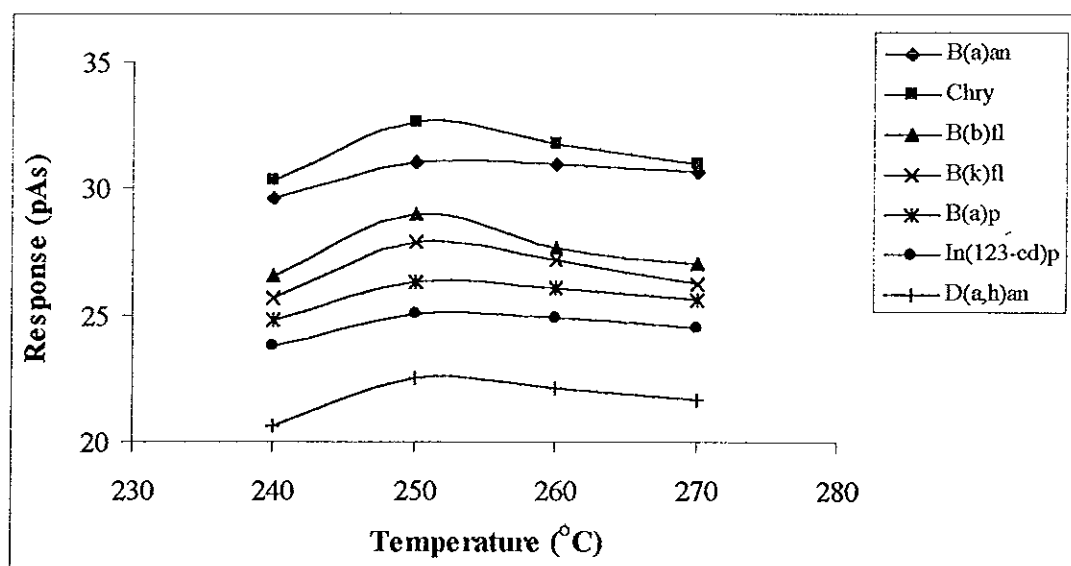


Figure 28 The responses of $10 \mu\text{g ml}^{-1}$, $1\text{-}\mu\text{l}$ PAHs standard working solution at different injector temperature

3.1.4 Optimization of detector temperature

The detector for this research was based on the flame ionization detector (FID). FID consists of a small hydrogen–air flame burning jet situated at the tip of the capillary tubing. When organic compounds are introduced into the flame from the column, electrically charged species are formed. These are collected by applying a voltage across the flame. The resulting current is amplified by an electrometer (Grob, 1985). The Hewlette Packard, GC manual suggested that the detector temperature should be set above 150°C, if the temperature was less than the recommend temperature flame would not lit. Table 33 and Figure 29 show the results of the optimization of detector temperature (2.3.3.4). The optimum detector obtained was 300°C *i.e.* the temperature which gave the highest response of PAHs for split mode injection analysis.

Table 33 The effect of detector temperature on the response of $10 \mu\text{g ml}^{-1}$, $1\text{-}\mu\text{l}$ PAHs standard working solution

Temperature (°C)	Response (pAs)*						
	B(a)an	Chry	B(b)fl	B(k)fl	B(a)p	In(123-cd)p	D(a,h)an
270	24.61	27.32	22.81	21.32	19.57	18.31	17.20
280	27.68	28.95	24.58	23.33	22.82	21.68	18.63
290	29.26	30.62	25.32	24.24	24.65	23.56	20.36
300	31.02	32.65	28.99	27.92	26.35	25.02	22.54

* 5 replication, RSD < 4%

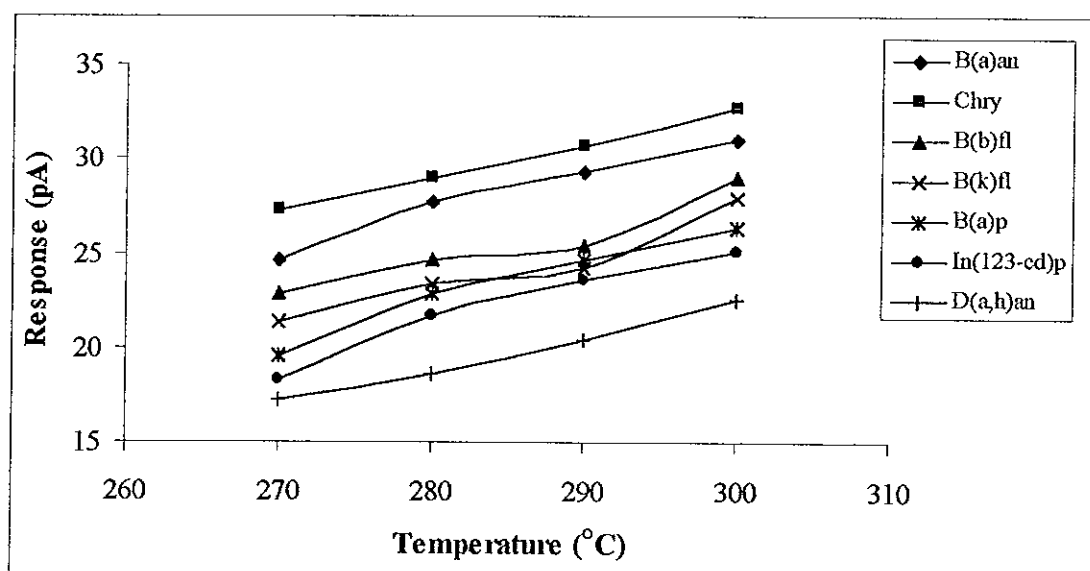


Figure 29 The responses of $10 \mu\text{g ml}^{-1}$, $1\text{-}\mu\text{l}$ PAHs standard working solution at different detector temperature

3.1.5 Optimization of make up gas flow rate

FID requires make up gas to carry the analyte that exists the column into the detection zone. Lighter carrier gas (He) operated at relatively low flow rates (1.5 ml/min), so a make up gas is added to the stream just before it enters the detector. The addition of this gas provided the high flow rate that met the detector requirement. Without the make up gas, the analyte will lag at the end of the column because the volume of gas that flows through the column is not sufficient to drive it through the relative large volume of the detector (www.chem.missouri.edu/Greenlief/courses/GC_HPLC_Instrumentation.pdf, 2001). In this study nitrogen was used as additional make up gas in the FID system and its flow rate was optimized for high sensitivity.

Table 34 and Figure 30 show the effect of make up gas flow rate. The highest response of PAHs was obtained at 30 ml/min for split mode injection analysis. This condition agreed with the rate recommended by the manufacture, *i.e.* the make up flow rate should be in the ranged 10 to 60 ml/min, and the suggested flow is 30 ml/min.

Table 34 The effect of make up gas flow rate on the response of $10 \mu\text{g ml}^{-1}$, $1\text{-}\mu\text{l}$ PAHs standard working solution

Flow rate (ml/min)	Response (pAs)*						
	B(a)an	Chry	B(b)fl	B(k)fl	B(a)p	In(123-cd)p	D(a,h)an
10	31.02	32.65	28.99	27.92	26.35	25.02	22.54
20	40.65	41.63	37.62	37.19	34.67	33.31	31.33
30	49.37	49.87	46.32	38.35	35.95	34.54	32.63

* 5 replication, RSD < 4%

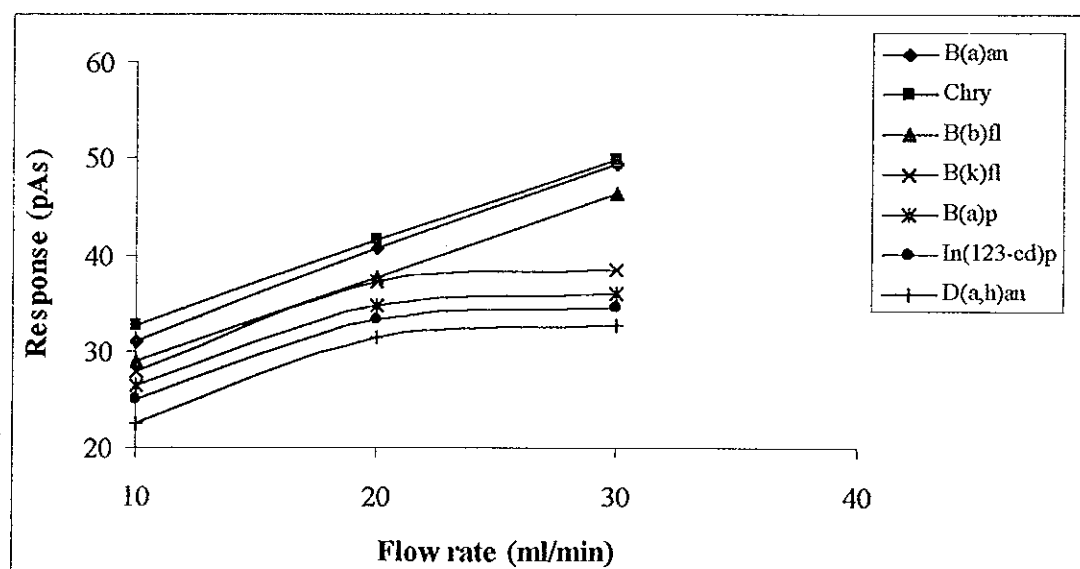


Figure 30 The responses of $10 \mu\text{g ml}^{-1}$, $1\text{-}\mu\text{l}$ PAHs standard working solution at different make up gas flow rate

3.1.6 Optimization of fuel gas flow rate

The FID detector requires fuel (H_2) and oxidant (air) to support a flame. As the detector consists of a small hydrogen – air flame burning jet, thus the flow rates of fuel and oxidant gas are significantly influence the noise level and the sensitivity of the detector.

In the experiment, hydrogen gas was used as fuel gas and was optimized (experiment 2.3.3.5). Table 35 and Figure 31 show the effect of fuel gas flow rate to the response of FID. Although 50 ml/min gave the best response, but a flow rate of 30 ml/min hydrogen flow rate was selected. The discussion of this selection will be accounted together in 3.1.7

Table 35 The effect of fuel gas flow rate on the response of $10 \mu\text{g ml}^{-1}$, $1\text{-}\mu\text{l}$ PAHs standard working solution

Flow rate (ml/min)	Response (pAs)*						
	B(a)an	Chry	B(b)fl	B(k)fl	B(a)p	In(123-cd)p	D(a,h)an
20	30.25	30.99	27.89	27.13	25.01	24.22	20.97
30	31.02	32.65	28.99	27.92	26.35	25.02	22.54
40	42.62	43.54	40.57	39.41	37.93	37.33	33.96
50	54.61	54.99	52.21	51.63	50.31	49.01	44.65

* 5 replication, RSD < 4%

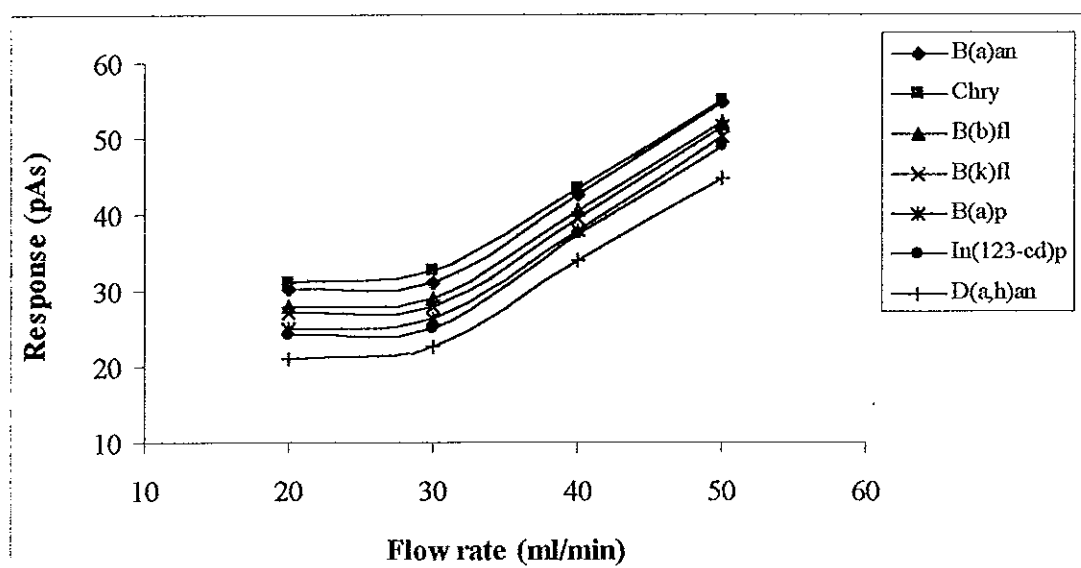


Figure 31 The responses of $10 \mu\text{g ml}^{-1}$, $1\text{-}\mu\text{l}$ PAHs standard working solution at different fuel gas flow rate

3.1.7 Optimization of oxidant gas flow rate

In this study, air (zero grade) was used as oxidant for FID. The responses at different flow rate were shown in Table 36 and Figure 32. According to the recommendation from the manufacture the fuel – oxidant ratio should be between 8 and 12% to keep the flame lit. From the results, hydrogen and air flow rates at 50 and 500 ml/min, respectively, showed the best response, and complied with the recommended range – 10%. However these value gave too high baseline output (high analysis background) and this affected the signal integration. Eventually, hydrogen and air flow rates at 30 and 300 ml/min, respectively, were selected as optimum, since they provided an acceptable baseline output.

Table 36 The effect of oxidant gas flow rate on the response of $10 \mu\text{g ml}^{-1}$, $1\text{-}\mu\text{l}$ PAHs standard working solution

Flow rate (ml/min)	Response (pAs)*						
	B(a)an	Chry	B(b)fl	B(k)fl	B(a)p	In(123-cd)p	D(a,h)an
20	29.65	30.64	27.89	25.35	24.74	23.69	20.46
300	31.02	32.65	28.99	27.92	26.35	5.02	22.54
400	44.06	43.66	41.64	49.45	49.32	47.13	44.95
500	56.05	58.34	53.48	52.01	51.52	48.56	46.48

* 5 replication, RSD < 4%

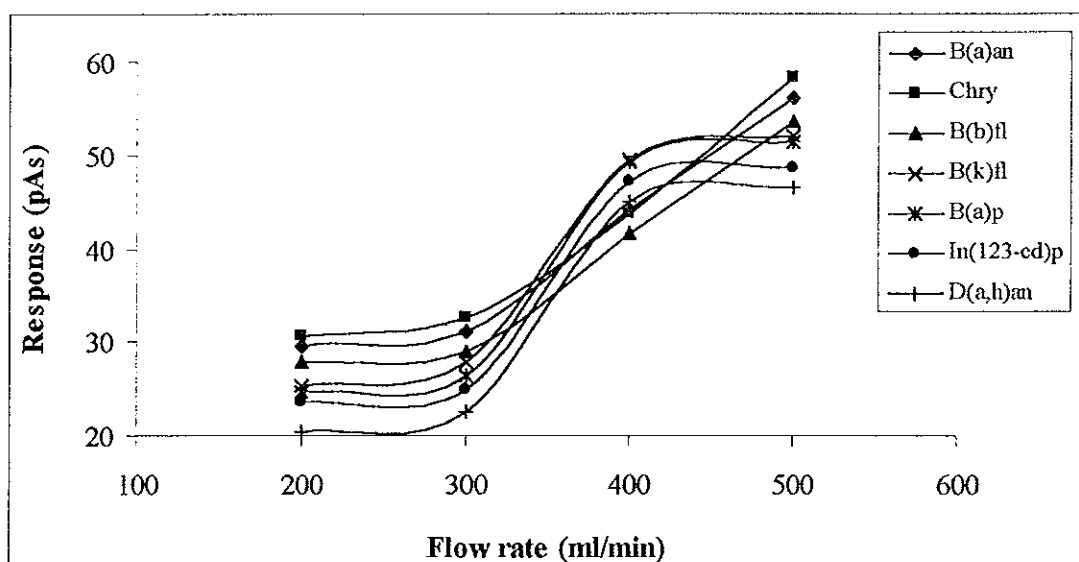


Figure 32 The responses of $10 \mu\text{g ml}^{-1}$, $1\text{-}\mu\text{l}$ PAHs standard working solution at different oxidant gas flow rate

3.1.8 Limit of detection

The determination of limit of detection for trace PAHs in this work was based on signal-to-noise ratio (S/N). The S/N was calculated from the chromatogram. The concentrations of PAHs where a S/N was more than 3.0 are shown in Table 37. The different efficiency of the FID to each PAHs was due

to the different structure of the PAHs (see 1.2.1). The limits of detection for individual PAHs were summarized in Table 38.

Table 37 The relationship between the response of PAHs ($S/N > 3$) and concentration

Concentration ($\mu\text{g ml}^{-1}$)	Response (pAs)*						
	B(A)an	Chry	B(b)fl	B(k)fl	B(a)p	In(123-cd)p	D(a,h)an
0.35	N.D	1.33	N.D	N.D	N.D	N.D	N.D
0.50	1.78	1.91	1.65	1.25	N.D	N.D	N.D
0.60	2.14	2.30	1.98	1.43	1.38	1.28	N.D
0.70	2.45	2.65	2.31	1.56	1.60	1.50	1.36
0.75	2.89	3.67	3.12	2.35	2.40	2.23	2.16

* 5 replication, RSD < 4%

Table 38 The limits of detection for individual PAHs with split mode injection

PAHs	Limit of detection ($\mu\text{g ml}^{-1}$)
B(a)an	0.50
Chry	0.35
B(b)fl	0.50
B(k)fl	0.50
B(a)p	0.60
In(123-cd)p	0.60
D(a,h)an	0.70

3.1.9 Linear dynamic range

As indicated in experiment 2.3.3.7, the linear dynamic range was demonstrated experimentally by running various concentration. Table 39 and Figure 33 show the response and linear regression, R^2 , of individual PAHs at

various concentration. The system provided a wide linear dynamic range from 0.50 to 75.00 $\mu\text{g ml}^{-1}$ with a good linear regression, $R^2 > 0.99$.

Table 39 The response of individual PAHs at various concentration

Concentration ($\mu\text{g ml}^{-1}$)	Response (pAs)*						
	B(a)an	Chry	B(b)fl	B(k)fl	B(a)p	IN(123-cd)p	D(a,h)an
0.50	1.78	1.91	1.65	1.25	1.60	1.50	1.45
0.75	2.89	3.67	3.12	2.35	2.40	2.23	2.16
1.00	4.31	3.86	6.12	3.13	3.20	3.10	3.02
5.00	17.62	19.63	17.55	15.66	16.02	15.21	15.08
10.00	33.64	38.17	35.11	31.33	32.05	31.02	30.15
25.00	83.64	95.43	91.77	78.32	82.12	77.55	75.39
50.00	163.24	201.87	185.54	166.64	170.24	160.10	156.77
75.00	244.63	286.31	263.31	234.95	240.36	232.66	224.16

* 5 replication, RSD < 4%

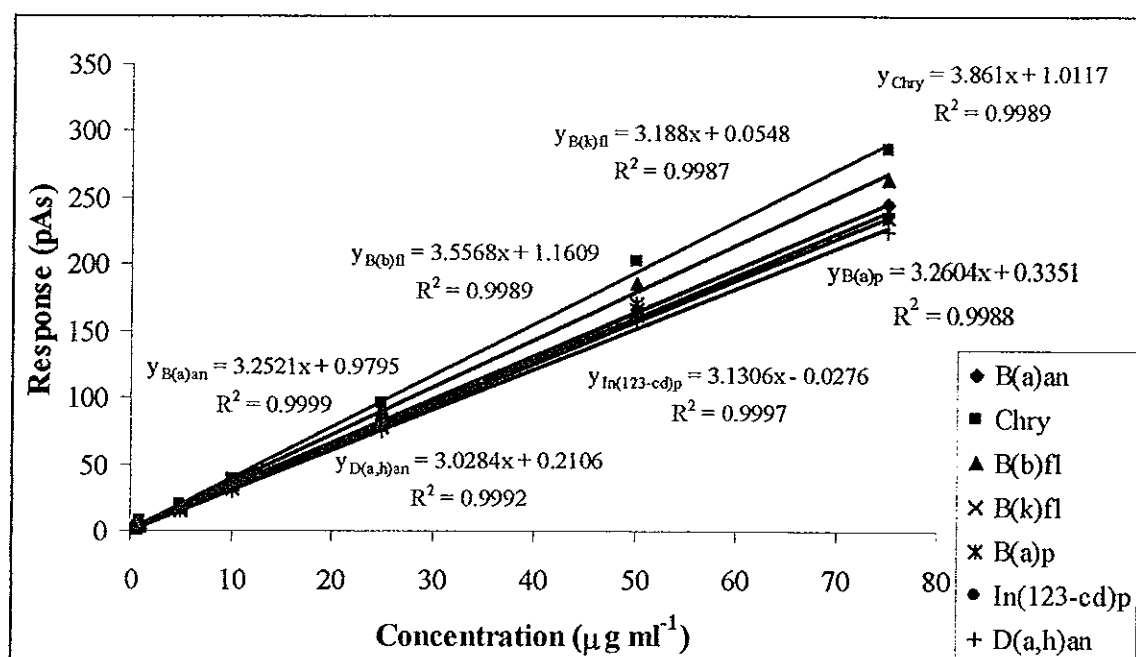


Figure 33 The linear dynamic range of seven PAHs

Second injection mode: Optimization of splitless injection mode

3.1.10 Optimization of carrier gas flow rate

The carrier gas flow rate was optimized as shown in experiment 2.3.3.8. The optimum flow rate was considered by the relationship between the height equivalent to a theoretical plate (HETP) and the carrier gas flow rate. The HETP was calculated by the van Deemter equation. The *HETP* and the carrier gas flow rate were plot as van Deemter graph. The results are shown in Table 40, and Figure 34. The narrowest HETP was at the carrier gas flow rate as 1.5 ml/min for all seven PAHs.

Table 40 The Height Equivalent to a Theoretical Plate (HETP) of $10 \mu\text{g ml}^{-1}$, $1\text{-}\mu\text{l}$ seven PAHs mixture at various carrier gas flow rate

Flow rate (ml/min)	HETP (cm)*						
	B(a)an	Chry	B(b)fl	B(k)fl	B(a)p	In(123-cd)p	D(a,h)an
1.5	0.33	0.14	1.38	0.84	0.48	1.17	0.94
2.0	0.47	0.15	1.44	0.87	0.49	1.23	1.02
2.5	0.60	0.23	1.51	1.06	0.54	1.29	1.03
3.0	0.71	0.34	1.57	1.13	0.63	1.34	1.08
3.5	0.87	0.51	1.73	1.26	0.75	1.42	1.17
4.0	0.91	0.67	1.82	1.38	0.85	1.50	1.27
4.5	1.13	0.86	1.93	1.46	0.93	1.58	1.33
5.0	1.31	1.00	2.04	1.64	1.05	1.68	1.42

* 5 replication, RSD < 4%

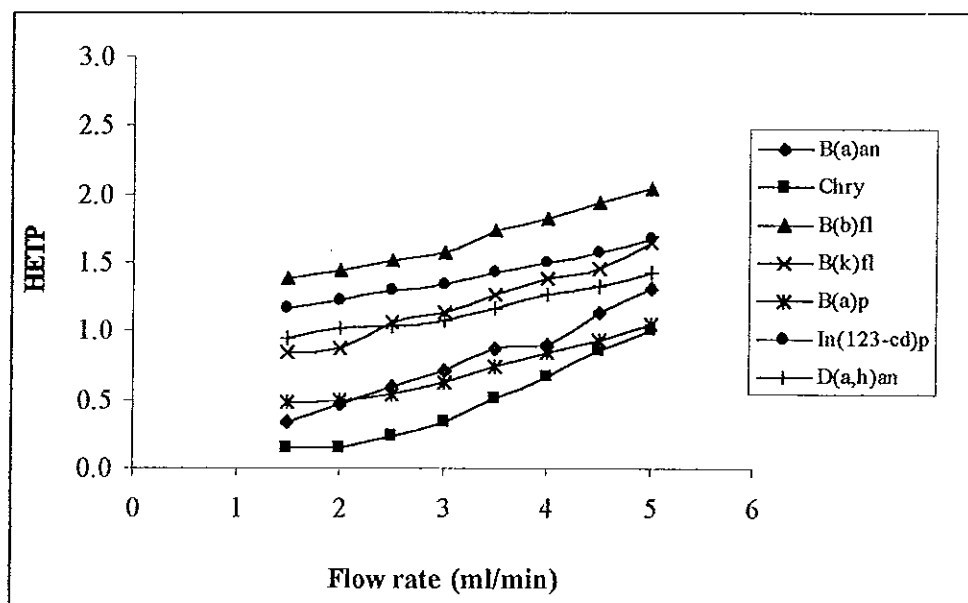


Figure 34 The van Deemter plot of seven PAHs

3.1.11 Optimization of column temperature programming

In splitless mode injection, the volume of analyte enter into the column is larger than in the split mode injection. Operating at the optimum column temperature programming for the split mode in the splitless mode gave an overlapping between the 1st and 2nd, 3rd and 4th and 6th and 7th peaks. To separate these peaks, the column temperature programming was reoptimized for the splitless mode. To achieve more separation two stages of temperature ramping were optimized. The initial temperature was ramped immediately with a ramp rate of 20°C/min to 200°C. Then ramped with a rate of 10°C/min to 300°C and held for 5 min.

Table 41 and Figure 35 shown the effect of initial temperature on the response and analysis time. The temperatures between 130 to 150°C provided the responses which differed less than 10%. The minimum analysis time was achieved at 150°C However when the baseline resolution was taken into consideration, initial temperature of 130°C indicated the best response with acceptable baseline resolution, therefore temperature 130°C was selected.

Table 41 The effect of initial temperature on the response and analysis time of $10 \mu\text{g ml}^{-1}$, $1\text{-}\mu\text{l}$ PAHs standard working solution

Temperature (°C)	Response (pAs)*							Analysis time (min)*
	B(a)an	Chry	B(b)fl	B(k)fl	B(a)p	In(123-cd)p	D(a,h)an	
120	173.60	193.34	186.47	143.25	128.54	56.54	47.97	19.00
130	241.65	265.67	251.83	202.60	174.62	76.71	63.35	18.50
140	246.32	284.62	264.33	219.48	200.61	91.27	69.89	18.00
150	238.47	278.62	259.36	208.55	195.59	87.17	66.85	17.50

* 5 replication, RSD < 4%

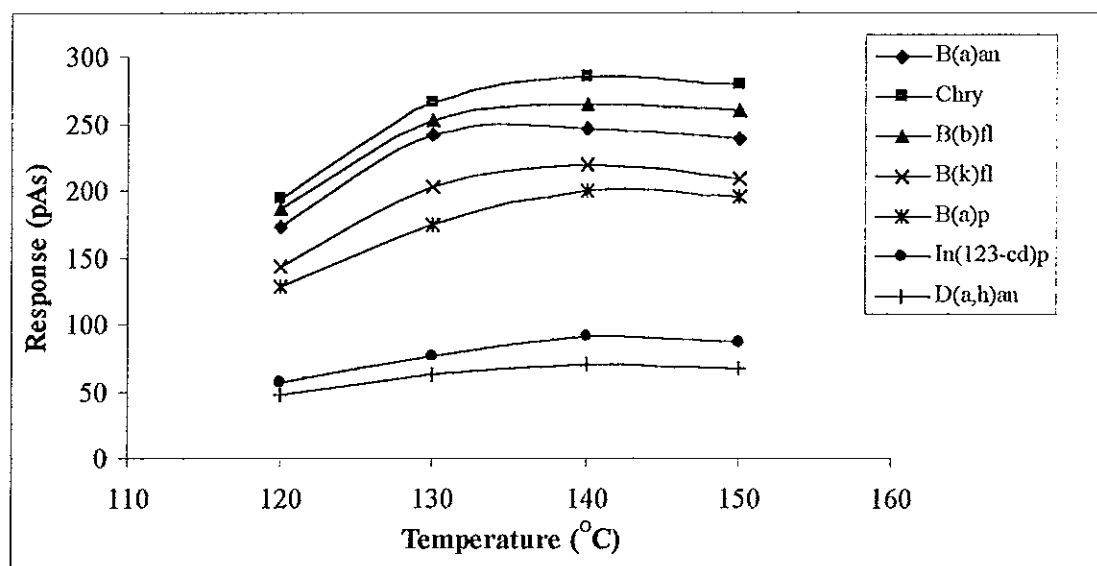


Figure 35 The responses of $10 \mu\text{g ml}^{-1}$, $1\text{-}\mu\text{l}$ PAHs standard working solution at different initial temperature

The effect of the initial temperature holding time on the response was shown in Table 42 and Figure 36, the difference between different hold time less than 10%. Therefore, the holding time for initial temperature was not necessary.

Table 42 The effect of hold time on the response and analysis time of $10 \mu\text{g ml}^{-1}$, $1\text{-}\mu\text{l}$ PAHs standard working solution

Time (min)	Response (pAs)*							Analysis time (min)*
	B(a)an	Chry	B(b)fl	B(k)fl	B(a)p	In(123-cd)p	D(a,h)an	
0	241.65	265.67	251.83	202.60	174.62	76.71	63.35	18.50
1	238.25	260.23	249.47	200.62	177.31	78.54	65.35	19.50
2	231.61	255.86	253.65	205.38	198.36	86.64	68.67	20.50
3	245.93	254.61	234.61	213.76	200.98	85.62	79.32	21.50

* 5 replication, RSD < 4%

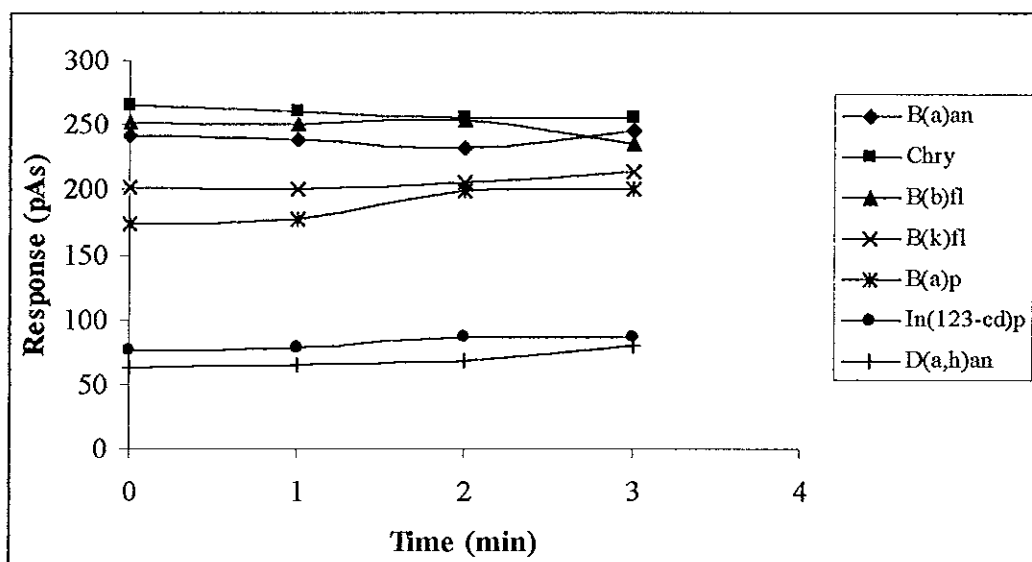


Figure 36 The responses of $10 \mu\text{g ml}^{-1}$, $1\text{-}\mu\text{l}$ PAHs standard working solution at different hold time

The initial temperature was ramped to 200°C at different ramp rate as shown in Table 43 and Figure 37. The rate 15°C/min was selected even though it gave lesser response than 20°C/min and 25°C/min but it gave a better baseline resolution .

Table 43 The effect of the first stage ramp rate on the response and analysis time of 10 µg ml⁻¹, 1-µl standard working solution

Ramp rate (°C/min)	Response (pAs)*							Analysis time (min)
	B(a)an	Chry	B(b)fl	B(k)fl	B(a)p	In(123-cd)p	D(a,h)an	
10	225.36	257.31	220.85	205.69	163.17	73.96	58.36	21.00
15	241.65	265.67	251.83	202.61	174.62	76.71	63.25	19.00
20	256.55	294.63	288.34	233.83	215.66	96.64	80.54	17.50
25	295.63	325.64	339.56	259.12	214.65	98.44	82.76	16.60

* 5 replication, RSD < 4%

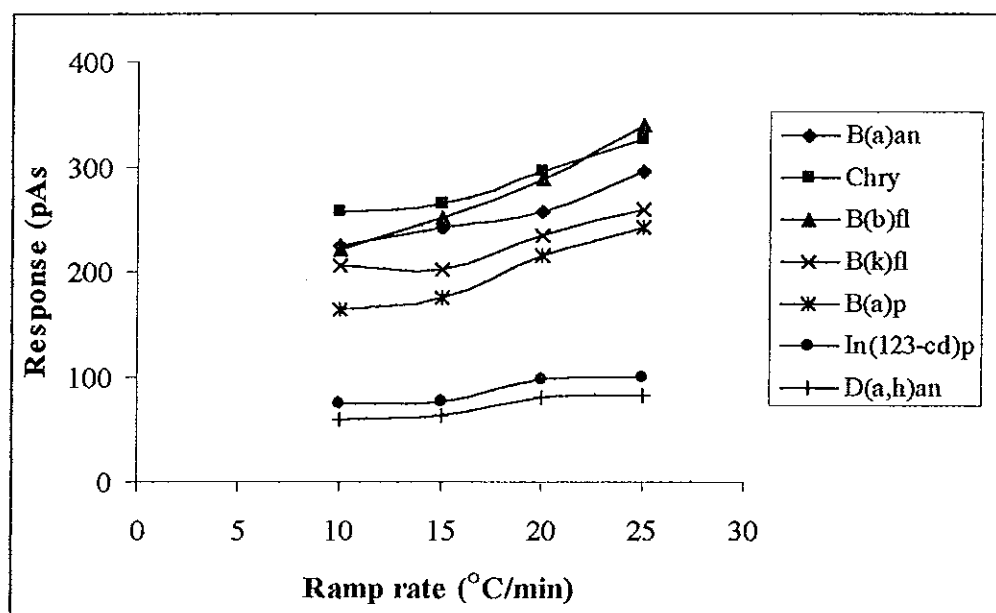


Figure 37 The responses of 10 µg ml⁻¹, 1-µl PAHs standard working solution at different first stage ramp rate

The second stage of temperature programming was obtained and the results are shown in Table 44 and Figure 38. The results indicated 220°C was optimum temperature *i.e.* it gave the highest response.

Table 44 The effect of second stage temperature on the response and the analysis time of 10 $\mu\text{g ml}^{-1}$, 1- μl standard working solution

Temperature (°C)	Response (pAs)*							Analysis time (min)
	B(a)an	Chry	B(b)fl	B(k)fl	B(a)p	In(123-cd)p	D(a,h)an	
200	187.33	220.82	198.91	169.34	158.47	65.64	52.34	18.50
210	232.92	244.09	232.45	189.16	176.90	87.52	67.32	18.00
220	256.45	277.47	264.3	202.89	189.57	91.28	77.41	17.50
230	249.12	262.84	256.94	196.55	182.45	88.28	71.53	17.00

* 5 replication, RSD < 4%

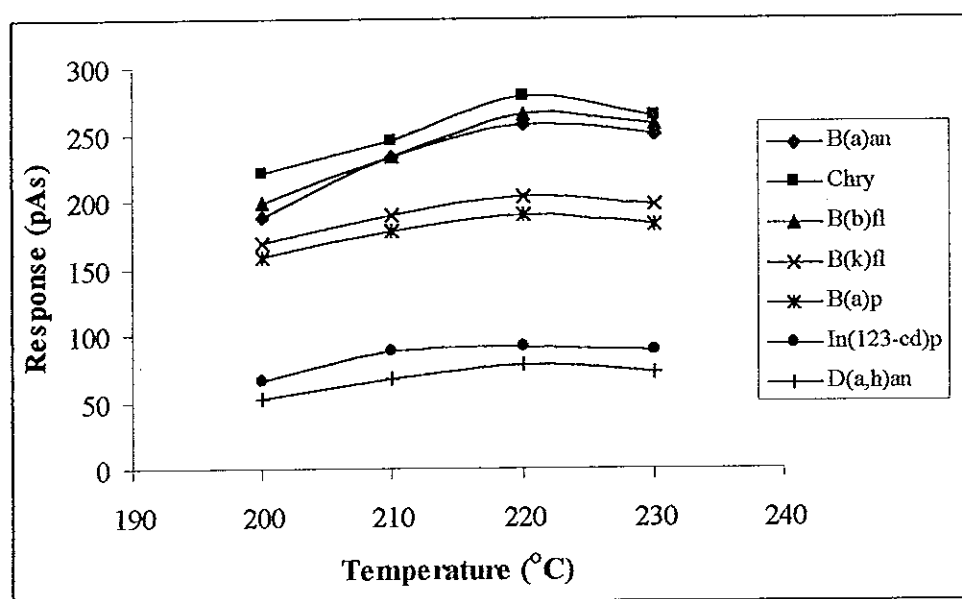


Figure 38 The responses of 10 $\mu\text{g ml}^{-1}$, 1- μl PAHs standard working solution at different second stage temperature

Table 45 and Figure 39 showed the responses of PAHs at various second stage temperature hold time. The responses were quite close between 1 to 3 min. So the hold time 1min was selected.

Table 45 The effect of hold time at the second stage temperature on the response and the analysis time of $10 \mu\text{g ml}^{-1}$, $1\text{-}\mu\text{l}$ standard working solution

Time (min)	Response (pAs)*							Analysis time (min)
	B(a)an	Chry	B(b)fl	B(k)fl	B(a)p	In(123-cd)p	D(a,h)an	
0	246.45	267.47	259.30	202.89	179.57	91.28	77.41	19.00
1	276.15	289.64	273.43	251.52	183.64	112.87	85.56	20.00
2	281.67	285.58	278.21	268.28	185.94	95.44	80.48	21.00
3	276.38	287.55	272.31	267.64	190.22	96.35	86.42	22.00

* 5 replication, RSD < 4%

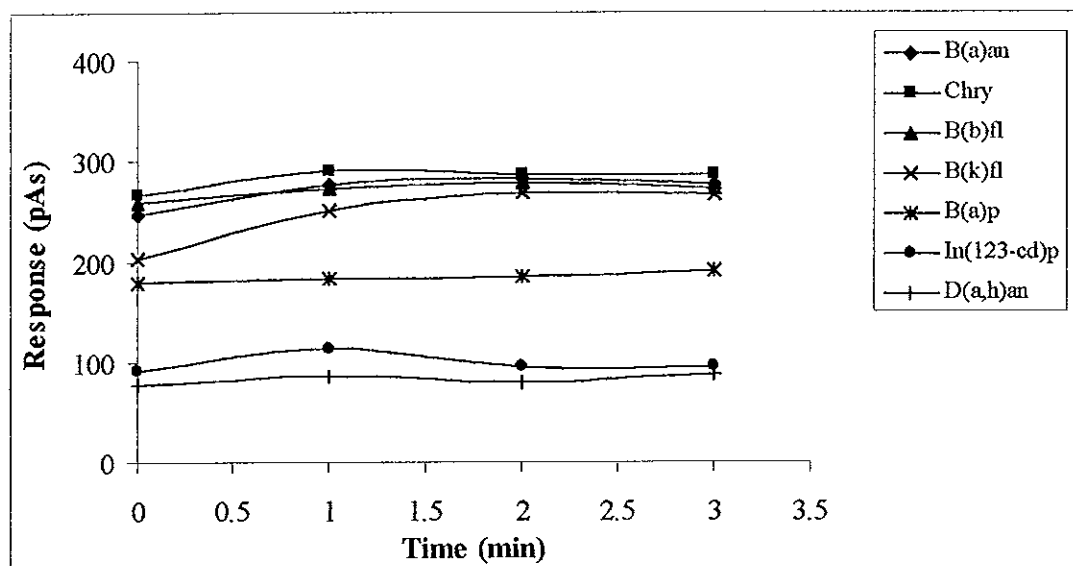


Figure 39 The responses of $10 \mu\text{g ml}^{-1}$, $1\text{-}\mu\text{l}$ PAHs standard working solution at different second stage temperature holding time

At the second ramp rate 5 and 7°C/min provided high responses (Table 46, Figure 40) but they gave unacceptable resolution between the 3rd and 4th peaks. While, 3°C/min provided a better baseline resolution between the 1st and 2nd and 6th and 7th peaks and also showed an acceptable resolution for the 3rd and 4th peak. So ramp rate at 3°C/min was the optimum.

Table 46 The effect of ramp rate at the second stage temperature on the response and the analysis time of 10 µg ml⁻¹, 1-µl standard working solution

Ramp rate (°C/min)	Response (pAs)*							Analysis time (min)*
	B(a)an	Chry	B(b)fl	B(k)fl	B(a)p	In(123-cd)p	D(a,h)an	
2	249.32	251.74	239.47	214.95	156.61	87.15	64.16	52.00
3	276.15	289.64	273.43	251.52	183.64	112.87	85.56	38.67
5	276.51	293.46	283.34	251.72	231.64	106.84	79.56	28.00
7	281.38	287.06	295.82	259.56	235.24	115.93	83.16	19.00

* 5 replication, RSD < 4%

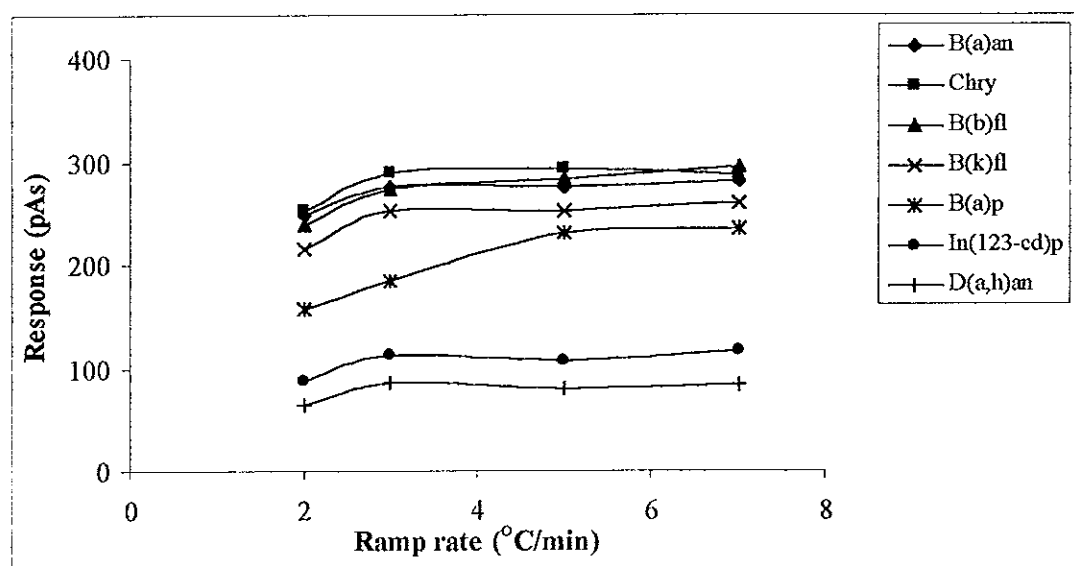


Figure 40 The responses of 10 µg ml⁻¹, 1-µl PAHs standard working solution at different second stage of ramp rate

The final temperature was optimized (experiment 2.3.3.11 step VII) and the results are shown in Table 47 and Figure 41. The highest responses of most PAHs were obtained at 290°C. it also gave the least analysis time. Therefore, 290°C was selected as the optimum final temperature.

Table 47 The effect of final temperature on the response and the analysis time of 10 µg ml⁻¹, 1-µl standard working solution

Temperature (°C)	Response (pAs)*							Analysis time (min)*
	B(a)an	Chry	B(b)fl	B(k)fl	B(a)p	In(123-cd)p	D(a,h)an	
270	179.97	195.63	184.87	166.74	141.69	77.48	60.93	28.67
280	250.06	282.38	274.71	228.56	196.37	94.56	68.85	32.00
290	275.48	314.78	290.88	249.42	234.24	119.98	80.58	35.33
300	276.15	289.64	273.43	251.52	183.64	112.87	85.56	38.67

* 5 replication, RSD < 4%

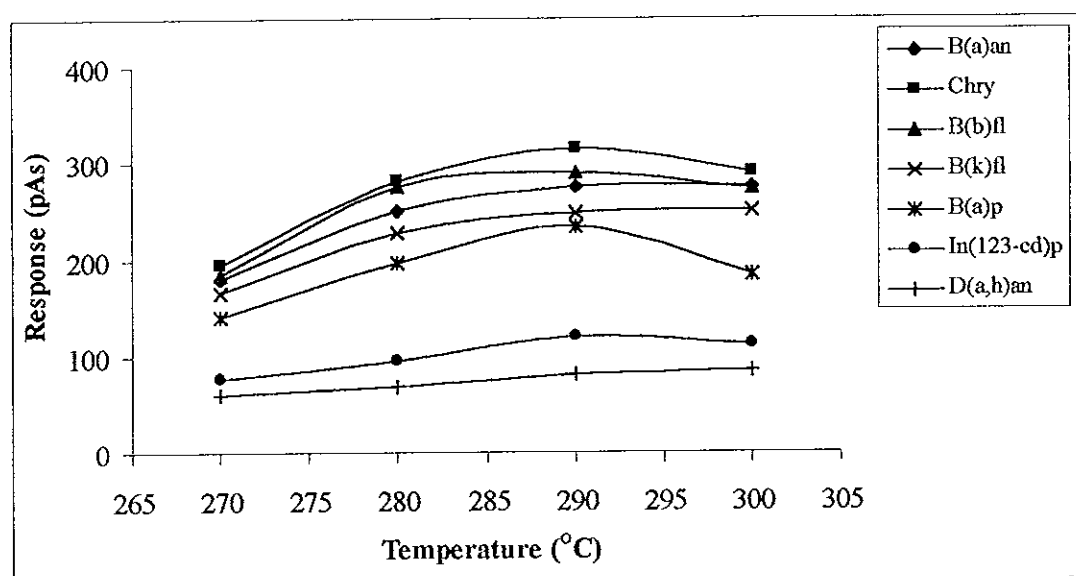


Figure 41 The responses of 10 µg ml⁻¹, 1-µl PAHs standard working solution at different final temperature

In summary the optimum conditions of the column temperature programming, with splitless mode injection, started at 130°C then ramped at a rate of 15°C/min to 220°C, held for 1 min. After that the second stage temperature of 220°C was ramped with a rate of 3°C/min to the final temperature of 290°C and held for 2 min (Figure 42). The purpose of holding the final temperature was for the signal to return to the baseline. The holding time at this temperature had no effect on the response and baseline resolution.

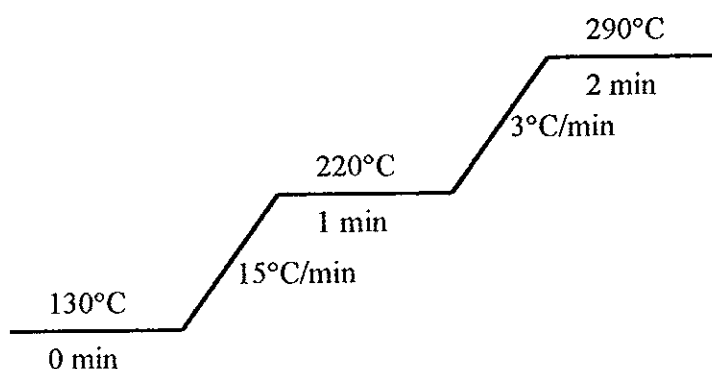


Figure 42 The optimum column temperature programming by splitless injection mode

3.1.12 Optimization of injector temperature

The FID gave the highest response for all seven PAHs at 280°C (Table 48, Figure 43) and this was selected to be the optimum injector temperature for splitless mode injection analysis.

Table 48 The effect of injector temperature on the response of 10 µg ml⁻¹, 1-µl PAHs standard working solution

Temperature (°C)	Response (pAs)*						
	B(a)an	Chry	B(b)fl	B(k)fl	B(a)p	In(123-cd)p	D(a,h)an
250	275.48	314.78	290.88	249.42	234.24	119.98	80.58
260	279.32	297.33	283.58	262.43	246.59	138.78	89.94
270	286.84	293.78	289.97	277.88	265.43	157.17	94.92
280	299.66	316.52	307.34	289.22	279.47	195.16	118.88
290	287.38	296.17	291.65	285.72	268.85	189.37	106.27

*5 replication, RSD < 4%

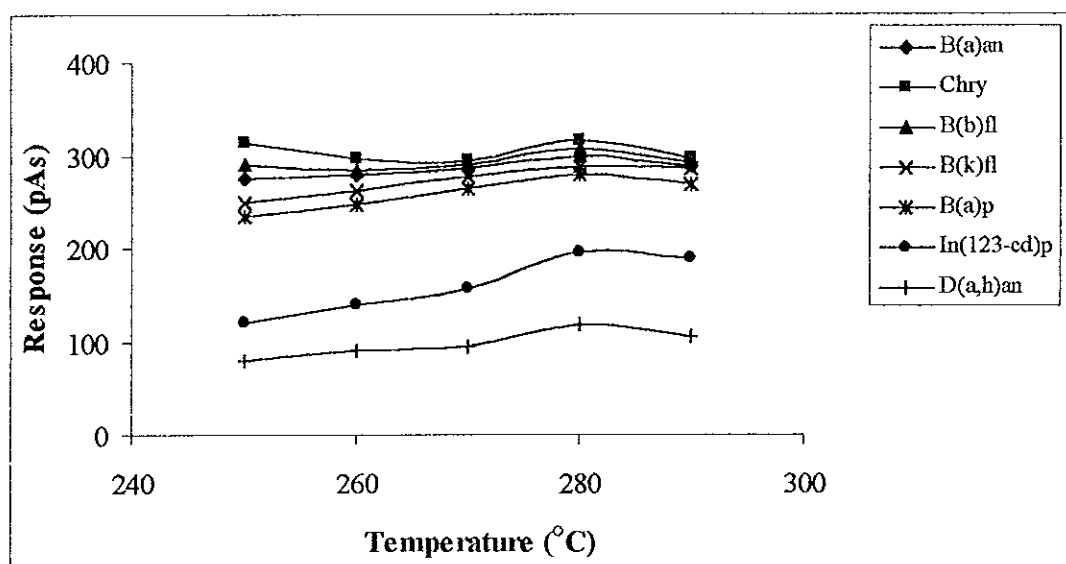


Figure 43 The responses of 10 µg ml⁻¹, 1-µl PAHs standard working solution at different injector temperature

3.1.13 Optimization of detector temperature

The responses from different detector temperature (experiment 2.3.3.11) are shown in Table 49 and Figure 44. The highest response of PAHs was obtained at 300°C, and this was the optimum detector temperature for splitless mode injection analysis.

Table 49 The effect of detector temperature on the response of 10 µg ml⁻¹, 1-µl PAHs standard working solution

Temperature (°C)	Response (pAs)*						
	B(a)an	Chry	B(b)fl	B(k)fl	B(a)p	In(123-cd)p	D(a,h)an
270	238.45	252.34	249.53	227.98	218.98	135.83	69.46
280	254.67	270.85	267.26	246.75	235.34	166.11	82.65
290	273.86	289.82	275.45	264.57	258.45	184.24	93.41
300	299.66	316.52	307.34	289.22	279.47	195.16	118.88

* 5 replication, RSD < 4%

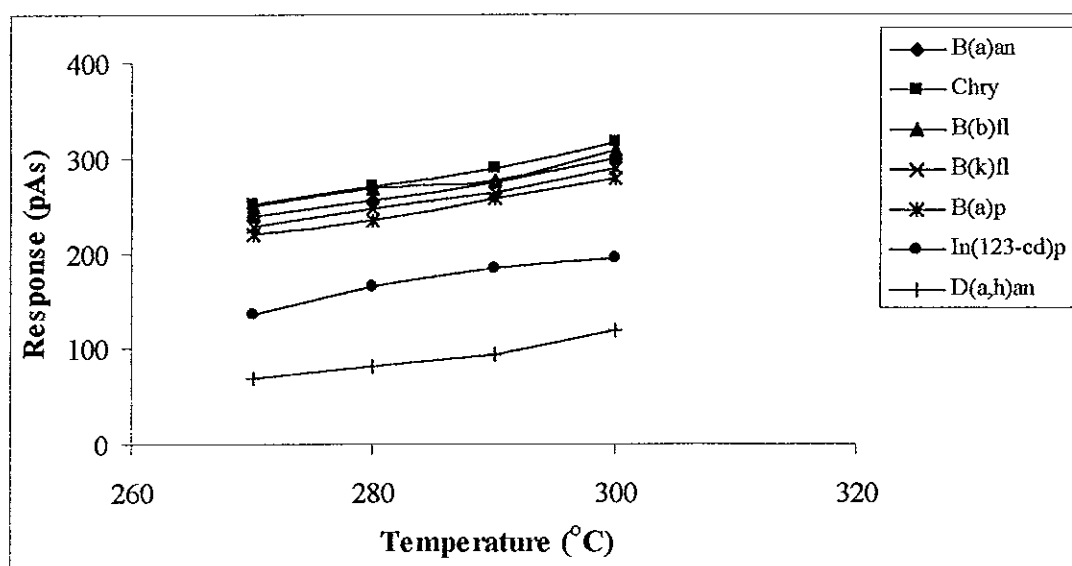


Figure 44 The responses of 10 µg ml⁻¹, 1-µl PAHs standard working solution at different detector temperature

3.1.14 Limit of detection (LOD)

The concentrations of PAHs where S/N is more than 3.0 are shown in Table 50. The different response of the FID to each PAHs was due to the structure of the compound (see 1.2.1). The limits of detection for all PAHs are summarized in Table 51. These LOD are better than those obtained by Jaouen-Madoulet *et al.*, (2000) where the analysis was done by DB-5 (60 m × 0.25 mm i.d. × 0.25 μm thickness) and DB-608 (30 m × 0.53 mm i.d. × 0.5 μm thickness) with on-column injection mode and equipped with GC-FID. The LOD for seven PAHs in group B2 in their work were ranged from 0.90 to 2.47 ng μl⁻¹.

Table 50 The relationship between the response of PAHs and concentrations

Concentration (μg ml ⁻¹)	Response (pAs)*						
	B(a)an	Chry	B(b)fl	B(k)fl	B(a)p	In(123-cd)p	D(a,h)an
0.025	N.D	1.48	N.D	N.D	N.D	N.D	N.D
0.050	1.55	1.85	1.12	N.D	N.D	N.D	N.D
0.100	3.11	3.71	2.25	2.11	2.19	N.D	N.D
0.250	6.34	7.42	4.51	4.23	4.38	1.28	N.D
0.500	12.57	14.79	8.81	7.89	8.08	2.50	2.42
0.750	20.19	23.62	14.68	13.21	14.37	4.94	5.00

* 5 replication, RSD < 4%

Table 51 The limits of detection for individual PAHs with the optimum splitless mode injection GC conditions

PAHs	Limit of detection (ng ml ⁻¹)
B(a)an	50
Chry	25
B(b)fl	50
B(k)fl	100
B(a)p	100
In(123-cd)p	250
D(a,h)an	500

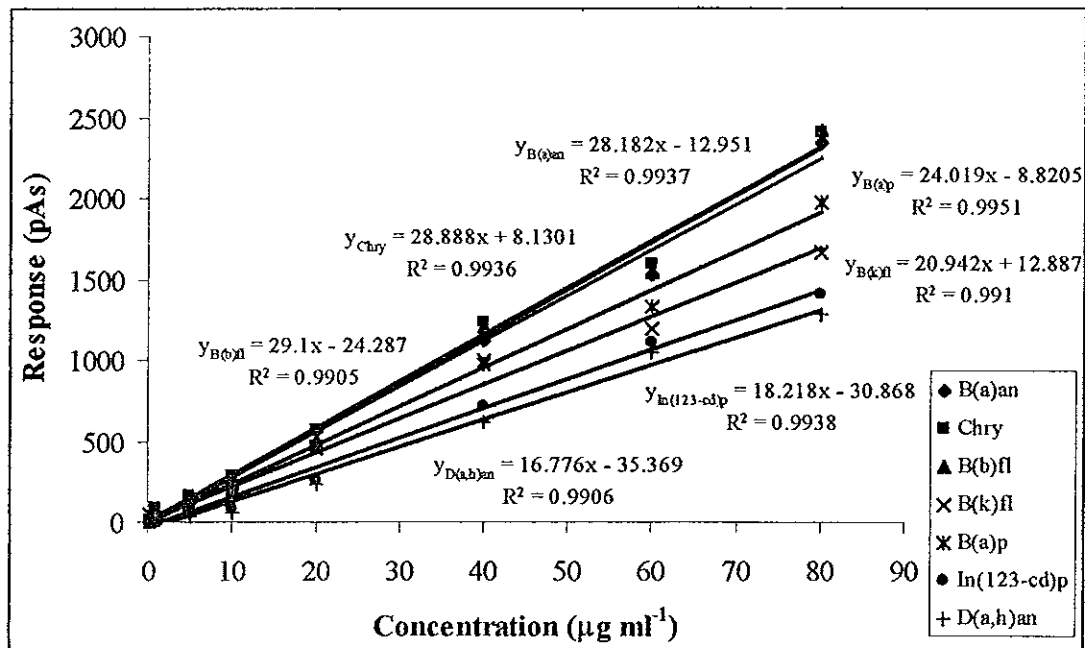
3.1.15 Linear dynamic range

As in experiment 2.3.3.13, the linear dynamic range was investigated experimentally by running various concentration. Table 52 and Figure 45 show the responses and linear regression, R^2 , of individual PAHs at various concentration. The system provided a wide linear dynamic range from 0.25 to 80.00 $\mu\text{g ml}^{-1}$ with a good linear regression, $R^2 > 0.99$. The linear dynamic range in this work are better than in the work by Jaouen-Madoulet and co-worker (2000). The linear dynamic range in their work was found to be between 2 to 40 $\text{ng } \mu\text{l}^{-1}$ analyzed by DB-5 and DB-608 GC-FID.

Table 52 The response of individual PAHs at various concentration

Concentration ($\mu\text{g ml}^{-1}$)	Response (pAs)*						
	B(a)an	Chry	B(b)fl	B(k)fl	B(a)p	In(123-cd)p	D(a,h)an
0.25	6.34	7.42	4.51	4.23	43.89	1.28	1.37
0.50	12.57	14.79	8.81	7.89	8.08	2.5	2.42
0.75	20.19	23.62	14.68	13.21	14.37	4.94	5.00
1.00	37.95	89.03	48.34	28.39	41.84	3.16	5.56
5.00	125.13	154.97	114.23	109.26	90.67	47.11	32.42
10.00	231.46	284.05	210.28	202.60	170.04	89.65	63.31
20.00	564.49	562.94	510.58	453.16	475.28	266.07	235.79
40.00	1123.79	1233.91	1212.65	1001.41	973.45	712.19	617.42
60.00	1527.65	1587.60	1541.57	1203.01	1338.67	1116.68	1050.67
80.00	2350.53	2406.03	2420.76	1660.66	1979.67	1404.19	1281.06

* 5 replication, RSD < 4%

**Figure 45** The linear dynamic range of seven PAHs

By comparing the response, limit of detection, and linear dynamic range between two modes of injection – split and splitless mode. It can be seen that at optimum conditions splitless mode provided the higher response, lower detection limit and more extensive linear dynamic range than the split mode at the same concentration. Thus, the optimum GC-FID conditions with splitless mode injection was used for trace analysis of PAHs in water.

The difference between split and splitless mode injection was the amount of sample introduced (analyte) into the column. The liner, an open end glass tube situated in the inlet part beneath the septum of injection port. The liner types were different in the split and splitless modes and a suitable liner would provide a correct amount of sample (analyte) that enters the column. In this thesis, both types of liners, split and splitless liners were investigated. Figure 46 and 47 show the configuration of each liner type and their connection to capillary column. From the figure it can easily explain how the liner controls the amount of sample (analyte). The split liner has a space between the inner wall of the liner and the outer surface of the capillary column, therefore it could split some portion of analyte to the purge vent valve. For splitless liner, it is a good fit to the capillary column and very little solvent can pass through to the purge vent valve. Therefore the amount of analyte entering the column is more than in the split mode. Figure 48 shows the comparison of chromatogram profile, response and analysis time between split and splitless injection mode.

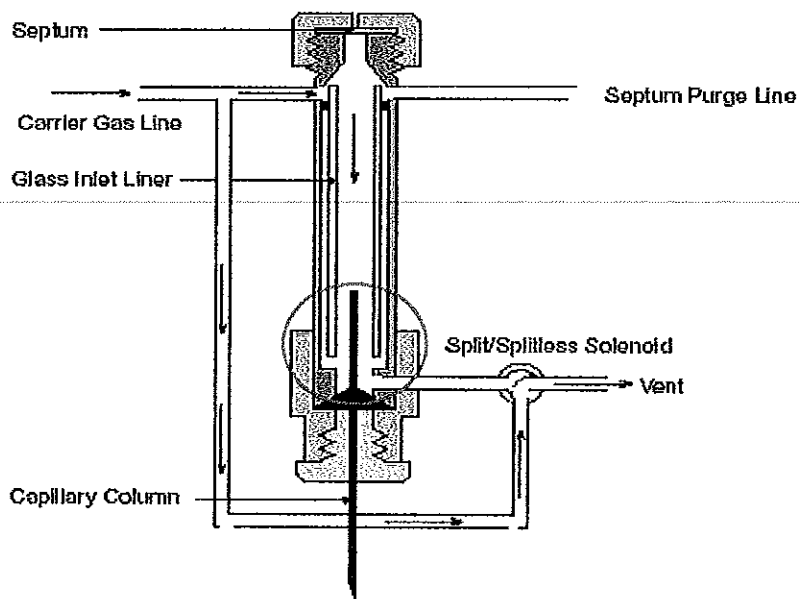


Figure 46 Split liner

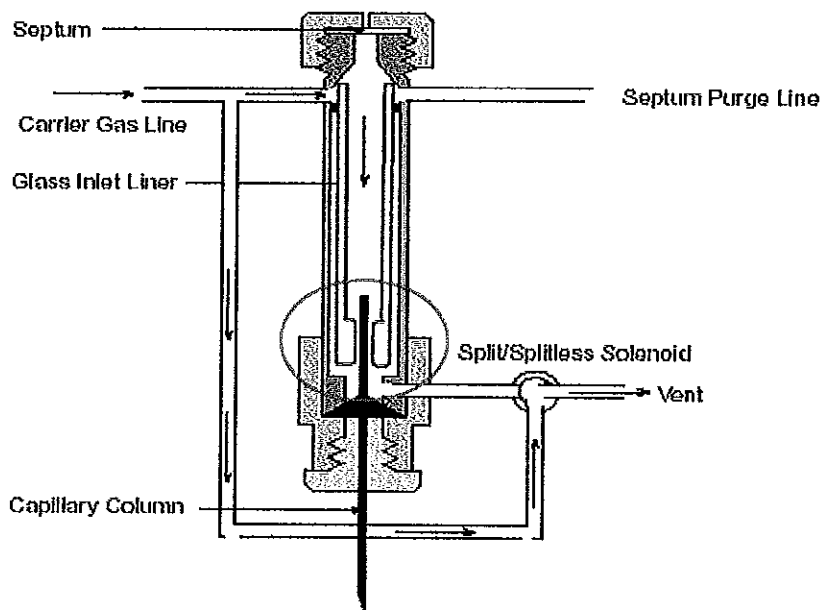
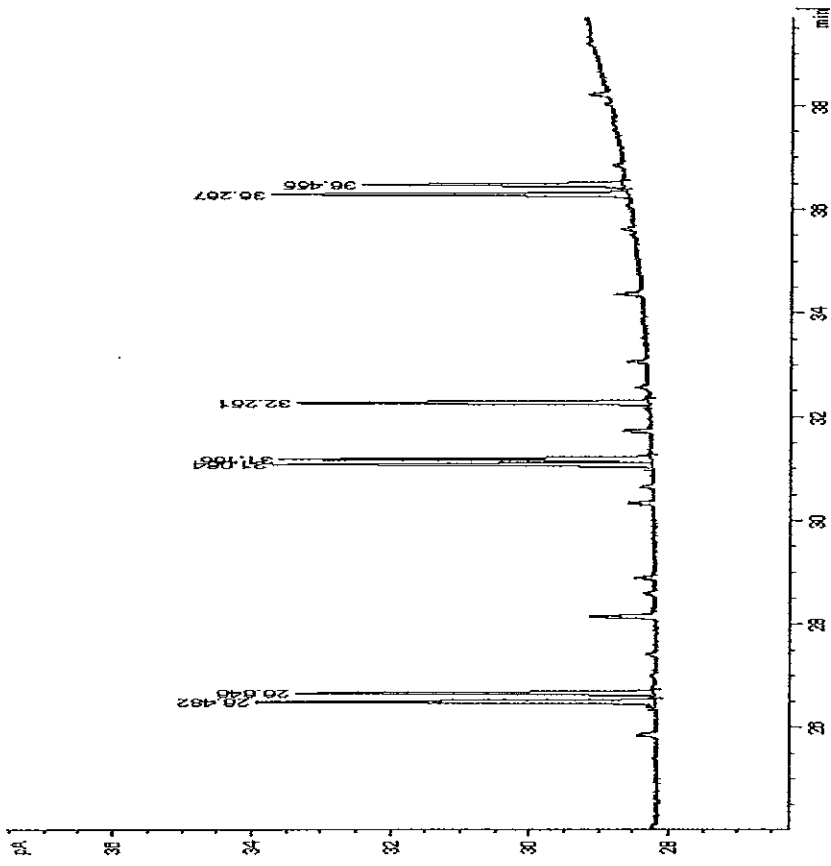


Figure 47 Splitless liner

(a) split injection



(b) splitless injection

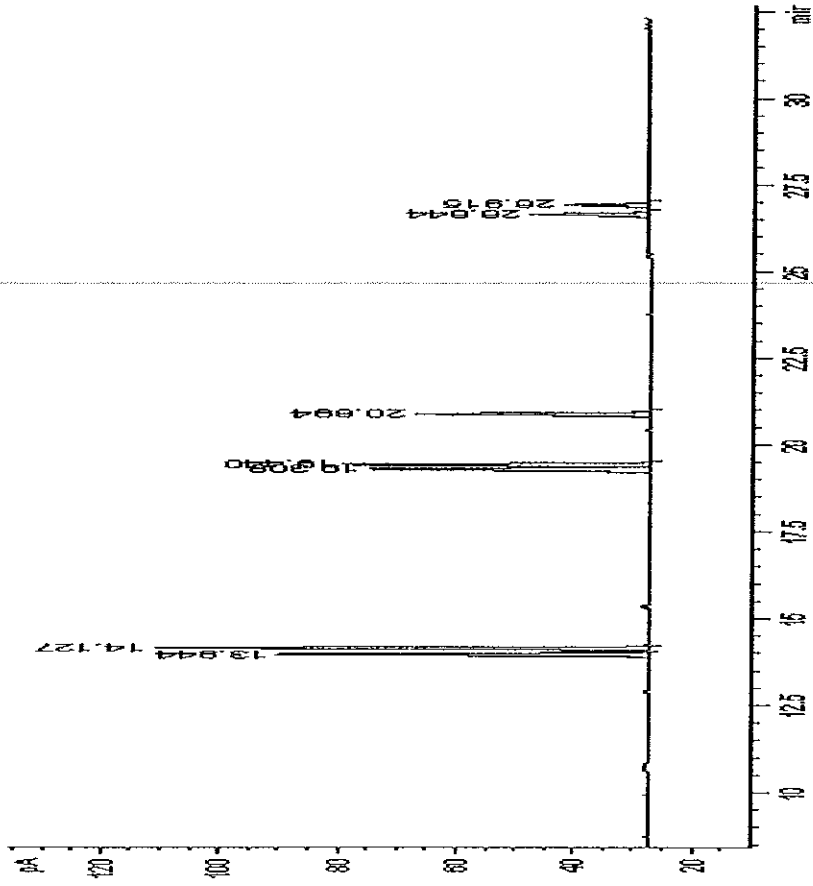


Figure 48 Comparison the response and analysis time obtained from split and splitless injection

3.1.16 Response factor (RF)

The response factors were determined using the integrated peak response of each analyte at various concentration compared with the integrated peak response of B(a)p, assigned response factor = 1. The results shown the precision of RF of each PAHs (Table 53).

Table 53 Relative response factor of seven PAHs at various concentration

Concentration ($\mu\text{g ml}^{-1}$)	Response Factor (RF)*						
	B(a)an	Chry	B(b)fl	B(k)fl	B(a)p	In(123-cd)p	D(a,h)an
0.50	1.15	1.33	1.05	0.77	1.00	0.31	0.23
0.75	1.17	1.34	1.02	0.81	1.00	0.34	0.24
1.00	1.17	1.34	1.04	0.76	1.00	0.33	0.22
1.25	1.16	1.33	1.02	0.81	1.00	0.35	0.21
1.50	1.18	1.36	1.04	0.81	1.00	0.34	0.21
Average	1.17±0.01	1.34±0.01	1.05±0.01	0.79±0.02	1.00	0.33±0.01	0.22±0.01

* 5 replication, RSD < 4%

3.1.16 Internal standardization plot method

Experiment 2.3.3.15 gave the relationship between the concentration of seven PAHs and the ratio of the analyte to the internal standard peak area (Table 54 and Figure 49).

In chemical analysis, this method combines the sample and standard into one injection. A calibration mixture is prepared containing known amounts of each component to be analyzed, plus an added compound that is not present in the analytical sample. From the results the internal standardization method provided a good linear regression (0.9934 – 0.9987). For the determination of PAHs in real sample by this method, the signal intensity was converted to concentration. The concentration of analyte *i.e.* a peak area, M_a is proportional to signal for the analyte, A_a as

$$M_a = RF \times A_a$$

Table 54 The relation between the concentration of PAHs and the ratio of peak area of analyte to internal standard (A_a/A_{is})

Concentration ($\mu\text{g ml}^{-1}$)	A_a/A_{is}^*						
	B(a)an	Chry	B(b)fl	B(k)fl	B(a)p	In(123-cd)p	D(a,h)an
0.50	0.31	0.21	0.28	0.19	0.28	0.23	0.15
0.75	0.59	0.60	0.55	0.57	0.56	0.47	0.44
1.00	0.92	0.92	0.84	0.86	0.84	0.73	0.69
1.25	0.26	1.31	1.26	1.24	1.20	0.91	1.10
1.50	0.67	1.75	1.58	1.55	1.49	1.16	1.34

* 5 replication, RSD < 4%

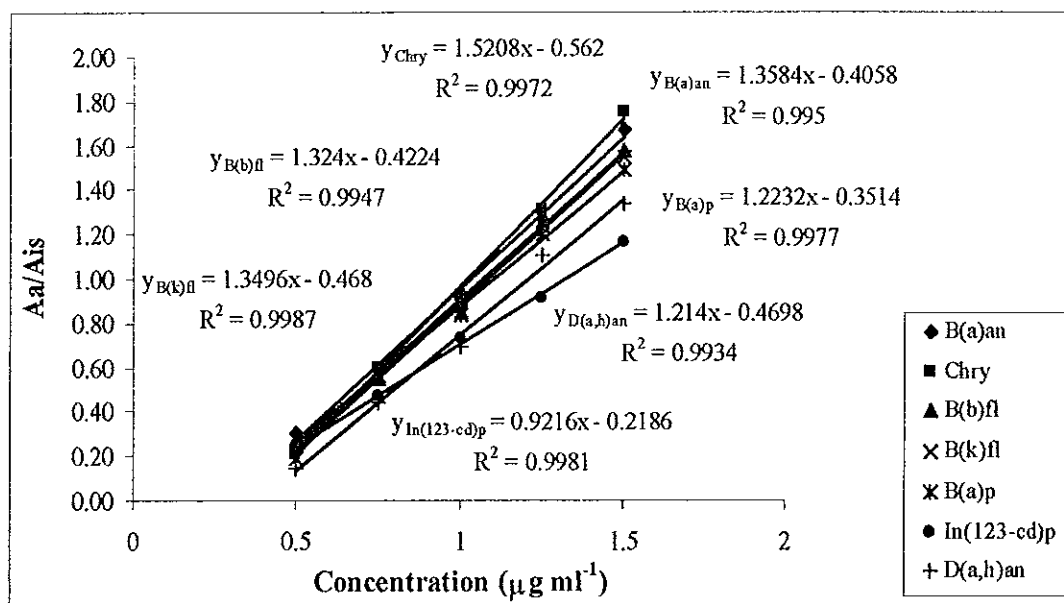


Figure 49 The relationship between concentration of PAHs and the ratio of peak area of analyte to internal standard

3.2 Sample preparation by Solid Phase Extraction

3.2.1 Elution solvent

In the experiment 2.3.4.1, ultrapure water spiked with known concentration of seven PAHs mixture was used as water sample. The suitable used to elute PAHs that retained on the disk were studied. Once the analytes are retained on the disk, they can be eluted by an organic solvent such as methanol, dichloromethane, ethyl acetate or mixture of them (Manoli and Samara, 1999). The polarity of the solvent must be considered, the dipole moment informs the polarity strength of molecule *i.e.* the molecule that have high dipole moment will have strong polarity. The dipole moment of methanol, ethyl acetate and dichloromethane are 1.7, 1.7 and 1.6 respectively (Merck KgaA, Germany, 1999/2000). In addition, the dielectric constant provided good information for predicting the suitable solvent for PAHs. An organic solvent with high dielectric constant will have high polarity. The dielectric constant at 20°C of methanol, ethyl acetate and dichloromethane are 3.26, 0.6 and 0.91 respectively (Merck KgaA, Germany, 1999/2000). From the described properties, the PAHs can be partition into dichloromethane as well as ethyl acetate. From the results (Table 55, Figure 50), show that ethyl acetate provided the highest recovery: 67 – 112% for extraction of all seven PAHs with a good precision, %RSD less than 10, dichloromethane: 58 – 93%, methanol: 65 – 94% and dichloromethane: ethyl acetate (1:1): 64 – 97%. Therefore, ethyl acetate was selected as the appropriate solvent to extract PAHs in water sample.

Table 55 The percentage recovery of seven PAHs extraction with dichloromethane, ethyl acetate, methanol and dichloromethane: ethyl acetate (1:1)

PAHs	DCM*		EtOAc*		MeOH*		DCM:EtOAc (1:1)*	
	%Recovery	%RSD	%Recovery	%RSD	%Recovery	%RSD	%Recovery	%RSD
B(a)an	93.8	7.6	110.6	3.5	94.7	3.3	97.1	9.2
Chry	79.5	4.0	88.5	5.5	84.5	4.6	92.5	8.1
B(b)fl	91.4	6.3	112.3	7.5	94.0	7.5	97.8	5.6
B(k)fl	79.7	4.4	97.8	4.9	89.1	5.8	90.6	5.5
B(a)p	74.3	3.8	87.4	2.9	81.0	7.4	80.6	4.6
In(123-cd)p	79.4	3.4	96.0	4.2	79.9	3.6	82.6	7.2
D(a,h)an	58.1	5.2	67.6	5.5	65.3	6.8	64.1	3.8

* 5 replication, RSD < 10%

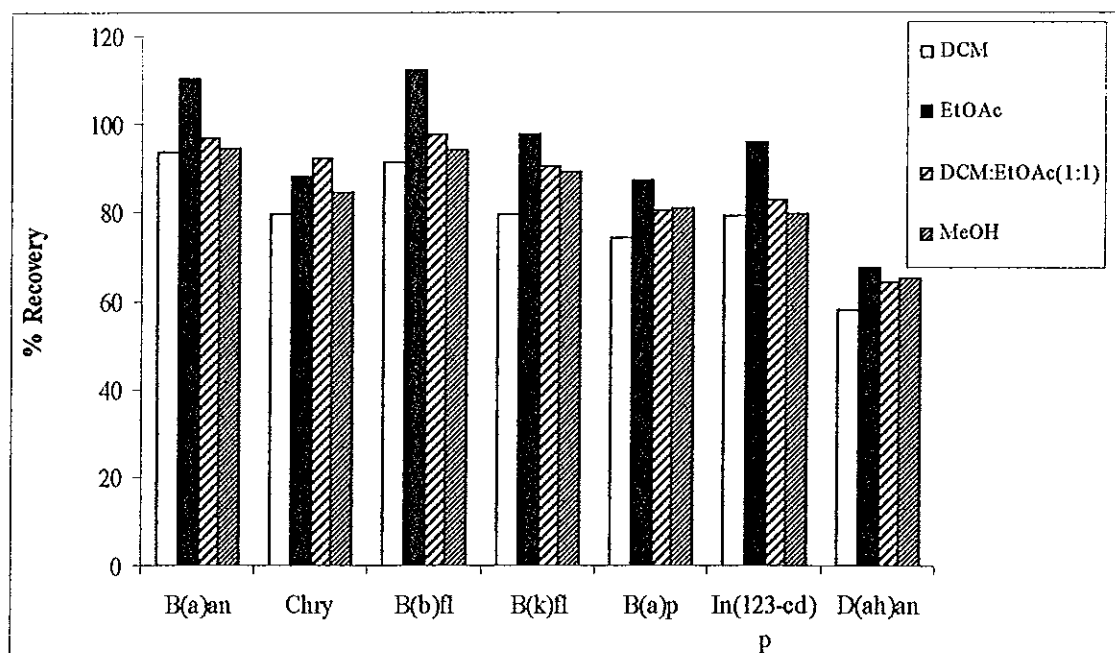


Figure 50 The effect of type of eluting solvent to the recovery of PAHs extraction

3.2.2 Volume of eluting solvent

The volume of organic solvent used in extraction processes was an important parameter because it would affect the extraction efficiency. If the volume is too small it may not be sufficient to elute the analyte on the disk. SPE is a technique which does not require large volumes of (toxic) organic solvents, unlike LLE. Therefore, it was necessary to optimize the volume of eluting solvent. Experiment 2.3.4.2 varied two portions of different eluting solvent and results (Table 56 and Figure 51) showed that recoveries from two portions of 3 to 5 ml ethyl acetate were not much different and the recoveries were less for two portions of 2 ml ethyl acetate. Therefore, to minimize solvent used, two portions of 3 ml ethyl acetate was selected to be the appropriate solvent volume to extract PAHs in water sample.

Table 56 The percentage recovery of seven PAHs with 2×2 ml, 2×3ml, 2×4 ml and 2×5 ml ethyl acetate

PAHs	2×2 ml*		2×3 ml*		2×4 ml*		2×5 ml*	
	%Recovery	%RSD	%Recovery	%RSD	%Recovery	%RSD	%Recovery	%RSD
B(a)an	74.3	6.8	112.9	4.7	111.6	5.6	110.6	3.5
Chry	67.3	8.4	89.3	5.3	88.4	6.4	88.5	5.5
B(b)fl	71.9	9.4	111.7	6.2	11.65	3.9	112.3	7.5
B(k)fl	69.5	7.1	96.9	4.8	95.6	5.7	97.8	4.9
B(a)p	69.2	6.8	89.6	5.7	89.3	7.7	87.4	2.9
In(123-cd)p	54.3	5.4	95.6	5.5	97.3	4.8	96.0	4.2
D(a,h)an	44.6	6.5	67.3	4.5	65.1	4.9	67.6	5.5

* 5 replication, RSD < 10%

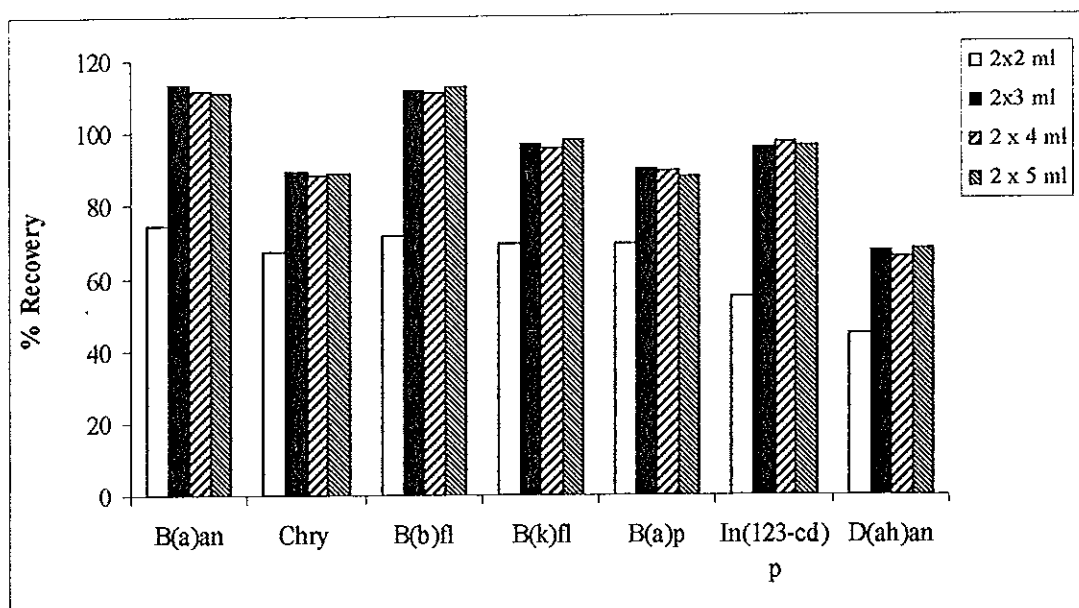


Figure 51 The effect of volume of solvent to the recovery of PAHs extraction

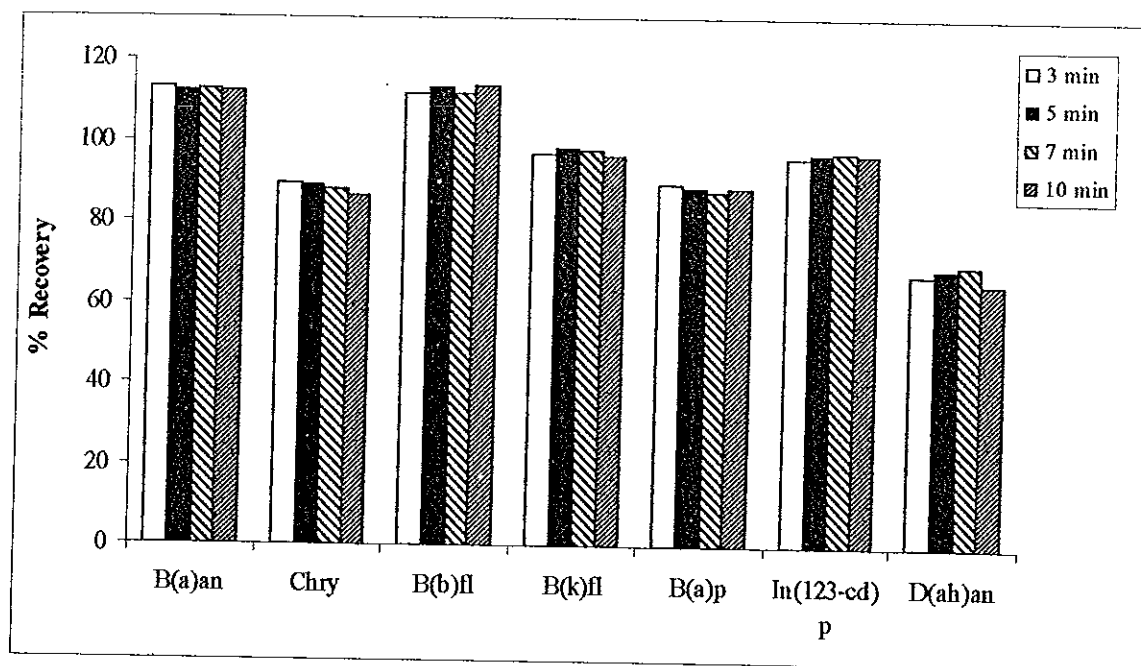
3.2.3 Drying time

Drying of the SPE disk after sample loading is also an important aspect to be taken into account. Water must be removed from the disk before elution otherwise it would affect the recovery. Table 57 and Figure 52 show the comparison of different drying time. There was difference in each variation of the drying time, thus to minimize the extraction time, 3 min was selected to dry the disk after sample loading.

Table 57 The percentage recovery of drying time as 3, 5, 7 and 10 min

PAHs	3 min*		5 min*		7 min*		10 min*	
	%Recovery	%RSD	%Recovery	%RSD	%Recovery	%RSD	%Recovery	%RSD
B(a)an	112.9	4.7	112.9	4.7	111.6	5.6	112.3	8.4
Chry	89.3	5.3	89.3	5.3	88.4	6.4	86.4	5.6
B(b)fl	111.7	6.2	111.7	6.2	110.6	3.9	113.4	7.4
B(k)fl	96.9	4.8	96.9	4.8	95.6	5.7	96.3	5.3
B(a)p	89.6	5.7	89.62	5.7	89.3	7.7	88.5	3.7
In(123-cd)p	95.6	5.5	95.6	5.5	97.3	4.8	96.9	4.5
D(a,h)an	67.3	4.5	67.3	4.5	65.1	4.9	65.3	6.8

* 5 replication, RSD < 10%

**Figure 52** The effect of drying time to the recovery of PAHs extraction

3.4.3 Percentage of modifier

The solid-phase extraction of PAHs seems like a simple process since it expected no breakthrough problems. However, the solubility of PAHs, decreased as the molecular weight increased. This brought up a problem because it could led to an adsorption problem during sampling and storage. To increase the solubility, an organic solvent is usually added to the sample. The concentration of the organic solvent is a critical parameter. If it is too small it can not solubilize the high molecular weight of PAHs. If the amount is too large, the breakthrough volume will be low for the low molecular weight PAHs. Thus, the percentage of adding modifier must be optimized. In this research 2-propanol was selected as the solubilized modifier (experiment 2.3.4.4). Three different amount were studied. Table 58 and Figure 53 show the results and 0.5% (v/v) 2 – propanol was the appropriate concentration to be added to the sample since it provided the best recovery.

Table 58 Comparison of percentage recovery of percentage organic modifier as 0, 5 and 10

PAHs	0%*		0.5%*		1.0%*	
	%Recovery	%RSD	%Recovery	%RSD	%Recovery	%RSD
B(a)an	55.3	6.4	112.9	4.7	104.6	7.8
Chry	46.4	5.8	89.3	5.3	84.4	5.6
B(b)fl	61.6	7.4	111.7	6.2	110.5	8.3
B(k)fl	45.6	5.3	96.9	4.8	95.0	4.8
B(a)p	43.0	8.1	89.6	5.7	8.7	7.2
In(123-cd)p	48.5	4.5	95.6	5.5	93.6	5.8
D(a,h)an	32.7	6.2	67.3	4.5	67.4	7.6

* 5 replication, RSD < 10%

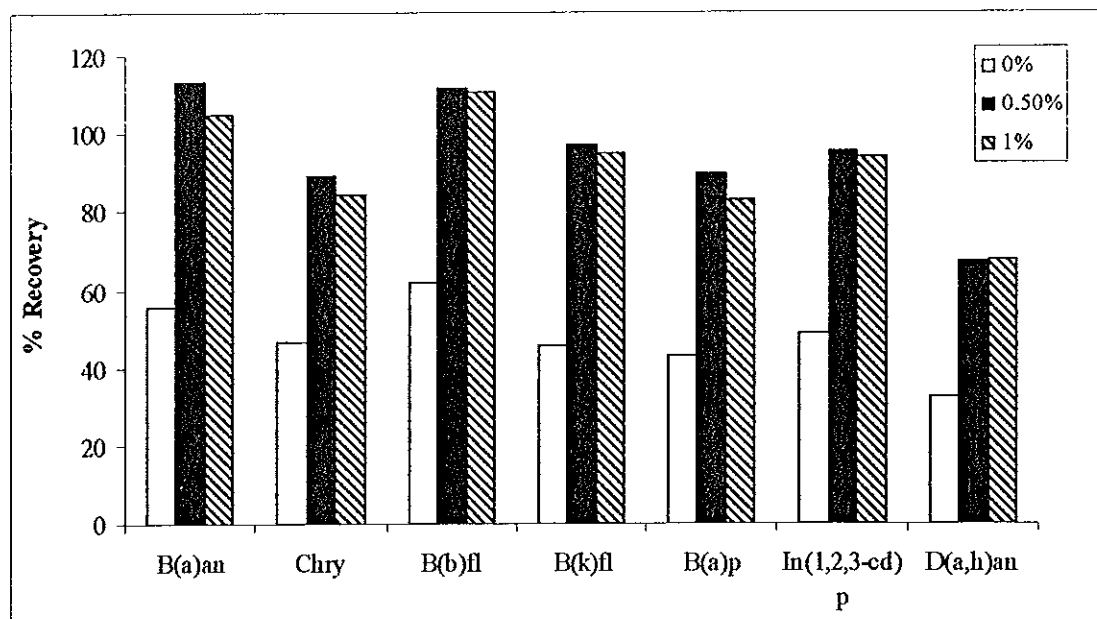


Figure 53 The effect of percentage of 2-propanol to the recovery of PAHs extraction

Table 59 summarized the percentage of recovery for the seven PAHs when extracted and enriched by SPE C₁₈ disk. In this work, 0.5% v/v of 2-propanol was added to sample before loading to the disk. After the water sample was loaded to the disk, it was dried for 3 minutes and then eluted by two portions of 3 ml ethyl acetate. The recoveries are better than those obtained by Urbe and Ruana (1997). They applied C₁₈ with glass fiber matrix to extract Fluoranthene, Benzo(b)fluoranthene (85±9), Benzo(k)fluoranthene (85±9), Benzo(a)pyrene (85±6), Benzo(ghi)perylene and Indeno(1,2,3-cd)pyrene (78±10). The recovery in this study also showed the better values than the work by Kootstra and co-worker (1995). They used C18 cartridge to extract 16 PAHs and the recovery of seven PAHs (group B2) from there are ranged in 51 to 75.

Table 59 The recovery of seven PAHs from C₁₈ disk

PAHs	%Recovery	%RSD
B(a)an	112.9	4.7
Chry	89.3	5.3
B(b)fl	111.7	6.2
B(k)fl	96.9	4.8
B(a)p	89.6	5.7
In(123-cd)p	67.3	5.5

3.3 Qualitative and quantitative analysis of PAHs in water

Water samples were collected from 3 sites, *i.e.* two water treatment ponds of Songklanagarind Hospital and Sri trang pond, and analyzed at the optimum conditions of this work. The studies showed that the concentration of PAHs in water were at trace levels and lower than the limit of detection. Therefore, the sample preparation (optimum SPE conditions) was used to extract, clean up and preconcentrate PAHs in water before analyzed by GC-FID. When water samples were extracted by SPE and analyzed by GC-FID at the optimum conditions by the internal standardization method PAHs components were not detectable. Therefore, the standard addition method was applied with the same samples. The results and standard addition calibration curves of each sample were shown in Tables 60 – 66 and Figures 54 – 60. Since the limit of detection of each component was different, so the level of concentration of each PAHs added into the samples were not the same (Table 8, experiment 2.3.5.4).

Table 67 shows the PAHs concentrations of the samples analyzed by standard addition methods. From the studies with the real water samples, the matrix in the sample showed no interference and the chromatogram of the seven PAHs was relative cleared. The unknown peak appeared in the chromatogram at a retention time of about 15 min, was not overlapping with any peak of PAHs. The standard addition method confirmed that the concentrations of PAHs in all real water samples were lower than the limit of detection *i.e.* 1.16-12.44 ng ml⁻¹. According to the work of Wolska and co-worker (1999), PAHs in water were extracted by SPE and analyzed by GC-MS. They found the PAHs concentration in water in range of 0.01 to 0.1 ng ml⁻¹, but for PAHs in group B2 they found 0.01 to 0.03 ng ml⁻¹.

Table 60 The response of B(a)an for sample site 1, 2 and 3 at various spiked concentration level

Spiked concentration (ng ml ⁻¹)	B(a)an (pAs)		
	Site 1	Site 2	Site 3
50	24.44	21.75	29.89
70	34.22	28.45	37.65
90	43.99	36.15	48.40
110	48.88	45.85	59.16

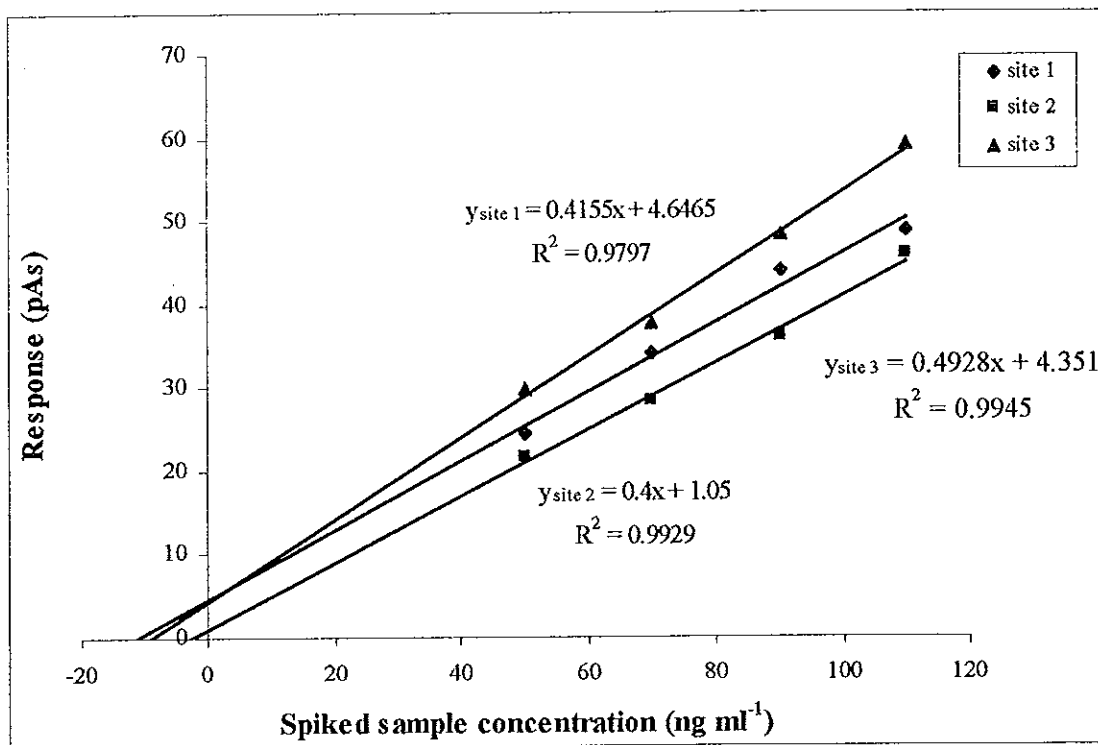


Figure 54 The standard addition calibration curve of B(a)an

Table 61 The response of Chry for sample site 1, 2 and 3 at various spiked concentration level

Spiked concentration (ng ml ⁻¹)	Chry (pAs)		
	Site 1	Site 2	Site 3
30	21.67	20.54	22.05
50	33.17	26.57	34.73
70	45.56	34.59	48.48
90	60.01	47.62	60.15

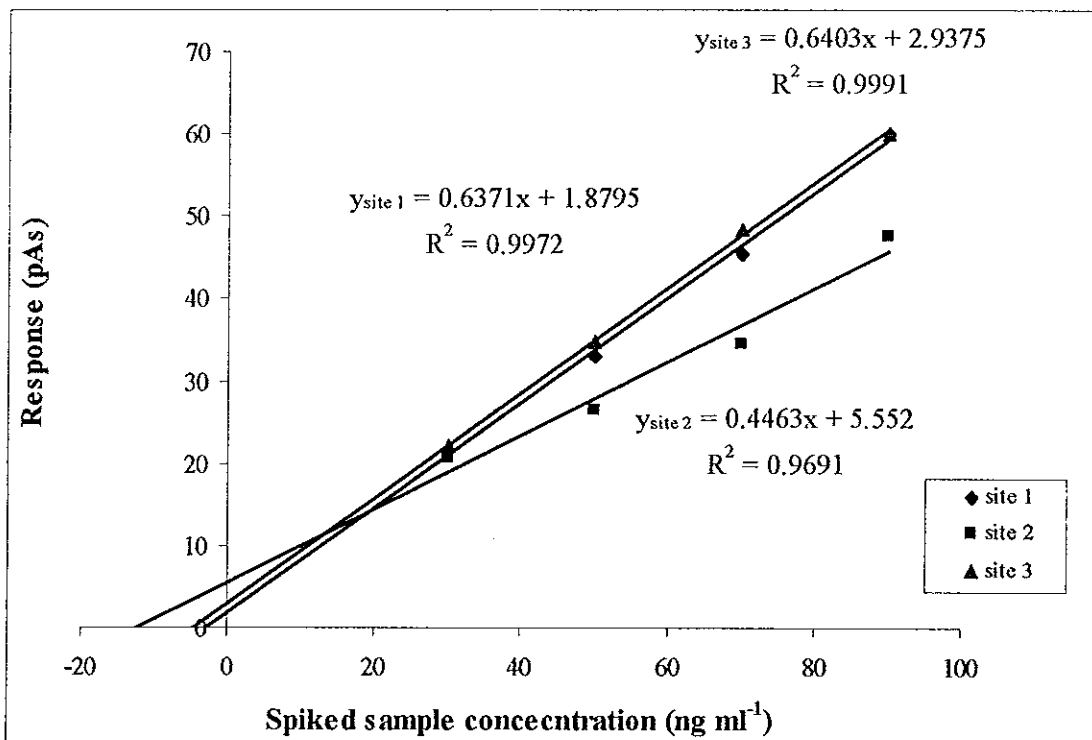


Figure 55 The standard addition calibration curve of Chry

Table 62 The response of B(b)fl for sample site 1, 2 and 3 at various spiked concentration level

Spiked concentration (ng ml ⁻¹)	B(b)fl (pAs)		
	Site 1	Site 2	Site 3
50	21.68	17.68	19.55
70	28.35	22.25	27.77
90	36.02	229.22	34.99
110	44.70	36.50	42.21

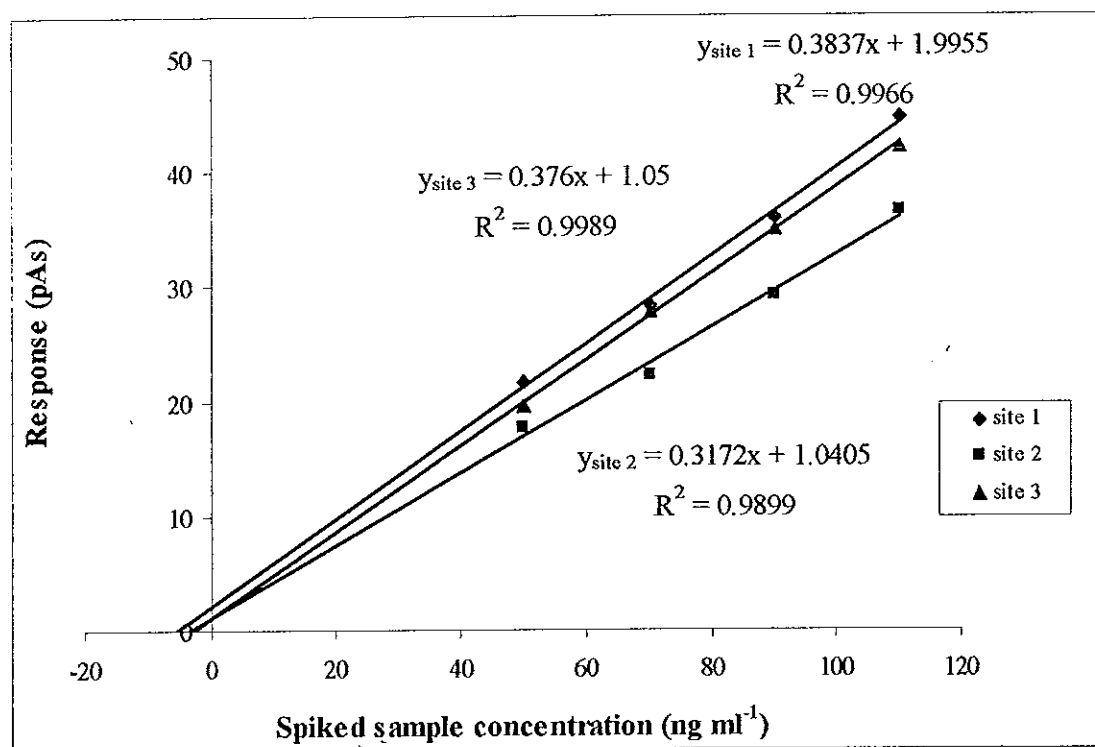


Figure 56 The standard addition calibration curve of B(b)fl

Table 63 The response of B(k)fl for sample site 1, 2 and 3 at various spiked concentration level

Spiked concentration (ng ml ⁻¹)	B(k)fl (pAs)		
	Site 1	Site 2	Site 3
100	21.35	15.24	22.68
120	24.62	19.69	28.22
140	28.89	22.14	31.75
160	33.16	24.58	36.29

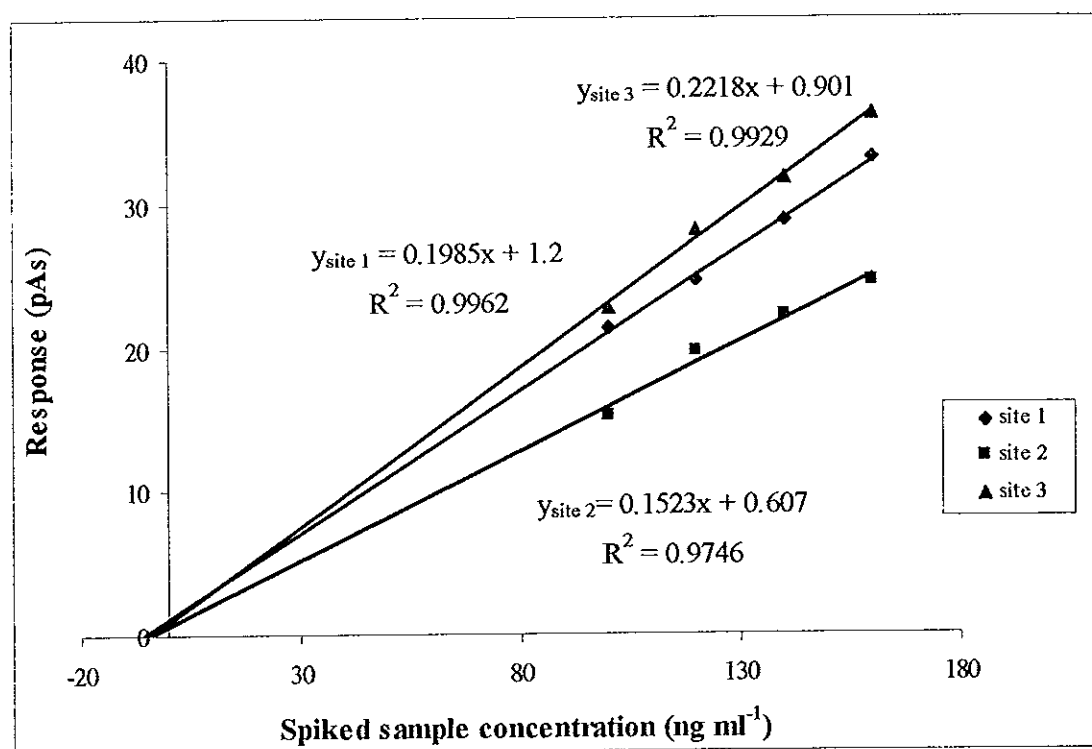


Figure 57 The standard addition calibration curve of B(k)fl

Table 64 The response of B(a)p for sample site 1, 2 and 3 at various spiked concentration level

Spiked concentration (ng ml ⁻¹)	B(a)p (pAs)		
	Site 1	Site 2	Site 3
100	18.64	17.35	20.97
120	22.37	21.82	25.63
140	27.09	25.29	29.34
160	30.82	28.76	33.66

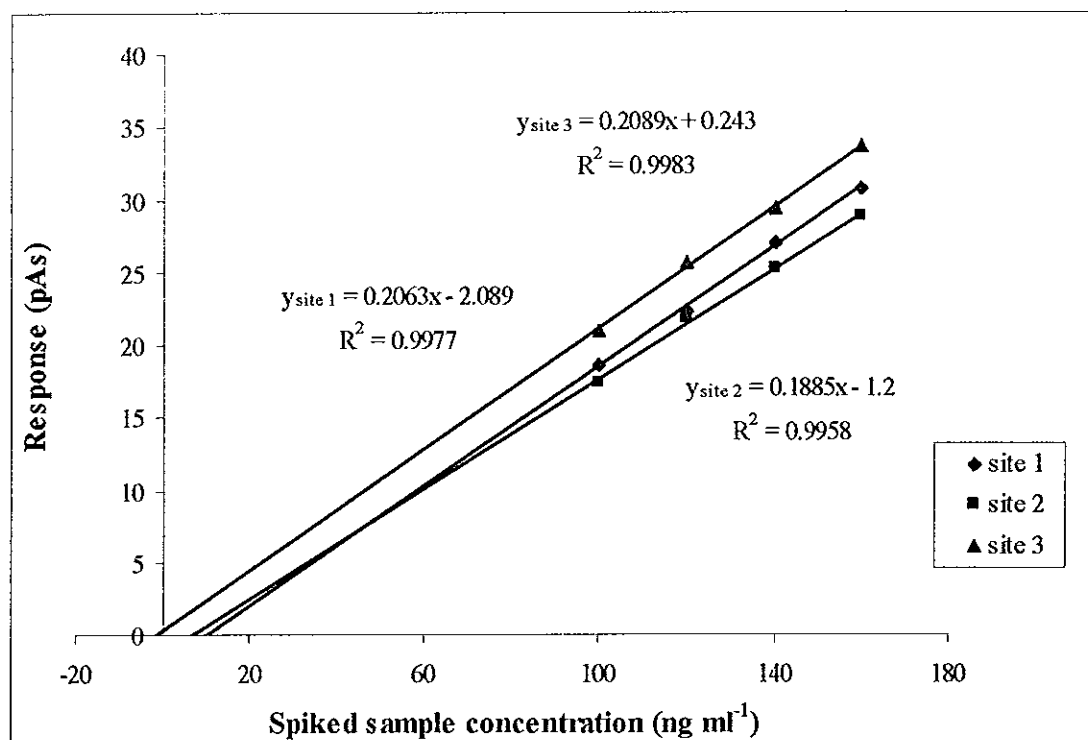


Figure 58 The standard addition calibration curve of B(a)p

Table 65 The response of In(123-cd)p for sample site 1,2 and 3 at various spiked concentration level

Spiked concentration (ng ml ⁻¹)	In(123-cd)p (pAs)		
	Site 1	Site 1	Site 1
250	18.32	20.95	22.13
270	20.79	22.43	23.34
290	21.85	24.51	25.67
310	22.94	25.78	27.14

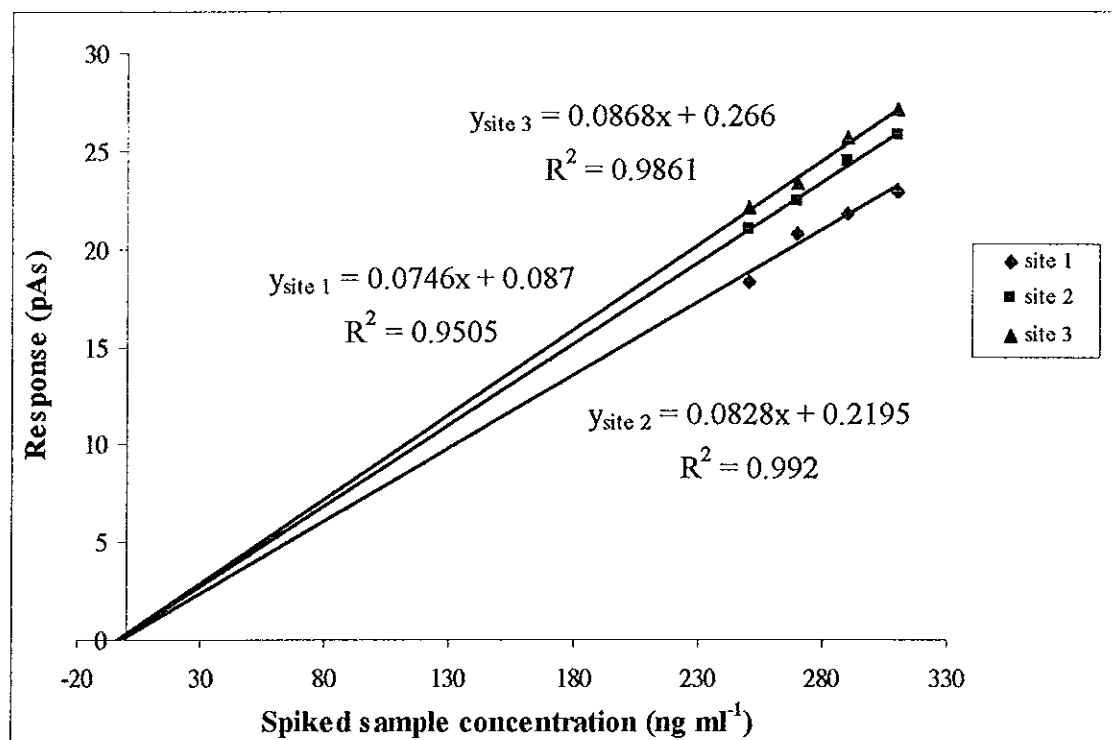


Figure 59 The standard addition calibration curve of In(123-cd)p

Table 66 The response of D(a,h)an for sample site 1,2 and 3 at various spiked concentration level

Spiked concentration (ng ml ⁻¹)	D(a,h)an (pAs)		
	Site 1	Site 2	Site 3
500	22.61	23.12	25.19
520	23.48	24.14	26.88
540	24.54	25.06	27.18
560	25.23	25.89	28.47

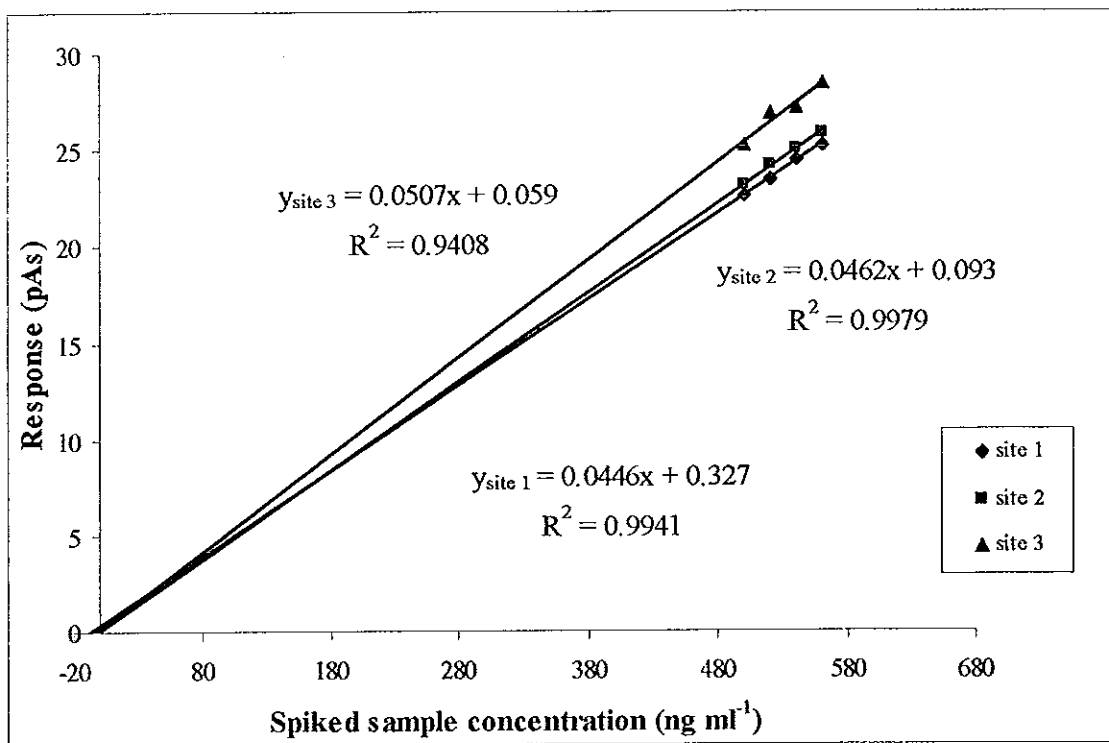


Figure 60 The standard addition calibration curve of D(a,h)an

Table 67 The PAHs concentrations of samples determined by standard addition method

PAHs	Sample (ng ml ⁻¹)		
	Site 1	Site 2	Site 3
B(a)an	11.2	8.8	2.6
Chry	2.9	12.4	4.6
B(b)fl	5.0	3.2	2.7
B(k)fl	6.0	4.0	4.0
B(a)p	10.1	6.3	1.1
In(123-cd)p	1.2	2.6	3.0
D(a,h)an	7.3	2.0	1.1

Chapter 4

CONCLUSIONS

Polycyclic aromatic hydrocarbons, or PAHs, in natural waters derive mainly from many origins. Their concentrations show significant spatial variation, depending on the relative contribution of individual sources, and generally lower than part-per-million level. This thesis demonstrated the method for determination of these PAHs, by focusing on seven PAHs which were classified as priority pollutant group B2 by US EPA. The qualitative and quantitative analysis method was carried out on a GC-FID. The separation process was by a HP 5 capillary column.

GC-FID conditions were optimized for the simultaneous analysis of the seven PAHs. Two modes of injection (the introduction of sample to GC system) were compared. The splitless injection mode gave higher responses for all compounds than the split mode. It also provided the lower limit of detection and wider linear dynamic range.

In the optimization process, the carrier gas (He) flow rate of 1.5 ml/min provided the highest theoretical plate numbers for PAHs. The optimum temperature programming was achieved as: initial temperature 130°C, ramped to 220°C with 15°C/min, hold at 220°C for 1 min, ramped to 290°C with 3°C/min, and finally hold for 2 min. The optimum injector and detector temperatures were 280 and 300°C respectively. In the part of FID detector, make up gas (N₂) flow rate was 30 ml/min and fuel (H₂): oxidant (air) flow rate was 30: 300 ml/min. These optimum conditions are appropriate for the simultaneous analysis of seven PAHs in trace level with high resolution and selectivity. The optimum conditions provided an analysis time of 32.33 minutes, limit of detections in the range of 50 to 250 ng ml⁻¹, and a linear

dynamic range in the range of 25 ng ml^{-1} to $80 \text{ } \mu\text{g ml}^{-1}$ with linear regression, R^2 of more than 0.99.

In real water samples the matrix is complex and the concentrations of PAHs are low, lower than limit of detection, thus a suitable sample pretreatment method is needed. In this research, solid phase extraction (SPE) using C_{18} Empore disk was applied to simultaneously extract, clean up and preconcentrate PAHs. High recovery and clean matrix of extractant are the purpose of using SPE, and the optimum conditions of SPE were used. The water sample was loaded into the extraction reservoir and vacuumed through the C_{18} extraction disk. Analytes were adsorbed on the disk and then eluted by organic solvent. The suitable solvent for elution of PAHs is ethyl acetate at an optimum volume of two portions of 3 ml. The drying of the disk after loading the sample is an important step, 3 minutes of drying time is enough to remove water that was retained on the extraction disk. In this study, 2-propanol was an organic modifier used to increase the solubility of PAHs. A 0.5% v/v of 2-propanol is an optimum amount for adding into the sample. The extraction coefficient of SPE expressed by percentage of recovery yield gave a percentage of relative standard deviation lower than 10. The percentage recovery of each components are, B(a)an: 112.9%, Chry: 89.3%, B(b)fl: 111.7%, B(k)fl: 96.9%, B(a)p: 89.6%, In(123-cd)p: 95.6% and D(a,h)an: 67.3%.

The large amount of suspended particle matter content in the sample could be a problem in the collecting step and it will also affect the concentration of PAHs during storage. The most important problem cause by the suspended particle matter is the clogging of the C_{18} extraction disk which will decrease the extraction coefficient. Therefore, a lab built prefiltration unit was used to minimize the suspended particle content before loaded the sample to the disk. The prefiltration unit provided the advantage of reducing the quantity of suspended particle matters by filtering off those with particle size more than $10 \text{ } \mu\text{m}$.

For qualitative and quantitative analysis of the seven PAHs in group B2 in real water samples. The water samples were collected from three sampling sites (Songklanakarind Hospital's wastewater treatment ponds). PAHs were analyzed and the concentrations were in the range of 1.1 to 11.2 ng ml⁻¹.

There are many advantages of SPE over the conventional method of LLE used by Wong and Wang (2000). Firstly, SPE provided 4 to 40% higher percentage of recovery. Secondly was less, the extraction time when applied the SPE disk (~ 30 minutes) than LLE (> 10 hours). Lastly, the solvent used in the extraction by SPE was 75 fold less than LLE. In conclusion, the procedures developed in this thesis successfully combined a rapid extraction technique with a highly effective method for analysis. PAHs could be identified by submitting the sample only to a single extraction and purification treatment, with evident savings in terms of time and cost. In addition, a reduction in the use of solvent is to be welcomed as it helps safeguard both the operator's health and the environment – an important aspect for a project which aims to determine the quality of the environment in order to identify possible dangers to human beings and nature.

REFERENCES

- Agency for Toxic Substances and Disease Registry (ASTDR). 1992. Appendix C. B(A)P and 2,3,7,8-TCDD Equivalent Concentrations. [Online]. Available: http://www.astdr.cdc.gov/HAC/PHA/popile/pop_p4.html.
- Agency for Toxic Substances and Disease Registry (ASTDR). 1995. Toxicological profile for polycyclic aromatic hydrocarbons (PAHs) (Update June 22, 2001). Atlanta, GA: US Department of Health and Human Services, Public Health Service.
- Agency for Toxic Substances and Disease Registry (ASTDR). 1996. ToxFaqS for polycyclic aromatic hydrocarbons (PAHs). Atlanta, GA:
- Barranco A., Alonso-Salces, R.M., Bakkali, A. Berrueta, L.A., Gallo, B., Vicenta, F. and Sarobe, M. 2003. Solid-phase clean-up in the liquid chromatographic determination of polycyclic aromatic hydrocarbons in edible oils. *Journal of chromatography A*. 988: 33-40.
- Bernal, J., Nozal, M.J., Toribio, L., Serna, M.L., Borrull, F., Marcé, R.M. and Pocurull, E. 1997. Determination of polycyclic aromatic hydrocarbons in waters by use of supercritical fluid chromatography coupled on-line to solid-phase extraction with disks. *Journal of chromatography A*. 778: 321-328.
- Bruzzonoti, M.C., Saranini, C. and Mentasti, E. 2000. Preconcentration of contaminants in water analysis. *Journal of chromatography A*. 902: 289-309.

Certificate of Analysis from Materials Safety Data Sheet (Restek, USA)

Chromatographic Instrumentation, 2001. GC. [Online]. Available:
http://www.chem.missouri.edu/Greenlief/courses/GC_HPLC_Instrumentation.pdf.

Doong R. and Chang S. 2000. Determination of distribution coefficients of priority polycyclic aromatic hydrocarbons using solid-phase microextraction. *Analytical Chemistry*. 72: 3647-3652.

Eisert, R. and Levsen, K. 1996. Solid-phase microextraction coupled to gas chromatography: a new method for the analysis of organics in water. *Journal of chromatography A*. 733: 143-157.

Grob, R.L. 1985. *Modern Practice of Gas Chromatography* (2nd ed.), 897 pp. New York: A Wiley-Interscience, John Wiley & Sons.

Hagestuen, E.D. and Campiglia, A.D. 1999. New approach for screening polycyclic aromatic hydrocarbons in water samples. *Talanta*. 49: 547-560.

Information on Toxic Chemicals, 2001. Polycyclic Aromatic Hydrocarbons (PAHs). [Online]. Available: <http://www.dhfs.state.wi.us/ch>.

Irwin, R. J. 1997. *Environmental Contaminants Encyclopedia*, Colorado: National Park Service.

Jaouen-Madoulet, A., Abarnou, A., Le Guellec, A.-M., Loizeau, V. and Leboulenger, F. 2000. Validation of an analytical procedure for

polychlorinated biphenyls, coplanar polychlorinated biphenyls and polycyclic aromatic hydrocarbons in environmental samples. *Journal of chromatography A*. 886: 153-173.

Kebbekus, B.B. and Mitra, S. 1998. *Environment Chemical Analysis* (1st ed.), 330 pp. London: Blackie Academic & Professional.

Kootstra, P.R., Straub, M.H.C., Stil, G.H., van der Velde, E.G., Hesselink, W. and Land, C.C.J. 1995. Solid-phase extraction of polycyclic aromatic hydrocarbons from soil samples. *Journal of chromatography A*. 697: 123-129.

Li, N. and Lee, H.K. 2001. Solid-phase extraction of polycyclic aromatic hydrocarbons in surface water negative effect of humic acid. *Journal of chromatography A*. 921: 255-263.

Manoli, E. and Samara, C. 1999. Polycyclic aromatic hydrocarbons in natural waters: sources, occurrence and analysis. *Trends in analytical Chemistry*. 18: 417-428.

Marcé, R.M. and Borrull, F. 2000. Solid-phase extraction of polycyclic aromatic compounds. *Journal of chromatography A*. 885: 273-290.

Marriott, P.J., Haglund, P. and Ong, R.C.Y. 2003. A review of environmental toxicant analysis by using multidimensional gas chromatography and comprehensive GC. *Clinica Chimica Acta*. 328: 1-19.

McGowin, A.E., Adom, K.K. and Obubuafo, A.K. 2001. Screening of compost for PAHs and pesticides using static subcritical water extraction. *Chemosphere*. 45: 857-864.

Merck KgaA Catalog. 1999/2000. Chemical Reagent. Germany: Dr. Theodor Schuchardt & Co.

Michor, G. Carron, J., Bruce, S. and Cancilla, D.A. 1996. Analysis of 23 polynuclear aromatic hydrocarbons from natural water at the sub-ng l⁻¹ level using solid-phase disk extraction and mass-selective detection. *Journal of chromatography A*. 732: 85-99.

Namieśnik, J., Zygmunt, B. and Jastrzebska, A. 2000. Application of solid-phase microextraction for determination of organic vapours in gaseous matrices. *Journal of chromatography A*. 885: 405-418.

Nguyen, A.-L. and Luong, J.H.T. 1997. Separation and determination of polycyclic aromatic hydrocarbons by solid phase microextraction/cyclodextrin-modified capillary electrophoresis. *Analytical Chemistry*. 69: 1726-1731.

Pichon, V., Bouzige, M. and Hennion, M.-C. 1998. New trends in environmental trace-analysis of organic pollutants: class-selective immunoextraction and clean-up in one step using immunosorbents. *Analytica Chimica Acta*. 376: 21-35.

Popp, P., Bauer, C., Möder, M. and Paschke, A. 2000. Determination of polycyclic aromatic hydrocarbons in waste water by off-line coupling

of solid-phase microextraction with column liquid chromatography. *Journal of chromatography A*. 897: 153-159.

Singh, A.K., Spassova, D. and White, T. 1998. Quantitative analysis of polychlorinated biphenyls, organochlorine insecticides, polycyclic aromatic hydrocarbons in spiked samples of soil, water and plasma by selected-ion monitoring gas chromatography-mass spectrometry.

Spectrum Laboratories, 2001. Chemical Fact Sheet. [Online]. Available: <http://www.speclab.com/compund.htm>.

Szolar, O.H.J., Brown, S. and Loung, J.H.T. 1995. Separation of PAHs by capillary electrophoresis with laser-induced fluorescence detection using mixture of neutral and anionic β -cyclodextrin. *Analytical Chemistry*. 67: 3004-3010.

Townshend A. 1995. Encyclopedia of Analytical Science (1st ed.), London: Academic Press Limited.

Urbe, I. and Ruana, J. 1997. Application of solid-phase extraction discs with a glass fiber matrix to fast determination of polycyclic aromatic hydrocarbons in water. *Journal of chromatography A*. 778: 337-345.

US Environmental Protection Agency. 1984. EPA 40 CFR, Part 136 Method for Organic Chemical Analysis of Municipal and Industrial Wastewater, Method 610-Polynuclear Aromatic Hydrocarbons, Fed. Regist. 49, Washington, DC.

US Environmental Protection Agency. 1986. Method 8100-Polynuclear Aromatic Hydrocarbons, Revision 0, September.

US Environmental Protection Agency. 1988. Method 525 in: Methods for the Determination of Organic Compounds in Drinking Water, EPA/600/4-88/039. Office of Research and Development, Washington, DC.

van der Oost, R, Beyer, J. and Vermeulen, N.P.E. 2003. Fish bioaccumulation and biomarkers in environmental risk assessment: a review. *Environmental Toxicology and Pharmacology*. 13: 57-149.

Wolska, L., Galer, K., Górecki, T and Namieśnik, J. 1999. Surface water preparation procedure for chromatographic determination of polycyclic aromatic hydrocarbons and polychlorinated biphenyls. *Talanta*. 50: 985-991.

Wong, P.K. and Wang, J. 2001. The accumulation of polycyclic aromatic hydrocarbons in lubricating oil over time – a comparison of supercritical fluid and liquid-liquid extraction methods. *Environmental Pollution*. 112: 407-415.

VITAE

Name Miss. Sathida Malee

Birth date April 8, 1979

Education Attainment

Degree	Name of Institution	Year of Graduation
B.Sc. (Chemistry-Biology)	Prince of Songkla University	2000

Scholarship Awards during Enrolment

The scholarship support from Higher Education Development Project: Postgraduate Education and Research Program in Chemistry (PERCH), Funded by The Royal Thai Government.

Poster Presentations

Sathida Malee and Proespichaya Kanatharana. Trace analysis of polycyclic aromatic hydrocarbons in water sample by capillary gas chromatography. The First PERCH Annual Scientific Conference (PERCH Conference I), May 12 – 15, 2002, Chonburi, Thailand.

Sathida Malee and Proespichaya Kanatharana. Trace analysis of PAHs in water sample by capillary gas chromatography. International Conference & Exhibition on Pure and Applied Chemistry 2002, May 29 – 31, 2002, Bangkok, Thailand.

Sathida Malee and Proespichaya Kanatharana. Sample preparation for trace analysis of PAHs in water sample. The First PSU Symposium on Graduate Research, March 12, 2003, Songkla, Thailand.

Sathida Malee and Proespichaya Kanatharana. Sample preparation of trace PAHs in water by solid phase extraction (SPE). The Second PERCH Annual Scientific Conference (PERCH Conference II), May 11 – 14, 2003, Chonburi, Thailand.

Oral Presentation

Sathida Malee, Jongjit Jantra, Triranat Pengubon, Sucheera Loyprasert, Proespichaya Kanatharana and Panote Thavarungkul. Sample preparation techniques for polycyclic aromatic hydrocarbons (PAHs) analysis in various sample. International Conference on Environmental Management and Technology, August 4-6, 2003, Kuala Lumpur, Malaysia.